

Proceedings of Anticancer Research

Honorary Editor-in-Chief

Behnam Mahdavi

Department of Chemistry, Faculty of Science, Hakim Sabzevari University, Iran

Editor-in-Chief

Shixiang Guo

Chongqing General Hospital, China

BIO-BYWORD SCIENTIFIC PUBLISHING PTY LTD

(619 649 400)

Level 10

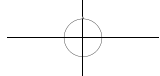
50 Clarence Street

SYDNEY NSW 2000

Copyright © 2024. Bio-Byword Scientific Publishing Pty Ltd.

Complimentary Copy





ISSN (ONLINE): 2208-3553

ISSN (PRINT): 2208-3545



Proceedings of Anticancer Research

Focus and Scope

Proceedings of Anticancer Research is an international peer-reviewed and open access journal, which is devoted to the rapid publication of high quality original articles, reviews, case reports, short communication and letters on all aspects of experimental and clinical oncology.

- Cellular research and bio-markers
- Identification of bio-targets and agents with novel mechanisms of action
- Preventative and integrated treatment for cancer patients
- Radiation and surgery
- Palliative care
- Patient adherence, quality of life, satisfaction
- Anticancer medicine

About Publisher

Bio-Byword Scientific Publishing is a fast-growing, peer-reviewed and open access journal publisher, which is located in Sydney, Australia. As a dependable and credible corporation, it promotes and serves a broad range of subject areas for the benefit of humanity. By informing and educating a global community of scholars, practitioners, researchers and students, it endeavors to be the world's leading independent academic and professional publisher. To realize it, it keeps creative and innovative to meet the range of the authors' needs and publish the best of their work.

By cooperating with University of Sydney, University of New South Wales and other world-famous universities, Bio-Byword Scientific Publishing has established a huge publishing system based on hundreds of academic programs, and with a variety of journals in the subjects of medicine, construction, education and electronics.

Publisher Headquarter

BIO-BYWORD SCIENTIFIC PUBLISHING PTY LTD Level 10
50 Clarence Street
Sydney NSW 2000
Website: www.bbwpublisher.com Email: info@bbwpublisher.com

Table of Contents

- 1 Application Value of Artificial Intelligence-Assisted Diagnostic Systems in CT Diagnosis of Pulmonary Nodules**
Yang Xue, Mingqiang Diao, Bing Han
- 8 Advantages and Application Prospects of Traditional Chinese Medicine Granules**
Xiaohua Sun
- 14 Effectiveness of High-Frequency Electrosurgical Knife Surgery Under Painless Digestive Endoscopy in Elderly Patients with Gastrointestinal Polyps**
Yumin Lu
- 21 Effectiveness of Multi-Modal Teaching Based on Online Case Libraries in the Education of Gene Methylation Combined with Spiral CT Screening for Pulmonary Ground-Glass Opacity Nodules**
Yong Zhou, Xi Zhang, Shuyi Liu, Zhuoyi He, Weili Tian, Shuping You
- 27 Infrared Thermography-Based Predictive Model for Syndrome Differentiation of Chaihu Guizhi Ganjiang Decoction**
Huisi Hong, Yiming Yuan, Na Li, Xiaoxing Huang, Leyu Li, Tingting Zeng
- 37 Advances in Artificial Intelligence for Predicting Breast Cancer Using Chest CT Scans**
Jingxiang Sun, Guang Zhang
- 45 Advances in Radiomics for Individualized and Precision-Based Diagnosis and Treatment of Lung Cancer**
Tongtong Liu, Fang Wang, Shuai Qie, Xuefeng Wang, Kuan Liu, Yang Li, Hongyun Shi
- 52 The High Expression of EXOSC3 in OSCC is Associated with Poor Prognosis and Immune Infiltration**
Yucunxi Liu, Jianguo Liu
- 62 Comparative Effectiveness of Medical Radiation Protection Spray and Triethanolamine Cream in Preventing and Treating Radiodermatitis in Breast Cancer Patients**
Yuge Ran, Chan Liu, Lanhui Yuan, Huibin Yang, Lei Su, Kunjie Wang, Qianqian Han, Xiaoxi Wu, Hongyun Shi

- 68 Research Progress on the Mechanism of Action of Traditional Chinese Medicine Extracts in the Prevention and Treatment of Periodontitis**
Tian Ke, Rao Lu, Tang Jing
- 82 Symptom Experiences and Coping Patterns in Pancreatic Cancer Patients During Chemotherapy: A Qualitative Study**
Xin Tian, Ping Chen, Wen Zhou, Peiyang Mao, Jian Li, Cheng Lei, Xiaojing Xue, Changlin Li, Yuxian Nie, Feng Gao, Jie Li, Gang Feng, Xiaobo Du, Qiuling Shi, Jingyu Zhang
- 97 The Predictive Value of *SPPI* Gene Expression for the Survival of Advanced Liver Cancer Treated with Transarterial Chemoembolization**
Yu Cai, Pu Yan, Chang Tian, Yuqing Li, Yuanyuan Jia, Siqi Wang
- 108 Clinical Efficacy and Safety Analysis of Toripalimab Combined with GC Chemotherapy for Advanced Urothelial Carcinoma**
Song Xue, Dongli Ruan
- 115 Application of Artificial Neural Networks in Predicting Malignant Lung Nodules on Chest CT Scans**
Wenhui Li, Yuping Yang, Yixian Liang, Pengliang Xu, Qiuqiang Chen
- 122 Study on the Clinical Efficacy of Levofloxacin Combined with Ambroxol in the Treatment of Elderly Patients with Chronic Obstructive Pulmonary Disease and Pulmonary Infection**
Yuanyuan Chen
- 128 Plasma Technology: Unlocking a New Path for Precise Elimination of Cancer Cells**
Jie Bai

Application Value of Artificial Intelligence-Assisted Diagnostic Systems in CT Diagnosis of Pulmonary Nodules

Yang Xue*, Mingqiang Diao, Bing Han

Deyang People's Hospital, Deyang 618000, Sichuan Province, China

*Corresponding author: Yang Xue, 26917269@qq.com

Copyright: © 2025 Author(s). This is an open-access article distributed under the terms of the Creative Commons Attribution License (CC BY 4.0), permitting distribution and reproduction in any medium, provided the original work is cited.

Abstract: *Objective:* To explore the application value of artificial intelligence-assisted diagnostic systems in the computed tomography (CT) diagnosis of pulmonary nodules. *Methods:* A total of 80 patients with pulmonary nodules, treated from June 2023 to May 2024, were included. All patients underwent pathological examination and CT scans, with pathological results serving as the gold standard. The diagnostic performance of CT alone and CT combined with the artificial intelligence-assisted diagnostic system was analyzed, and differences in CT imaging features and evaluation results of benign and malignant pulmonary nodules were compared. *Results:* The sensitivity, specificity, and accuracy of CT combined with the artificial intelligence-assisted diagnostic system were significantly higher than those of CT alone ($P < 0.05$). Moreover, the false-positive and false-negative rates were significantly lower for the combined approach compared to CT alone ($P < 0.05$). *Conclusion:* The artificial intelligence-assisted diagnostic system effectively identifies malignant features in pulmonary nodules, providing valuable clinical reference data and enhancing diagnostic accuracy and efficiency.

Keywords: Artificial intelligence-assisted diagnostic system; Pulmonary nodule; CT diagnosis

Online publication: January 16, 2025

1. Introduction

Lung cancer is one of the most prevalent and deadly malignant tumors globally, posing a severe threat to human health. Early detection, diagnosis, and treatment are critical for improving survival rates and outcomes for lung cancer patients. Pulmonary nodules are common radiological findings in the lungs, some of which may represent early-stage lung cancer^[1]. Therefore, accurately differentiating between benign and malignant pulmonary nodules is of great clinical importance.

Traditionally, the diagnosis of pulmonary nodules relies primarily on imaging techniques, such as chest X-rays and computed tomography (CT) scans, along with the expertise and clinical experience of physicians^[2,3].

However, the imaging characteristics of pulmonary nodules are often complex and varied, with overlaps in morphology, size, and density between benign and malignant nodules, which presents challenges for accurate diagnosis ^[4]. Additionally, factors such as subjectivity, fatigue, and workload can affect the diagnostic accuracy of physicians.

With the rapid development of artificial intelligence (AI) technology, AI-assisted diagnostic systems are being increasingly applied in medicine. These systems can learn from and analyze large volumes of medical imaging data, automatically extract features from images, and provide diagnostic and predictive insights. In the context of pulmonary nodule diagnosis, AI-assisted diagnostic systems can quickly and accurately identify the location, size, and morphology of nodules, assess their benign or malignant nature, and offer critical diagnostic support for clinicians ^[5].

Several studies have demonstrated the high accuracy and reliability of AI-assisted diagnostic systems in diagnosing pulmonary nodules. However, these studies often involve relatively small sample sizes, limiting the generalizability and scalability of their findings. This study aims to analyze a larger cohort of pulmonary nodule patients to further evaluate the application value of AI-assisted diagnostic systems in CT diagnosis, providing more reliable evidence for clinical practice.

2. Materials and methods

2.1. General information

Eighty patients with pulmonary nodules who visited our hospital from June 2023 to May 2024 were selected for this study, including 45 males and 35 females, aged 35–75 years, with an average age of 52.57 ± 10.54 years.

Inclusion criteria: (1) Pulmonary nodules detected via chest CT; (2) Patients who signed informed consent forms and were willing to cooperate with the study.

Exclusion criteria: (1) Concurrent diagnoses of other malignant tumors; (2) Severe dysfunction of critical organs such as the heart, liver, or kidneys; (3) Patients with mental illnesses who could not cooperate with examination and treatment.

2.2. Methods

2.2.1. CT examination

All patients underwent chest CT using a 64-slice spiral CT scanner (Brand: Shanghai United Imaging Healthcare Co., Ltd.; Model: uCT 760). Scanning parameters: tube voltage 120 kV, tube current 200–300 mAs, slice thickness 5 mm, and slice spacing 5 mm. The scanning range extended from the thoracic inlet to the diaphragm. After the scan, image data were transmitted to a workstation for post-processing, including multiplanar reconstruction (MPR) and volume rendering (VR).

2.2.2. Artificial intelligence-assisted diagnostic system

The artificial intelligence-assisted diagnostic system used in this study was developed by Pu'er iFLYTEK Information Technology Co., Ltd. This system, based on deep learning algorithms, was trained with extensive pulmonary nodule CT images to establish a classification model for distinguishing benign from malignant nodules. Patient CT images were imported into the system, which automatically identified and analyzed pulmonary nodules, providing an evaluation of their benign or malignant nature.

2.2.3. Pathological examination

All patients underwent pathological examination within 1–2 weeks after CT scanning. Depending on the location and size of the pulmonary nodules, appropriate pathological examination methods were selected, including percutaneous lung biopsy, bronchoscopic biopsy, or thoracoscopic surgery. Pathological results were jointly assessed by two experienced pathologists to determine the nature of the pulmonary nodules.

2.3. Observation indicators

2.3.1. Diagnostic performance metrics

Using pathological results as the gold standard, the diagnostic performance of CT alone and CT combined with the artificial intelligence-assisted diagnostic system was analyzed. Diagnostic performance metrics included sensitivity (true positive rate), specificity (true negative rate), false positive rate, false negative rate, and accuracy.

$$\text{Sensitivity} = \frac{\text{True positives}}{\text{True positives} + \text{False negatives}} \times 100\%$$

$$\text{Specificity} = \frac{\text{True negatives}}{\text{True negatives} + \text{False positives}} \times 100\%$$

$$\text{False positive rate} = \frac{\text{False positives}}{\text{True negatives} + \text{False positives}} \times 100\%$$

$$\text{False negative rate} = \frac{\text{False negatives}}{\text{True positives} + \text{False negatives}} \times 100\%$$

$$\text{Accuracy} = \frac{\text{True positives} + \text{True negatives}}{\text{Total cases}} \times 100\%$$

2.3.2. Differences in pulmonary nodule evaluation results

The CT imaging features of benign and malignant pulmonary nodules were compared, including nodule size, shape, margins, density, and the presence of lobulation, spiculation, or pleural indentation. Additionally, differences in evaluations by the artificial intelligence-assisted diagnostic system were analyzed. Malignant pulmonary nodules were scored within a range of 60–100 points, while benign nodules were scored between 0–40 points.

2.4. Statistical analysis

Statistical analysis was performed using SPSS 27.0 software. Quantitative data were expressed as mean \pm standard deviation (SD) and compared using the *t*-test. Categorical data were presented as frequencies and percentages and compared using the χ^2 -test. Statistical significance was set at $P < 0.05$.

3. Results

3.1. Pathological examination results

Among the 80 patients with pulmonary nodules, pathological examination confirmed 30 cases of malignant nodules and 50 cases of benign nodules (**Table 1**).

Table 1. Comparison of pathological examination results

Pathological examination		Number of cases (<i>n</i>)
Malignant nodules	Adenocarcinoma	20
	Squamous carcinoma	5
	Small cell carcinoma	3
	Other	2
Benign nodules	Inflammatory nodules	30
	Tuberculoma	10
	Hamartoma	5
	Other	5

3.2. Diagnostic performance of CT and AI-assisted CT examination

The sensitivity, specificity, and accuracy of AI-assisted CT examination were significantly higher than those of CT examination alone ($P < 0.05$), while the false positive and false negative rates were significantly lower ($P < 0.05$) (**Table 2**).

Table 2. Comparison of diagnostic performance between CT and AI-assisted CT examination

Diagnostic method	True positive (<i>n</i>)	False positive (<i>n</i>)	False negative (<i>n</i>)	True negative (<i>n</i>)	Sensitivity (%)	Specificity (%)	False positive rate (%)	False negative rate (%)	Accuracy (%)
CT examination	20	10	10	40	66.67	80.00	20.00	33.33	75.00
AI-assisted CT examination	25	5	5	45	83.33	90.00	10.00	16.67	87.50
χ^2	-	-	-	-	7.402	3.922	3.922	7.402	5.128
<i>P</i>	-	-	-	-	0.007	0.048	0.048	0.007	0.024

3.3. Comparison of CT imaging features between benign and malignant pulmonary nodules

There were significant differences in CT imaging features between benign and malignant pulmonary nodules, including nodule size, shape, margins, density, and the presence of lobulation, spiculation, and pleural indentation ($P < 0.001$) (**Table 3**).

Table 3. Comparison of CT imaging features between benign and malignant pulmonary nodules

CT feature	Malignant nodules (<i>n</i> = 30)	Benign nodules (<i>n</i> = 50)	χ^2 value	<i>P</i> value
Malignant nodules (mean \pm SD, cm)	3.54 \pm 1.20	1.81 \pm 0.87	7.451	< 0.001
Irregular shape [<i>n</i> (%)]	20 (66.67%)	10 (20.00%)	17.422	< 0.001
Blurry edges [<i>n</i> (%)]	22 (73.33%)	15 (30.00%)	14.163	< 0.001
Uneven density [<i>n</i> (%)]	25 (83.33%)	20 (40.00%)	14.307	< 0.001
Lobulation [<i>n</i> (%)]	20 (66.67%)	5 (10.00%)	28.024	< 0.001
Spiculation [<i>n</i> (%)]	18 (60.00%)	8 (16.00%)	16.547	< 0.001
Pleural indentation [<i>n</i> (%)]	15 (50.00%)	5 (10.00%)	16.000	< 0.001

3.4. Differences in AI-assisted evaluation of benign and malignant pulmonary nodules

The AI-assisted diagnostic system produced significantly higher evaluation scores for malignant nodules compared to benign nodules ($P < 0.001$) (Table 4).

Table 4. Comparison of AI-assisted evaluation scores for benign and malignant pulmonary nodules

Group (<i>n</i>)	Score (mean \pm SD, points)
Malignant pulmonary nodules (<i>n</i> = 30)	80.57 \pm 10.54
Benign pulmonary nodules (<i>n</i> = 50)	20.54 \pm 8.56
<i>t</i> value	27.815
<i>P</i> value	< 0.001

4. Discussion

The AI diagnostic assistance system has been a significant innovation in the medical field in recent years and has been extensively applied to cancer diagnosis and differential diagnosis. As cancer incidence continues to rise, precise and efficient diagnostic tools have become increasingly critical. Traditional imaging diagnostics are inevitably influenced by factors such as the physician's expertise, experience, and subjective judgment, leading to variability and interpretative differences^[6]. Different physicians may provide varying diagnostic results for the same imaging data, which can affect subsequent treatment and lead to the inefficient use of medical resources.

The AI diagnostic assistance system, with its powerful data analysis and learning capabilities, can perform deep learning on large volumes of cancer imaging data. It can rapidly and accurately identify characteristic information in images, effectively reducing diagnostic variability caused by human factors^[7,8]. By providing precise image analysis, AI systems deliver more consistent diagnostic results, significantly improving diagnostic consistency^[9]. Moreover, the system's rapid processing capabilities can substantially reduce diagnostic time, enhancing efficiency and securing valuable treatment time for patients^[10].

The results of this study demonstrate that the AI diagnostic assistance system combined with CT imaging has high application value in diagnosing pulmonary nodules. Compared to standalone CT imaging, the AI-

assisted system significantly improves the detection rate, sensitivity, specificity, and accuracy of malignant pulmonary nodules while reducing false positive and false negative rates.

A comparison of CT imaging features between benign and malignant pulmonary nodules revealed that malignant nodules exhibit typical imaging characteristics, such as larger size, irregular shape, blurred margins, uneven density, lobulation, spiculation, and pleural indentation. Conversely, benign nodules are more likely to appear smaller, with regular shape, clear margins, uniform density, and without lobulation, spiculation, or pleural indentation. The AI diagnostic system can accurately identify these features and assess the benign or malignant nature of pulmonary nodules, providing critical reference information for physicians^[11-13].

Furthermore, the system showed significant differences in its assessment of benign and malignant pulmonary nodules, with higher evaluation scores for malignant nodules compared to benign ones. This indicates that the AI diagnostic assistance system can effectively assess the malignancy of pulmonary nodules through CT image analysis, offering valuable information for the formulation of clinical treatment plans.

5. Conclusion

In summary, the application of the AI diagnostic assistance system in pulmonary nodule CT diagnosis improves diagnostic accuracy and reliability, reduces misdiagnosis and missed diagnosis, and holds significant clinical value and application prospects. However, this study has certain limitations, such as a relatively small sample size and short research duration. Future studies should expand the sample size and conduct multi-center, large-sample clinical research to verify the long-term efficacy and safety of the AI diagnostic assistance system in pulmonary nodule diagnosis. Additionally, continuous optimization of AI algorithms and models is needed to enhance its diagnostic capabilities for complex pulmonary nodules, thereby providing more precise medical services for patients.

Funding

This work is supported by Chengdu University of Traditional Chinese Medicine “Xinglin Scholars” Subject Talent Scientific Research Enhancement Plan (No. YYZX2022056).

Disclosure statement

The authors declare no conflict of interest.

References

- [1] Liu YB, Li Q, Zhou W, et al., 2022, The Diagnostic and Nodule-Type Assessment Value of Artificial Intelligence-Based Chest CT Combined with AI Diagnostic Systems in Patients with Suspected Pulmonary Nodules. *Artif Intell Mod Biomed Prog*, 22(5): 955–959.
- [2] Jin CW, Guo YM, 2019, Application and Quality Control of Artificial Intelligence-Assisted Diagnostic Technology in Low-Dose CT Screening for Pulmonary Nodules. *Chin J Radiol*, 53(1): 6–8.
- [3] Wang HS, Shen JK, Zan PF, et al., 2021, Imaging Characteristics and Prognosis Analysis of Pulmonary Nodules of Uncertain Nature in Osteosarcoma Patients Using Artificial Intelligence. *Chin J Bone Joint*, 10(11): 834–839.

- [4] Zhou YP, Li S, Zhang X, et al., 2019, Clinical Application Value Study of an Artificial Intelligence-Based Deep Neural Network-Assisted Diagnostic System for High-Resolution MRI Rectal Lymph Nodes. *Chin J Surg*, 57(2): 108–113.
- [5] Huang L, Li YX, Wu LL, et al., 2020, Research on an Artificial Intelligence-Assisted Diagnostic System Based on Deep Learning for Benign and Malignant Gastric Ulcers. *Chin J Dig Endosc*, 37(7): 476–480.
- [6] Yi L, Zuo MJ, 2023, Research Progress of CT Radiomics-Based Artificial Intelligence in the Differential Diagnosis of Pulmonary Nodules. *Pract Radiol*, 39(11): 1894–1896.
- [7] Qiu L, Fang XM, Chen HW, 2019, Research Progress in Artificial Intelligence-Assisted CT for Distinguishing Benign and Malignant Pulmonary Nodules. *Clin Radiol J*, 38(12): 2453–2456.
- [8] Mao YX, Ren CY, Li SZ, et al., 2021, Diagnostic Value of Artificial Intelligence Combined with Low-Dose CT in the Screening of Pulmonary *In Situ* Carcinoma. *Chin Med Equip*, 18(12): 45–48.
- [9] Luo YM, Zhao L, Jiang YL, et al., 2022, Evaluation of the Application Value of Artificial Intelligence Diagnostic Systems in Pulmonary Nodule CT Screening. *South China J Def Med*, 36(7): 521–524.
- [10] Shen J, Liu YJ, Mo M, et al., 2023, Effectiveness Study of Artificial Intelligence-Assisted Ultrasound for Identifying Breast Lesions in Chinese Women. *Chin J Cancer*, 33(11): 1002–1008.
- [11] Liu HL, Chen GP, Tao JS, et al., 2022, Application Value of a CT Thin-Slice Imaging Feature-Based Pulmonary Nodule Grading Assessment System in Distinguishing Benign and Malignant Pulmonary Nodules. *Clin Pulmonol*, 27(1): 102–105.
- [12] Yang F, Fan J, Tian ZJY, et al., 2020, Preliminary Study on Artificial Intelligence-Based CT Screening for Subsolid Pulmonary Nodules in a Population. *Chin J Thorac Cardiovasc Surg*, 36(3): 145–150.
- [13] Chinese Medical Association Respiratory Disease Branch Lung Cancer Group, Chinese Lung Cancer Prevention and Treatment Alliance Expert Group, 2018, Chinese Expert Consensus on the Diagnosis and Treatment of Pulmonary Nodules (2018 Version). *Chin J Tuberc Respir Dis*, 41(10): 763–771.

Publisher's note

Bio-Byword Scientific Publishing remains neutral with regard to jurisdictional claims in published maps and institutional affiliations.

Advantages and Application Prospects of Traditional Chinese Medicine Granules

Xiaohua Sun*

Nanjing Xingyin Pharmaceutical Group Co., Ltd., Nanjing 210000, Jiangsu Province, China

*Corresponding author: Xiaohua Sun, 478512346@qq.com

Copyright: © 2025 Author(s). This is an open-access article distributed under the terms of the Creative Commons Attribution License (CC BY 4.0), permitting distribution and reproduction in any medium, provided the original work is cited.

Abstract: With the advancement of the modernization of traditional Chinese medicine (TCM), TCM granules have emerged and garnered widespread attention. This study provides a comprehensive review of the development of TCM granules, analyzing their characteristics in terms of ease of use, quality stability, and pharmacodynamic advantages. It also explores their broad application prospects in clinical TCM treatment and preventive healthcare. Through an integrative analysis of relevant research literature, the study highlights the significant value and vast development potential of TCM granules in modern medicine. The article aims to offer valuable references for the modernization and internationalization of TCM while promoting the continuous development and innovative application of TCM granules in the field of traditional Chinese medicine.

Keywords: TCM granules; Advantages; Clinical application; Preventive healthcare

Online publication: February 13, 2025

1. Introduction

Throughout the long history of traditional Chinese medicine (TCM) development, drug formulations have continually evolved and innovated to meet the demands of modern society and medical practices. As a novel TCM formulation, TCM granules have emerged based on traditional decoctions, integrating the essence of TCM theories with modern pharmaceutical technologies. They are gradually gaining prominence in clinical TCM treatment, the modernization of TCM, and public health care. TCM granules retain the characteristics and efficacy of TCM compound formulas while offering numerous advantages, including convenience, quality stability, and ease of storage and transport ^[1]. These features make TCM granules a prominent research and application focus in the field of TCM, paving new paths for its inheritance and development. They also provide patients with safer, more efficient, and more convenient medication options, showcasing broad application prospects and significant research value.

2. Development history of traditional Chinese medicine granules

The development of TCM granules can be traced back to the mid-20th century. Early preparation methods were relatively simple due to technological limitations, often involving the direct granulation of crushed TCM decoction pieces. This approach resulted in incomplete extraction of active ingredients and inconsistent granule quality ^[2]. With rapid advancements in science and technology, modern pharmaceutical techniques began to be applied to TCM granules in the 1970s. For example, in extraction technology, supercritical fluid extraction was introduced to extract active components, such as tanshinones from *Salvia miltiorrhiza* and ligustilide and total lactones from *Ligusticum chuanxiong*, which demonstrated enhanced efficacy in preventing cardiovascular and cerebrovascular diseases ^[3].

Drying technologies, such as spray drying and vacuum freeze-drying, have significantly improved the granules' formability and stability ^[4]. Granulation techniques have also evolved, with innovations such as fluidized bed granulation and dry granulation enabling more efficient and precise production processes. Entering the 21st century, advanced quality control methods, including TCM fingerprint technology and multi-component quantitative analysis, have been widely applied in the field of TCM granules. These methods effectively ensure product consistency and controllability ^[5].

3. Advantages of traditional Chinese medicine granules

3.1. Convenience in consumption

The preparation of traditional decoctions is laborious, requiring patients to spend significant time and effort in boiling herbs, with conditions such as heat, time, and water volume being difficult to control precisely, often leading to variations in efficacy. In contrast, TCM granules can be dissolved and consumed instantly, thanks to modern packaging technologies such as individual sachets or bottled designs. Patients only need to pour the granules into a cup and add a suitable amount of hot or warm water, and the medicine dissolves quickly, eliminating the need for the complicated decoction process and saving both time and effort. For example, in a study by Xu ^[6], patients using TCM granules found them more convenient to take compared to decoctions.

Additionally, during production, TCM granules benefit from precise weighing systems and automated packaging equipment, ensuring accurate dosing in each sachet or granule. This eliminates concerns of under-dosage or over-dosage during use, a problem often associated with pills or powders, especially for children and the elderly. The application of modern packaging technologies enables clear, pre-measured doses, which can be tailored to individual patient needs without worry of incorrect dosage ^[7].

Furthermore, pills are often hard-textured and difficult for some patients to swallow, while powders may have an unpleasant taste and can cause choking. TCM granules dissolve well and typically include flavor enhancers or sweeteners, improving patient compliance and therapeutic outcomes ^[8].

3.2. Quality stability

TCM granules ensure strict control over raw material quality. During procurement, factors such as the origin and harvest season are prioritized, with high-quality, authentic medicinal materials being preferred to ensure stable active ingredient content. For instance, Sanqi from Wenshan, Yunnan, and Zhe Beimu from Pan'an, Zhejiang, are widely used in granule production. Moreover, the preparation of raw herbs follows standardized management practices, combining traditional processing techniques with modern quality standards to reduce toxicity and

enhance pharmacological stability^[9].

During production, modern equipment and automated production lines enable precise control over every stage of the process. For example, in the extraction process, computer-controlled systems accurately regulate parameters such as temperature, pressure, and time to ensure efficient extraction without damaging active ingredients. In the case of Huangqin granules, optimal extraction conditions involve two water extractions: the first with 13 times the water volume, boiled for 1 hour, and the second with 11 times the water volume, also boiled for 1 hour^[10].

Production environments and process quality control strictly adhere to Good Manufacturing Practices (GMP) standards, effectively preventing microbial and cross-contamination. Advanced equipment such as vacuum concentrators and spray dryers efficiently extract and concentrate active components into granule form, minimizing losses during processing and ensuring the stability and consistency of active ingredients^[11]. Additionally, modern detection equipment, such as microbial limit detectors and heavy metal analyzers, performs comprehensive quality testing on finished products, further ensuring the stability and safety of TCM granules.

3.3. Pharmacodynamic advantages

Modern TCM granule preparation technologies efficiently extract and retain active ingredients from herbs. For example, Wang *et al.*^[12] found that ultrasound-assisted extraction of puerarin from *Pueraria lobata* achieved a 95.85% extraction rate, significantly higher than the 86.2% rate from ethanol reflux methods. For heat-sensitive or volatile components, such as menthol in Mint or volatile oils in Schizonepeta, low-temperature extraction, freeze-drying, or encapsulation technologies effectively prevent their loss during preparation.

TCM granules can be designed to exhibit different drug release characteristics according to therapeutic needs. Immediate-release granules disintegrate and release drugs rapidly, enabling quick therapeutic effects. For example, Su Xiao Jiu Xin Wan granules, used to treat acute angina pectoris, dissolve and absorb quickly when taken sublingually, alleviating symptoms within 1–2 minutes^[13].

Sustained-release granules, on the other hand, use specialized formulation techniques such as slow-release matrix materials or coating technologies to release drugs gradually and continuously within the body. This maintains stable blood drug concentrations, reduces dosing frequency, and improves patient adherence^[14].

4. Application prospects of traditional Chinese medicine granules

4.1. Application in clinical TCM treatment

In cardiovascular medicine, Astragalus granules improve cardiac function through multi-target mechanisms, enhancing myocardial contractility, dilating blood vessels, and reducing cardiac load, showing significant efficacy in chronic heart failure. In the study by Yang *et al.*^[15], patients with chronic heart failure who consumed Astragalus granules demonstrated better improvement in heart function classification compared to those using Western medicine. In respiratory medicine, Lianhua Qingwen granules have strong inhibitory effects on the influenza virus, effectively alleviating flu symptoms such as fever, cough, and fatigue, while maintaining good safety^[16]. In gastroenterology, the TCM granule Chaihu Shugan San provides mild and sustained therapeutic effects, gradually improving gastric symptoms in patients. For chronic gastritis, consuming Chaihu Shugan San can not only relieve discomforts such as stomach pain and bloating but also regulate emotions and prevent exacerbation caused by emotional distress. He^[17] suggested in his research that compared to the Western drug lansoprazole, Chaihu Shugan San has favorable clinical effects in treating chronic gastritis.

In surgery, the application of TCM granules is particularly noteworthy. For example, in fracture treatment, granules such as Jiegu Xujin granules promote blood circulation, reduce swelling and pain, accelerate fracture healing, and shorten recovery time ^[18]. In gynecology, Wuji Baifeng granules help regulate female endocrine functions, improving symptoms like menstrual irregularities, dysmenorrhea, and amenorrhea. Clinical practice has shown that Wuji Baifeng granules also assist in regulating menstrual cycles and ovulation functions in patients with polycystic ovary syndrome, improving pregnancy rates ^[19]. In pediatrics, considering the immature liver and kidney functions of children, TCM granules like Xiao'er Ganmao granules and Xiao'er Zhike granules offer high safety and confirmed efficacy. These granules, through proper formulation and dosage control, effectively alleviate symptoms, shorten recovery time, and provide safe and effective treatment for children.

4.2. Application in preventive healthcare

With the accelerating pace of modern life and heightened health awareness, people are increasingly focusing on wellness and prevention, seeking scientific methods to prevent diseases and enhance physical fitness. In this context, TCM granules have demonstrated their advantages. For instance, for common sub-health conditions such as fatigue, insomnia, and low immunity, TCM granules like Ginseng granules and Astragalus granules exhibit remarkable effects in boosting energy, nourishing blood, calming the mind, and enhancing immunity. These granules are convenient to carry and consume, have good taste, and exhibit minimal side effects, making them ideal for long-term use as part of modern health maintenance routines ^[20]. For the elderly, granules such as Liuwei Dihuang granules and Goji berry granules, which replenish kidney essence and delay aging, can improve physical fitness and enhance the quality of life ^[21]. For women, granules like Rose granules and Angelica granules, which promote beauty and regulate endocrine functions, can help maintain a youthful appearance and alleviate menopausal symptoms.

In today's society, with the increasing pace of life and worsening environmental pollution, the incidence of various diseases continues to rise, prompting greater attention to disease prevention. TCM granules, as a convenient, efficient, and widely accepted form of TCM, exhibit great potential in disease prevention. For instance, in preventing respiratory infections like influenza, granules such as Banlangen granules and Honeysuckle granules possess significant heat-clearing, detoxifying, and antiviral properties, making them suitable for daily preventive use during flu seasons. Long-term consumption can enhance immunity and reduce the risk of influenza virus infections ^[22].

5. Conclusion

As a significant outcome of TCM formulation reform, TCM granules have continuously integrated modern technology throughout their development, showcasing numerous advantages. Their convenience, quality stability, and pharmacodynamic benefits offer broad application prospects in both clinical TCM treatment and preventive healthcare. With further research and technological advancements, TCM granules are expected to play a greater role in more fields, advancing the modernization and internationalization of TCM. However, challenges remain, such as standardizing the quality of compound TCM granules and evaluating the safety of their combined use with Western medicines. These issues require further in-depth research and exploration by medical and pharmaceutical researchers to fully realize the potential of TCM granules and contribute more significantly to global health.

Disclosure statement

The author declares no conflict of interest.

References

- [1] Zhang X, 2021, Analysis of the Advantages and Problems of Traditional Chinese Medicine Formula Granules in Modern Pharmacy Management. *Xinjiang J Tradit Chin Med*, 39(4): 81–83.
- [2] Sun W, He G, Ye Z, 2001, Development and Improvement of Preparation Technology of Chinese Medicine Granules. *Res Inf Tradit Chin Med*, 2001(10): 21–23.
- [3] Yang H, 2019, A Granule Preparation for Preventing Cardiovascular and Cerebrovascular Diseases: CN201910927804.9.
- [4] Jia S, 2022, Application of Spray Granulation Technology in the Production of Traditional Chinese Medicine Granules. *Kang Yi*, 2022(1): 254–256.
- [5] Xiao J, 2015, Application of HHLSE Integrated Technical Equipment in the Secondary Development of Xia Sang Ju Compound, dissertation, Guangdong Pharmaceutical University.
- [6] Xu Y, 2015, Comparative Analysis of Traditional Chinese Medicine Decoctions and Granules. *Clin Med Lit Electr J*, 2015(1): 87–88.
- [7] Wang Y, Li L, 2016, Clinical Efficacy and Safety Comparison of Traditional Chinese Medicine Decoctions and Granules in Treating Various Types of Colds. *Mod J Integr Tradit Chin West Med*, 25(29): 3254–3256.
- [8] Du Y, Sun C, 2011, Analysis of the Advantages, Shortcomings, and Prospects of Traditional Chinese Medicine Formula Granules. *Chin Ethn Folk Med*, 20(5): 19–20.
- [9] Chen J, Liu Y, Jiang Y, et al., 2011, Experiences in the Application of Traditional Chinese Medicine Formula Granules. *Asia Pac Tradit Med*, 7(12): 186–188.
- [10] Xu Y, Xu H, Li S, 2000, Optimization of the Extraction Process of *Scutellaria baicalensis* Concentrated Granules. *J Shizhen Med Mater Medica Res*, 11(12): 1090–1091.
- [11] Yang R, Zhao L, Huang Y, et al., 2021, Exploratory Study on High Drug-Loading Granules Using Raw Chinese Medicine Powders as Carriers. *Chin J Chin Mater Med*, 46(13): 3356–3363.
- [12] Wang Z, Hu X, Chen X, 2016, Extraction of Puerarin Using Ultrasound-Assisted Method and Ethanol Reflux Method. *Food Res Dev*, 37(9): 47–51.
- [13] Zhang X, Xiao W, 2021, Pharmacoeconomic Evaluation of Su Xiao Jiu Xin Wan in Treating Stable Angina Pectoris. *Chin J Pharmacoecon*, 16(7): 44–49 + 56.
- [14] Ding X, Fan C, Xu J, et al., 2023, Effect of Self-Designed Traditional Chinese Medicine Enema Formula Combined with Sustained-Release Mesalazine Granules on Ulcerative Proctitis and TCM Syndrome Scores. *J North Sichuan Med Coll*, 38(4): 530–533.
- [15] Yang Q, Lu S, Sun H, 2010, Effect of Astragalus on Cardiac Function and Serum Tumor Necrosis Factor Levels in Patients with Chronic Heart Failure. *Chin J Integr Tradit West Med*, 30(7): 699–701.
- [16] Chen L, Wang Y, Huang H, 2017, Clinical Observation of Lianhua Qingwen Capsules Against Influenza Virus. *Gansu Med J*, 36(8): 666–667.
- [17] He Y, 2018, Modified Chaihu Shugan Powder (Granules) for Chronic Gastritis Treatment. *Chin Health Nutr*, 28(25): 316–317.
- [18] Zhu X, Zhou S, Feng W, et al., 2019, Effects of Xujin Jiegu Granules Combined with Surgery on Clinical Outcomes and Fracture Healing in Elderly Patients with Lower Limb Fractures. *Special Health*, 2019(25): 135–136.

- [19] Lin Q, 2023, Clinical Value of Wujibai Fengwan Combined with Metformin in Treating Polycystic Ovary Syndrome. *Matern Child Nurs*, 3(21): 5281–5283.
- [20] Li S, 2023, Study on Preparation Process of Astragalus and Goji Berry Health Granules. *J Weifang Eng Vocat Coll*, 36(5): 95–100.
- [21] Zhang M, Liu F, Chen Y, 2023, Clinical Observation of Liuwei Dihuang Pills in Treating Insomnia with Yin Deficiency and Fire Excess Syndrome in Elderly Patients. *Guangxi J Tradit Chin Med*, 46(6): 13–15.
- [22] Tian H, 2019, Banlangen Granules: Prevention and Treatment of Wind-Heat Colds. *Family Tradit Chin Med*, 26(11): 71.

Publisher's note

Bio-Byword Scientific Publishing remains neutral with regard to jurisdictional claims in published maps and institutional affiliations.

Effectiveness of High-Frequency Electrosurgical Knife Surgery Under Painless Digestive Endoscopy in Elderly Patients with Gastrointestinal Polyps

Yumin Lu*

Meili People's Hospital, Changshu 215511, Jiangsu Province, China

*Corresponding author: Yumin Lu, benben812@163.com

Copyright: © 2025 Author(s). This is an open-access article distributed under the terms of the Creative Commons Attribution License (CC BY 4.0), permitting distribution and reproduction in any medium, provided the original work is cited.

Abstract: *Objective:* To analyze the therapeutic effect of high-frequency electrosurgical knife surgery guided by painless digestive endoscopy (PDE) in elderly patients with gastrointestinal polyps (GP). *Methods:* A total of 100 elderly GP patients admitted between June 2021 and December 2022 were selected. Patients were randomly divided into two groups: the painless group (50 cases) underwent high-frequency electrosurgical knife surgery guided by PDE, while the conventional group (50 cases) underwent the same surgery guided by traditional digestive endoscopy (DE). The total treatment efficacy, perioperative indicators, gastrointestinal hormone levels, oxidative stress (OS) markers, and complication rates were compared between the two groups. *Results:* The total treatment efficacy in the painless group was higher than that in the conventional group, and perioperative indicators were superior in the painless group ($P < 0.05$). One week after treatment, the gastrointestinal hormone levels and OS-related markers in the painless group were better than those in the conventional group ($P < 0.05$). The complication rate in the painless group was lower than in the conventional group ($P < 0.05$). *Conclusion:* High-frequency electrosurgical knife surgery guided by PDE improves the effectiveness of polyp removal in elderly GP patients and accelerates postoperative recovery. It also protects gastrointestinal function, reduces postoperative OS, and ensures higher surgical safety.

Keywords: Painless digestive endoscopy; High-frequency electrosurgical knife surgery; Elderly gastrointestinal polyps

Online publication: February 13, 2025

1. Introduction

Gastrointestinal polyps (GP) are benign tumors located on the mucosa of the digestive tract, characterized by epithelial tissue protrusions. GP has a high incidence rate and, if left untreated, can progress and increase the risk of malignancy, affecting prognosis. Currently, digestive endoscopy (DE) is the standard diagnostic and therapeutic technology for GP, allowing precise control of the observation range, clear visualization of polyp status, and guidance for removal procedures^[1,2]. High-frequency electrosurgical knife surgery guided by DE utilizes high-

frequency currents and voltage to precisely separate tissues and completely excise polyps. This approach is simple, minimally invasive, and effective. However, traditional endoscopy often causes significant discomfort during insertion, such as nausea or palpitations, reducing patient cooperation. In contrast, PDE can alleviate the discomfort of endoscope insertion with the use of analgesics, thus improving surgical efficiency ^[3]. This study evaluated the efficacy of high-frequency electrosurgical knife surgery guided by PDE in 100 elderly GP patients.

2. Materials and methods

2.1. General information

A total of 100 elderly patients with GP treated in the hospital from June 2021 to December 2022 were included. The patients were randomly divided into two groups using a random number table:

- (1) Painless group: 50 cases, including 27 males and 23 females; ages ranged from 62 to 88 years, with a mean of (71.26 ± 3.12) years; polyp diameters ranged from 1.1 to 3.6 cm, with a mean of (1.95 ± 0.43) cm; 19 cases had multiple polyps, and 31 cases had single polyps.
- (2) Conventional group: 50 cases, including 29 males and 21 females; ages ranged from 63 to 89 years, with a mean of (71.37 ± 3.20) years; polyp diameters ranged from 1.2 to 3.8 cm, with a mean of (1.97 ± 0.59) cm; 20 cases had multiple polyps, and 30 cases had single polyps.

There was no significant difference in baseline data between the two groups ($P > 0.05$).

Inclusion criteria: Diagnosis of GP confirmed by gastroscopic pathology; age > 60 years; clear consciousness; complete clinical data; informed consent to participate.

Exclusion criteria: Presence of gastric perforation; primary diseases such as gastroesophageal bleeding; malignancies; history of open abdominal surgery; withdrawal during the study.

2.2. Methods

Before surgery, routine examinations of cardiac and liver functions were performed. Patients fasted for 8 hours and consumed compound polyethylene glycol electrolyte powder (137.15 g), dissolved in 2 L of warm water, and taken in divided doses.

2.2.1. Painless group

High-frequency electrosurgical knife surgery was performed under painless digestive endoscopy (PDE) guidance. Patients were positioned in the lateral decubitus position. Propofol emulsion injection ($1.0 \mu\text{g/kg}$) was administered intravenously 5 minutes before surgery. Fentanyl citrate injection ($0.5 \mu\text{g/kg}$) was also administered intravenously. After anesthesia onset (disappearance of eyelash reflex), the digestive endoscope (DE) was slowly inserted to observe the location, number, and morphology of the polyps. Surrounding fluids were suctioned to ensure a clear surgical field. The high-frequency electrosurgical knife was set at a coagulation power of 40 W, a current index of 4.0, and a power-on duration of 2 seconds per application. Polyps were lifted completely using non-damaging forceps and excised using the electrosurgical knife for coagulation and cutting.

2.2.2. Conventional group

High-frequency electrosurgical knife surgery was performed under traditional DE guidance. No anesthesia was administered before surgery. The digestive endoscope was slowly inserted to observe the polyps, followed by

coagulation and excision using the high-frequency electrosurgical knife. The procedure followed the same steps as in the painless group.

2.3. Observation indicators

- (1) Perioperative indicators: Observations included intraoperative blood loss, surgery duration, postoperative pain at 2 hours (measured using a visual analog scale, with scores ranging from 0 to 10, where higher scores indicate greater pain), postoperative exhaust time, and length of hospital stay.
- (2) Gastrointestinal hormones: Four milliliters of fasting venous blood was drawn, centrifuged for 12 minutes at 4,000 r/min to extract serum, and used to measure vasoactive intestinal peptide (VIP), gastrin (GAS), and motilin (MOT) levels using radioimmunoassay.
- (3) Oxidative stress (OS) markers: Fasting venous blood was processed similarly to measure 5-hydroxytryptamine (5-HT) and malondialdehyde (MDA) using enzyme-linked immunosorbent assay (ELISA). Glutathione peroxidase (GSH-Px) and total antioxidant capacity (T-AOC) were measured using a chemical colorimetry method.
- (4) Complication rate: Observed complications included gastrointestinal bloating, wound infection, gastric perforation, and gastric bleeding.

2.4. Efficacy evaluation criteria

- (1) Significant effect: Complete removal of polyps in one session with total symptom resolution.
- (2) Effective: Residual polyps with significant symptom alleviation.
- (3) Ineffective: Large residual polyps with no symptom relief.

2.5. Statistical analysis

Data were analyzed using SPSS 28.0. Measurement data were expressed as mean \pm standard deviation (SD) and compared using the *t*-test. Count data were expressed as [*n* (%)] and compared using the χ^2 test. Statistical significance was set at $P < 0.05$.

3. Results

3.1. Comparison of overall treatment effectiveness between groups

Table 1 shows that the overall treatment effectiveness rate in the painless group was significantly higher than that in the conventional group ($P < 0.05$).

Table 1. Comparison of overall treatment effectiveness between groups [*n* (%)]

Group	<i>n</i>	Significant effect	Effective	Ineffective	Total effectiveness
Painless	50	26 (52.0)	22 (44.0)	2 (4.0)	48 (96.0)
Conventional	50	21 (42.0)	20 (40.0)	9 (18.0)	41 (82.0)
χ^2	-	-	-	-	5.005
<i>P</i>	-	-	-	-	0.025

3.2. Comparison of perioperative indicators between groups

Table 2 shows that the perioperative indicators in the painless group were significantly better than those in the conventional group ($P < 0.05$).

Table 2. Comparison of perioperative indicators between groups (mean \pm SD)

Group	<i>n</i>	Blood loss (mL)	Surgery time (min)	Postoperative pain at 2 h (score)	Postoperative exhaust time (h)	Hospital stay (days)
Painless	50	15.62 \pm 2.34	27.11 \pm 4.03	1.85 \pm 0.56	24.10 \pm 3.56	6.61 \pm 1.58
Conventional	50	21.27 \pm 3.41	36.91 \pm 4.37	3.01 \pm 0.79	33.15 \pm 3.97	8.40 \pm 1.79
<i>t</i>	-	9.660	11.657	8.471	12.001	5.301
<i>P</i>	-	0.000	0.000	0.000	0.000	0.000

3.3. Comparison of gastrointestinal hormones between groups

Before treatment, there were no significant differences in gastrointestinal hormone levels between the groups ($P > 0.05$). After one week of treatment, the gastrointestinal hormone levels in the painless group were significantly better than those in the conventional group ($P < 0.05$), as shown in **Table 3**.

Table 3. Comparison of gastrointestinal hormones between groups before and after treatment (mean \pm SD, pg/mL)

Group	<i>n</i>	VIP		GAS		MOT	
		Before	After	Before	After	Before	After
Painless	50	36.15 \pm 4.19	40.15 \pm 5.98	150.36 \pm 18.74	130.52 \pm 15.39	262.64 \pm 19.85	240.56 \pm 18.02
Conventional	50	36.09 \pm 4.22	45.91 \pm 5.77	151.32 \pm 17.53	115.92 \pm 14.70	263.05 \pm 18.78	214.66 \pm 17.90
<i>t</i>	-	0.071	4.901	0.265	4.851	0.106	7.210
<i>P</i>	-	0.943	0.000	0.792	0.000	0.916	0.000

3.4. Comparison of oxidative stress markers between groups

Before treatment, there were no significant differences in OS markers between the groups ($P > 0.05$). After one week of treatment, the OS markers in the painless group were significantly better than those in the conventional group ($P < 0.05$), as shown in **Table 4**.

Table 4. Comparison of OS markers between groups before and after treatment (mean \pm SD)

Group	<i>n</i>	5-HT (ng/mL)		MDA (mmol/L)		GSH-Px (U/mL)		T-AOC (U/mL)	
		Before	After	Before	After	Before	After	Before	After
Painless	50	250.65 \pm 20.41	375.02 \pm 34.11	4.46 \pm 0.39	5.01 \pm 0.58	1,925.84 \pm 97.63	1,768.32 \pm 80.57	5.25 \pm 0.64	3.75 \pm 0.40
Conventional	50	250.31 \pm 21.47	470.12 \pm 39.52	4.48 \pm 0.40	6.42 \pm 0.63	1,924.33 \pm 98.06	1,620.53 \pm 77.32	5.28 \pm 0.69	2.89 \pm 0.37
<i>t</i>	-	0.081	12.881	0.253	11.643	0.077	9.358	0.225	11.160
<i>P</i>	-	0.935	0.000	0.801	0.000	0.939	0.000	0.822	0.000

3.5. Comparison of complication rates between groups

Table 5 shows the complication rate in the painless group was significantly lower than that in the conventional group ($P < 0.05$).

Table 5. Comparison of complication rates between groups [n (%)]

<i>Group</i>	<i>n</i>	Gastrointestinal bloating	Wound infection	Gastric perforation	Gastric bleeding	Total complications
Painless	50	1 (2.0)	0	0	0	1 (2.0)
Conventional	50	4 (8.0)	1 (2.0)	1 (2.0)	1 (2.0)	7 (14.0)
χ^2	-	-	-	-	-	4.891
<i>P</i>	-	-	-	-	-	0.027

4. Discussion

The development process of GP involves poor dietary habits and weakened gastrointestinal function, leading to inflammatory responses in the gastric mucosa. This results in the mucosal epithelium protruding and forming polyps^[4]. Elderly individuals have a higher likelihood of developing this condition due to their declining physical functions, prolonged dietary irregularities, preference for high-salt foods, and frequent constipation. These factors contribute to intestinal mucosal lesions, thereby triggering GP. Traditional diagnostic endoscopy (DE) can comprehensively diagnose GP and guide polyp removal. However, elderly patients remain conscious during the procedure, leading to significant stress reactions such as emotional tension, increased heart rate, and elevated blood pressure, which can hinder the smooth execution of the procedure^[5,6]. Additionally, in a conscious state, elderly patients experience faster gastrointestinal motility, delaying wound healing and prolonging postoperative recovery.

In contrast, PDE offers advantages such as ease of operation, rapid cutting, and efficient hemostasis. PDE allows patients to undergo endoscopy in a state resembling natural sleep, improving their tolerance to the endoscopic process and polyp removal. It also slows gastrointestinal motility and efficiently detects and removes small polyps^[7].

The results of this study indicate that the painless group had a higher overall treatment effectiveness rate and significantly better perioperative indicators compared to the conventional group ($P < 0.05$). The underlying reasons include the following: Local anesthesia administered 5 minutes before the procedure for elderly patients provided both analgesic and sedative effects, alleviating preoperative anxiety. This improved patient compliance and ensured the smooth and effective execution of the procedure, enhancing the reliability and safety of the surgery^[8]. PDE prevents reactions like tremors during the procedure, avoiding damage to healthy tissues and minimizing intraoperative blood loss. Additionally, PDE eliminates the risk factors associated with electrosurgical polypectomy and shortens the duration of the surgery. Consequently, the surgical outcomes are favorable, and postoperative recovery is quicker. Furthermore, anesthetic drugs reduce postoperative pain perception and provide prolonged analgesic effects, resulting in milder postoperative pain^[9].

VIP is produced by intestinal neurons and has dual biological effects. GAS, found in the duodenum and stomach and produced by pancreatic D cells, promotes gastrointestinal motility and enhances gastric contractions. MOT, located in the small intestine, stimulates phase III muscle contractions and accelerates gastric emptying. In this study, the gastrointestinal hormone levels in the painless group were more stable one week after treatment

compared to before treatment and showed less fluctuation^[10]. PDE alleviates pain and psychological distress, enabling patients to undergo endoscopy in a painless state, reducing excessive gastrointestinal motility, and stabilizing gastrointestinal hormone secretion.

Serotonin and MDA are common OS markers used to assess stress levels and evaluate surgical stability. In this study, the OS-related indicators in the painless group were significantly better one week after treatment compared to the conventional group ($P < 0.05$). This is attributed to the use of anesthetic agents like propofol in PDE, which act quickly to provide stable sedative and analgesic effects, stabilize hemodynamics, and reduce stress responses^[11]. Furthermore, the complication rate in the painless group was lower than in the conventional group ($P < 0.05$). PDE reduces the invasiveness of high-frequency electrosurgical procedures, improves resection precision, and prevents unnecessary damage, enhancing safety^[12]. The side effects of anesthetic drugs are minimal, primarily targeting the central nervous system, and they rarely cause residual drug accumulation, demonstrating higher anesthesia reliability.

5. Conclusion

In conclusion, high-frequency electrosurgical procedures guided by PDE demonstrate high success rates and facilitate postoperative recovery in elderly GP patients. This approach protects gastrointestinal function, reduces perioperative stress responses, and ensures high surgical safety, making it the preferred treatment option for elderly GP patients.

Disclosure statement

The author declares no conflict of interest.

References

- [1] Shang Z, 2023, Effect of Painless High-Frequency Electrosurgical Procedures Under Digestive Endoscopy on Elderly Patients with Gastrointestinal Polyps. *Chin J Med Health*, 35(3): 41–44.
- [2] Xu J, 2021, Effect of Painless High-Frequency Electrosurgical Procedures Under Digestive Endoscopy on Elderly Gastrointestinal Polyps and Oxidative Stress. *Huaxia Med J*, 34(5): 48–51.
- [3] Song Y, An M, Qin Y, et al., 2022, Impact of Painless High-Frequency Electrosurgical Procedures Under Digestive Endoscopy on Complications and Postoperative Recovery in Gastrointestinal Polyp Patients. *Mod Dig Interv Ther*, 27(5): 603–605.
- [4] Shao X, Yu S, Chen R, 2022, Clinical Effect and Complication Analysis of Painless High-Frequency Electrosurgical Procedures Under Digestive Endoscopy for Gastrointestinal Polyps. *Life Sci Instrum*, 20(Suppl 1): 3.
- [5] Shen L, 2020, Clinical Analysis of Painless High-Frequency Electrosurgical Polypectomy Under Digestive Endoscopy for Gastrointestinal Polyps. *J Hunan Norm Univ Med Sci*, 17(3): 114–117.
- [6] Yan X, Wu X, 2024, Clinical Effects of Painless High-Frequency Electrosurgical Procedures Under Digestive Endoscopy for Gastrointestinal Polyps. *Chin Med Equip Info*, 30(3): 125–127.
- [7] Lu M, 2020, Discussion on the Effect of Painless High-Frequency Electrosurgical Procedures Under Digestive Endoscopy for Gastrointestinal Polyps. *Chin Med Equip Info*, 26(15): 98–99.
- [8] Gu J, Li X, 2020, Analysis of the Short-Term Efficacy and Complications of High-Frequency Electrosurgical Snare

Resection of Larger Gastrointestinal Polyps Under Gastrointestinal Endoscopy. *Mod Dig Interv Ther*, 25(11): 1519–1521.

- [9] Wen J, Nie Y, Li C, et al., 2024, Effect of Painless High-Frequency Electrosurgical Procedures Under Digestive Endoscopy on Gastrointestinal Polyps and Factors Influencing Postoperative Recurrence. *Mod Dig Interv Ther*, 29(1): 21–24 + 30.
- [10] Lin H, 2024, Application Effect of Painless High-Frequency Electrosurgical Procedures Under Digestive Endoscopy for Gastrointestinal Polyps. *Fujian Med J*, 46(4): 77–80.
- [11] Guo M, Wang J, 2024, Clinical Effect Study of Painless High-Frequency Electrosurgical Procedures Under Digestive Endoscopy for Gastrointestinal Polyps. *Zhejiang J Trauma Surg*, 29(7): 1270–1272.
- [12] Yang S, Xiang Z, Chen X, et al., 2021, Effectiveness of EMR Under Endoscopy for Gastrointestinal Polyps and Changes in Gastrointestinal Hormone Levels. *China Med Herald*, 18(14): 111–114.

Publisher's note

Bio-Byword Scientific Publishing remains neutral with regard to jurisdictional claims in published maps and institutional affiliations.

Effectiveness of Multi-Modal Teaching Based on Online Case Libraries in the Education of Gene Methylation Combined with Spiral CT Screening for Pulmonary Ground-Glass Opacity Nodules

Yong Zhou¹, Xi Zhang¹, Shuyi Liu¹, Zhuoyi He¹, Weili Tian¹, Shuping You^{2*}

¹Third Clinical Medical College of Xinjiang Medical University (Affiliated Cancer Hospital), Urumqi 830011, Xinjiang Province, China

²Department of Basic Nursing, School of Nursing, Xinjiang Medical University, Urumqi 830000, Xinjiang Province, China

*Corresponding author: Shuping You, youshupin@163.com

Copyright: © 2025 Author(s). This is an open-access article distributed under the terms of the Creative Commons Attribution License (CC BY 4.0), permitting distribution and reproduction in any medium, provided the original work is cited.

Abstract: *Objective:* To explore the effectiveness of multi-modal teaching based on an online case library in the education of gene methylation combined with spiral computed tomography (CT) screening for pulmonary ground-glass opacity (GGO) nodules. *Methods:* From October 2023 to April 2024, 66 medical imaging students were selected and randomly divided into a control group and an observation group, each with 33 students. The control group received traditional lecture-based teaching, while the observation group was taught using a multi-modal teaching approach based on an online case library. Performance on assessments and teaching quality were analyzed between the two groups. *Results:* The observation group achieved higher scores in theoretical and practical knowledge compared to the control group ($P < 0.05$). Additionally, the teaching quality scores were significantly higher in the observation group ($P < 0.05$). *Conclusion:* Implementing multi-modal teaching based on an online case library for pulmonary GGO nodule screening with gene methylation combined with spiral CT can enhance students' knowledge acquisition, improve teaching quality, and have significant clinical application value.

Keywords: Multi-modal teaching based on online case library; Pulmonary nodules; Gene methylation; Computed tomography

Online publication: February 13, 2025

1. Introduction

Pulmonary nodules are an early clinical manifestation of lung cancer, with ground-glass opacity (GGO) nodules being a specific radiological feature of early-stage lung cancer. Clinical diagnosis primarily relies on pathological

biopsy via puncture, but small pulmonary nodule diagnoses are often affected by various factors ^[1]. Studies have shown that combining spiral computed tomography (CT) with gene methylation for the diagnosis of early pulmonary GGO nodules achieves the expected diagnostic value and has a high positive detection rate for small nodules, making it a feasible and commonly used diagnostic approach in radiology. This approach also places high demands on the operational skills of diagnostic physicians ^[2].

Undergraduate medical education includes medical imaging courses to enhance diagnostic quality. However, existing teaching methods lack diverse and innovative elements, making it difficult to effectively improve students' diagnostic skills. Multi-modal teaching using an online case library emphasizes the importance of case-based learning. This approach integrates diverse teaching methods around typical cases, offering strong comprehensiveness ^[3].

This study examines the teaching outcomes of multi-modal teaching based on an online case library in the context of gene methylation combined with spiral CT screening for pulmonary GGO nodules. A total of 66 medical imaging students from October 2023 to April 2024 were included in this research.

2. Materials and methods

2.1. General information

From October 2023 to April 2024, 66 medical imaging students were selected as study subjects and randomly divided into two groups of 33 each using a random number table method.

Control group: Average age ranged from 18 to 22 years (20.15 ± 0.66 years). Educational background: 16 students had a college diploma or below, while 17 were undergraduates or above.

Observation group: Average age ranged from 18 to 22 years (20.39 ± 0.59 years). Educational background: 16 students had a college diploma or below, while 17 were undergraduates or above.

There were no statistically significant differences in baseline characteristics between the two groups ($P > 0.05$).

2.2. Methods

Control group: The traditional lecture-based teaching approach was employed. The teaching content was aligned with the syllabus and focused on theoretical knowledge, including the definition, classification, imaging characteristics, anatomical and radiological signs, diagnosis, and differential diagnosis of pulmonary ground-glass opacity (GGO) nodules. The sessions predominantly utilized slide presentations. During the teaching sessions, imaging materials of pulmonary GGOs were intermittently introduced to guide students in writing reports. The final 10 minutes of each session were dedicated to discussing and analyzing challenging cases with the students.

Observation group: A multi-modal teaching method based on an online case library was adopted, incorporating the following approaches:

- (1) Online case library development: An online teaching case library was constructed using an electronic medical record system and PACS platform. This library included knowledge about pulmonary GGO nodules, gene methylation, and spiral CT detection. Thirty typical cases were collected from the hospital, covering conditions such as tumors, pneumonia, congenital diseases, and pulmonary connective tissue diseases. For each type, clinical data from five patients (medical history, specialized examinations, imaging findings, pathological results, etc.) were compiled. A web-based teaching material system was established for students to access and review online.

- (2) Case-based learning (CBL): Before teaching, three representative cases were selected from the online teaching case library. During the session, students were guided to search the case library, analyze cases in detail, and answer questions based on the syllabus. Students were encouraged to provide feedback on cases, which was evaluated by the instructor. At the end of the session, new questions were posed to stimulate further learning. Students were also instructed to use online tools for review and problem-solving, with unresolved queries addressed in the following class.
- (3) AI-assisted teaching: AI software systems were used to analyze cases from the online library. The system facilitated an in-depth study of the imaging characteristics of pulmonary GGO nodules, such as location, size, and density, including features like vacuole signs, air bronchogram signs, and vascular convergence signs. Teachers summarized and explained the AI-assisted analysis, helping students address questions related to the interpretation of pulmonary GGO imaging.

2.3. Observation indicators

- (1) A custom-designed assessment questionnaire was used to evaluate students. It included theoretical knowledge (objective and subjective questions) and practical knowledge. The total score was 100, with scores directly proportional to assessment outcomes.
- (2) A post-teaching survey assessed teaching quality using a self-designed questionnaire. This included dimensions such as learning enthusiasm, independent problem-solving abilities, foundational imaging knowledge, clinical diagnostic thinking, report writing skills, and teamwork/interactive communication. Each dimension was scored out of 100, with higher scores indicating better teaching quality.

2.4. Statistical methods

Statistical analysis was performed using SPSS 25.0. Measurement data were expressed as mean \pm standard deviation (SD) and analyzed using t-tests. Count data were expressed as [n (%)] and analyzed using the chi-squared (χ^2) test. Differences were considered statistically significant when $P < 0.05$.

3. Results

3.1. Comparison of assessment results between the two groups

The scores for theoretical and practical knowledge in the observation group were significantly higher than those in the control group ($P < 0.05$), as shown in **Table 1**.

Table 1. Comparison of assessment results between the two groups (mean \pm SD, points)

Group	<i>n</i>	Theoretical knowledge	Practical knowledge
Control group	33	80.23 \pm 4.45	81.61 \pm 4.02
Observation group	33	85.56 \pm 4.37	91.11 \pm 3.39
<i>t</i>		4.909	10.378
<i>P</i>		< 0.001	< 0.001

3.2. Comparison of teaching quality between the two groups

The observation group showed significantly higher teaching quality scores across all dimensions compared to the

control group ($P < 0.05$), as shown in **Table 2**.

Table 2. Comparison of teaching quality between the two groups (mean \pm SD, scores)

Group	<i>n</i>	Learning enthusiasm	Independent problem-solving	Foundational imaging knowledge	Clinical diagnostic thinking	Report writing skills	Teamwork & interaction
Control group	33	75.28 \pm 3.27	78.76 \pm 5.51	81.22 \pm 5.46	83.31 \pm 4.41	85.84 \pm 3.33	84.43 \pm 4.40
Observation group	33	80.16 \pm 3.38	84.47 \pm 5.36	88.75 \pm 4.49	91.18 \pm 3.62	92.64 \pm 3.59	95.56 \pm 2.79
<i>t</i>		5.961	4.267	6.119	7.924	7.978	12.272
<i>P</i>		< 0.001	< 0.001	< 0.001	< 0.001	< 0.001	< 0.001

4. Discussion

Gene methylation combined with spiral CT screening of pulmonary ground-glass nodules is a critical diagnostic procedure in radiology. The accuracy of diagnostic results is closely linked to the operator's experience and technical skills, necessitating educational models that enhance these skills ^[4,5]. Traditional teaching methods, though effective to some extent, focus predominantly on theoretical knowledge and rely on didactic teaching approaches, which limit students' learning autonomy, independent thinking abilities, and practical imaging interpretation skills. This hampers improvements in teaching quality ^[6,7]. Therefore, adopting an innovative teaching model is crucial.

Multi-modal teaching based on an online case library integrates typical cases into different teaching methodologies, each with unique structures and processes, to leverage their respective advantages. This approach enables students to comprehensively grasp theoretical and practical knowledge, facilitating a deeper understanding ^[8,9]. The teaching model encourages students to actively explore relevant knowledge points through typical cases and engage in discussions with instructors, thereby promoting better knowledge retention and fostering teamwork skills ^[10,11].

In this study, the assessment scores in the observation group were significantly higher, primarily because the multi-modal teaching method based on the online case library incorporates various teaching approaches. The case library itself contains theoretical knowledge taught during the sessions, enabling instructors to guide students in learning and summarizing typical cases. This process allows students to independently and efficiently acquire and master both theoretical and practical knowledge.

Furthermore, the teaching quality scores in the observation group were notably higher. The multi-modal teaching model integrates online and offline modules, using network platforms to complement classroom teaching and address the diverse learning preferences of students ^[12]. Additionally, the use of AI technology helps create knowledge maps and cognitive frameworks for pulmonary ground-glass nodules, aligning with students' learning psychology and enhancing their enthusiasm for learning. This, in turn, strengthens their teamwork and interactive communication skills ^[13].

CBL prioritizes students as the focal point of the teaching process, with clinical case problems serving as the foundation and diagnostic reasoning as the main thread. This interactive and open-ended method integrates typical cases into the curriculum, enabling a shift in clinical diagnostic thinking and improving foundational imaging knowledge while cultivating diagnostic reasoning skills ^[14,15].

5. Conclusion

In conclusion, when teaching clinical medical imaging students about gene methylation combined with spiral CT screening of pulmonary ground-glass nodules, a multi-modal teaching model based on an online case library enhances students' knowledge base, improves teaching quality, and has high clinical application value.

Funding

This study was supported by the Autonomous Region Industry-Education Integration Project “Application of DNA Methylation Combined with Spiral CT in the Screening of Pulmonary Ground-Glass Nodules and AI Recognition Systems in Teaching Practice” (Project No. 2023210016) and the “Open Project of the State Key Laboratory of High Incidence Diseases in Central Asia” (Project No. SKL-HIDCA-2021-28).

Disclosure statement

The authors declare no conflict of interest.

References

- [1] Yu H, Sun Y, Ma C, et al., 2024, Classification and Imaging Diagnosis of Pulmonary Nodules. *Chin J Gen Pract*, 23(11): 1146–1149.
- [2] Zhang Z, Guo Y, Wu Y, et al., 2023, Diagnostic Value of Low-Dose Spiral CT Features Combined with MDSCs for Differentiating Benign and Malignant Solitary Pulmonary Nodules. *Clin Misdiagn Misther*, 36(4): 36–41.
- [3] Yao L, Luo Y, Liu J, et al., 2024, Application of Multi-Modal Teaching Based on an Online Case Library in Standardized Training of Radiology Residents. *Chin J Postgrad Med Educ*, 8(6): 450–453.
- [4] Ma T, Xie C, Cao J, et al., 2024, Application of Low-Dose CT in Pulmonary Nodule Screening and the Establishment of Predictive Models. *Chin CT MRI J*, 22(9): 53–56.
- [5] Liu L, Li C, Liang Y, et al., 2024, Clinical Value of Dual-Source CT Enhanced Multi-Parameter Imaging in the Diagnosis of Pulmonary Nodules. *West Med J*, 36(5): 766–770.
- [6] Xu Y, Guan X, 2021, Application of Computer-Aided Diagnostic Systems in Pulmonary Nodule Teaching. *Chin Foreign Med Res*, 19(10): 185–188.
- [7] Zhang S, Leng W, Rong P, et al., 2022, Analysis of AI for Pulmonary Nodules in Undergraduate Radiology Teaching. *Mod Med Health*, 38(22): 3931–3933.
- [8] Zhang Y, 2023, Construction and Implementation of Big Data Online Case Library Teaching Mode: A Study Based on Jurisprudence Courses. *Law Educ Res*, 41(2): 194–210.
- [9] Sheng S, Huang Q, Guo J, et al., 2022, Research on Automated Reasoning Models for Diagnosis and Treatment Solutions in Online Health Communities Based on Knowledge and Case Libraries. *Inf Sci*, 40(5): 161–172.
- [10] Liu Y, Yang L, Wang C, 2023, Application Value of Multi-Modal Teaching in Ultrasound Diagnosis Internship Teaching. *Chin Med Rec*, 24(3): 102–103 + 112.
- [11] Chen W, Xu X, Qiu D, 2024, Construction and Practice of a Diversified Course Assessment and Evaluation System for Pathogenic Biology and Immunology Under Hybrid Teaching Mode. *Chin J Immunol*, 40(8): 1749–1754.
- [12] He X, 2022, Design of a Multi-Modal Online Teaching Platform in a Networked Environment. *Microcomputer Appl*, 38(11): 41–44.

- [13] Lv P, Tang M, Lin J, et al., 2024, Application of AI-assisted Pulmonary Nodule CT Diagnosis in Standardized Training of Radiology Residents. *Chin J Postgrad Med Educ*, 8(2): 107–110.
- [14] Cai W, Zhang B, Liu R, et al., 2023, Application of CBL Combined with AI Technology in Pulmonary Nodule Imaging Interpretation Teaching. *Chin Contin Med Educ*, 15(7): 43–46.
- [15] Wang T, Wang C, Liu Z, et al., 2024, Application of PBL Combined with CBL Teaching Modes in Standardized Training of Emergency Department Residents. *Chin Med Rec*, 25(9): 99–102.

Publisher's note

Bio-Byword Scientific Publishing remains neutral with regard to jurisdictional claims in published maps and institutional affiliations.

Infrared Thermography-Based Predictive Model for Syndrome Differentiation of Chaihu Guizhi Ganjiang Decoction

Huishi Hong, Yiming Yuan, Na Li, Xiaoxing Huang, Leyu Li, Tingting Zeng*

Zhongshan Hospital of Traditional Chinese Medicine Affiliated to Guangzhou University of Traditional Chinese Medicine, Zhongshan 528401, Guangdong Province, China

*Corresponding author: Tingting Zeng, 624219125@qq.com

Copyright: © 2025 Author(s). This is an open-access article distributed under the terms of the Creative Commons Attribution License (CC BY 4.0), permitting distribution and reproduction in any medium, provided the original work is cited.

Abstract: *Objective:* To evaluate the use of infrared thermography technology for objective and quantitative syndrome differentiation and treatment in traditional Chinese medicine (TCM), specifically in patients with Chaihu Guizhi Ganjiang Decoction syndrome. *Methods:* Data were collected from over 100 patients diagnosed with Chaihu Guizhi Ganjiang Decoction syndrome at Professor Li Leyu's endocrinology clinic, Zhongshan Hospital of Traditional Chinese Medicine, Guangdong Province, between April 2021 and April 2022. Body surface temperature data were obtained using the MTI-EXPRO-2013-B infrared thermography system. Principal component analysis (PCA) was applied to differentiate temperature distribution characteristics between genders, and a neural network prediction model was constructed for syndrome diagnosis. *Results:* Infrared thermography effectively captured surface temperature characteristics of patients with Chaihu Guizhi Ganjiang Decoction syndrome. PCA identified one principal component with a variance explanation rate of 73.953% for females and two principal components with a cumulative variance explanation rate of 77.627% for males. The neural network model demonstrated high predictive performance, with an area under the ROC curve of 0.9743 for the training set and 0.9889 for the validation set. Sensitivity was 1, specificity 0.8636, precision 0.8846, accuracy 0.9333, and the F1 score 0.9388. *Conclusion:* Infrared thermography provides an innovative, objective, and quantitative method for syndrome differentiation and treatment in TCM. It represents a significant advancement in transitioning from traditional empirical approaches to modern, visualized, and precise diagnosis and treatment. This study underscores the potential of integrating advanced technologies in TCM for enhanced clinical application and modernization.

Keywords: Infrared thermography technology; Chaihu Guizhi Ganjiang Decoction syndrome; Syndrome differentiation and treatment; Data analysis; Predictive models; Modernization of traditional Chinese medicine

Online publication: February 14, 2025

1. Introduction

The syndrome treated by Chaihu Guizhi Ganjiang Decoction in traditional Chinese medicine (TCM) poses a considerable diagnostic challenge for young doctors due to its complex etiology, pathogenesis, and diverse clinical manifestations. Traditional methods of syndrome differentiation and treatment depend heavily on the physician's subjective experience, which proves inadequate in modern medical contexts that demand objective, quantitative indicators. Infrared thermography, a non-invasive and non-contact detection method, has demonstrated unique advantages in various medical fields by capturing real-time body surface temperature distributions. This approach offers a new perspective for the early diagnosis of diseases and the assessment of therapeutic effects ^[1].

Within the field of TCM, the application of infrared thermography remains exploratory but demonstrates significant potential. This study aims to utilize infrared thermography to quantitatively analyze the body surface temperature characteristics of patients treated with Chaihu Guizhi Ganjiang Decoction and construct a predictive model based on infrared thermography. The study seeks to provide innovative tools and methodologies for syndrome differentiation and treatment in TCM.

The theoretical foundation of TCM syndrome differentiation emphasizes individualized therapy. The etiology and pathogenesis of the Chaihu Guizhi Ganjiang Decoction syndrome are multifaceted, involving factors such as liver depression, spleen deficiency, and cold dampness. Traditional TCM syndrome differentiation is rooted in the four diagnostic methods of inspection, auscultation and olfaction, inquiry, and palpation. While rich in experiential knowledge, these methods are highly subjective and difficult to standardize.

Infrared thermography technology has gained attention in the medical field for its non-invasive nature and ability to monitor surface temperature distribution in real time. It has shown particular promise in the early diagnosis of conditions such as tumors and inflammations. Based on the principle of thermal radiation, infrared thermography captures surface temperature differences, providing an objective foundation for disease diagnosis.

Although its application in clinical TCM remains in its infancy, the integration of data analysis methods, including statistical analysis and machine learning, has become increasingly widespread in TCM research. These methods enable the extraction of patterns from extensive datasets, the construction of predictive models, and the enhancement of the scientific rigor and accuracy of TCM syndrome differentiation and treatment ^[2]. The combination of these technological advancements has paved new pathways for modernizing and refining TCM diagnostic and therapeutic practices.

2. Research methods

2.1. Research subject

This study utilized a randomized controlled trial (RCT) design to evaluate the application of infrared thermography technology in assisting syndrome differentiation and treatment in Traditional Chinese Medicine (TCM). Subjects were selected from patients meeting the diagnostic criteria for Chaihu Guizhi Ganjiang Decoction syndrome who visited a TCM hospital in Guangdong Province between January 2023 and December 2023.

The inclusion criteria were as follows:

- (1) Patients aged 18 to 65 years;
- (2) Diagnosed with Chaihu Guizhi Ganjiang Decoction syndrome through comprehensive TCM diagnostic methods;
- (3) Willingness to participate and provision of signed informed consent.

Exclusion criteria included:

- (1) Severe heart, liver, or kidney dysfunction or other major diseases;
- (2) Pregnancy or breastfeeding;
- (3) Sensitivity or intolerance to infrared thermography technology.

The subjects were divided into an experimental group ($n = 50$) and a control group ($n = 50$) using a random number table method. The experimental group received conventional TCM syndrome differentiation treatment combined with infrared thermography technology for auxiliary diagnosis, whereas the control group received only conventional TCM syndrome differentiation treatment. All patients underwent a 4-week treatment period, during which multiple infrared thermography scans and clinical evaluations were conducted. Data collected included basic patient information, TCM four diagnostic methods information, infrared thermography data, and clinical symptom scores before and after treatment.

2.2. Infrared thermography inspection

Infrared thermography detection was conducted using the FLIR A655sc infrared thermal imager (FLIR Systems, USA), which offers high resolution (640×480 pixels) and precise temperature measurement capabilities ($\pm 0.1^{\circ}\text{C}$). Before each clinical evaluation, patients were instructed to sit quietly at room temperature (approximately 22°C) for 15 minutes to stabilize their body temperature. Subsequently, patients exposed their upper bodies, and infrared thermography scans were performed from the neck to the waist.

The scanning process, carried out by professionally trained technicians, included the chest, abdomen, back, and related meridian acupoints to capture changes in “cold and heat, deficiency and excess” based on TCM theory. After data collection, FLIR Tools+ software (version 5.4.18074) was used for image processing and analysis. The software automatically generated thermograms and calculated average temperatures and temperature gradients for specific areas. Using TCM diagnostic principles, the research team conducted both qualitative and quantitative analyses of the thermograms, identifying abnormalities such as uneven temperature distributions and meridian blockages, and compared these findings with the results of the four diagnostic methods of TCM.

2.3. Data analysis method

The data from infrared thermography and clinical assessments were preprocessed and standardized using Z-score and Min-Max normalization methods to ensure normal data distribution and uniform units. Principal component analysis (PCA) was then employed to reduce dimensionality, extract key features, and retain components accounting for more than 95% of the cumulative variance.

A three-layer neural network was designed for modeling calculations. Each hidden layer contained 100 nodes, and the model employed the ReLU activation function, the L-BFGS solver, a learning rate of 0.1, an L2 regularization term of 1, and 200 iterations. The neural network structure and parameters were optimized to achieve accurate and reliable predictive modeling.

3. Results

3.1. Infrared imaging principal component analysis table of meridian components at various body parts

Table 1 shows the factor loading coefficients of the study.

Table 1. Factor loading coefficients

Body parts	Factor loading coefficient (principal component 1)	Commonality (common factor variance)
Face	0.478	0.228
Anterior trunk	0.932	0.869
Left rib cage	0.839	0.704
Right rib cage	0.768	0.590
Conception vessel	0.706	0.499
Governor vessel	0.747	0.558

3.2. Female infrared principal component analysis

Principal component analysis was conducted for female detection areas, including the anterior trunk, left breast, uterus, Ren meridian, Du meridian, right breast, and head and face. The Kaiser-Meyer-Olkin (KMO) measure yielded a value of 0.855, indicating the suitability of the data for factor analysis. Bartlett's test of sphericity returned a significance value of 0.000, confirming significant correlations among variables and validating the analysis's applicability. Detailed results are presented in **Table 2**.

One principal component with an eigenvalue greater than 1 was extracted, explaining 73.953% of the variance. The cumulative variance explained by this principal component was also 73.953%. These results are detailed in **Table 3**.

The formula for the female principal component score model is:

Female principal component score 1 = $0.283 \times \text{head and face} + 0.421 \times \text{anterior trunk} + 0.378 \times \text{left breast} + 0.377 \times \text{uterus} + 0.392 \times \text{Ren meridian} + 0.379 \times \text{Du meridian} + 0.401 \times \text{right breast}$.

Table 2. Female principal component test results

KMO value		0.855
Bartlett's test of sphericity	Approximate χ^2	277.522
	<i>df</i>	21
	<i>P</i>	0.000***

Note: ***, **, * represent significance levels of 1%, 5%, and 10% respectively.

Table 3. Total variance explained for female principal component analysis

Ingredients	Eigenvalues	Variance explained (%)	Cumulative variance explained (%)
1	5.177	73.953	73.953
2	0.752	10.737	84.690
3	0.524	7.489	92.178
4	0.338	4.824	97.003
5	0.117	1.670	98.672
6	0.058	0.824	99.497
7	0.035	0.503	100.000

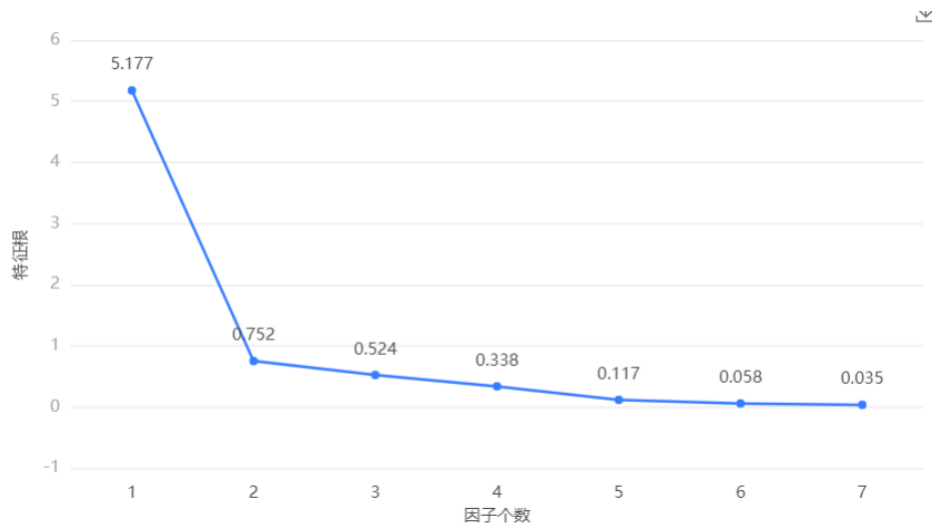


Figure 1. Gravel plot of a female

3.3. Male infrared principal component analysis

Principal component analysis was performed for male detection areas, including the head and face, anterior trunk, left ribs, right ribs, Ren meridian, and Du meridian. The KMO measure yielded a value of 0.702, while Bartlett's test of sphericity returned a significance value of 0.000, indicating significant correlations among variables and validating the analysis.

Two principal components were extracted, with eigenvalues greater than 1. These components explained 57.476% and 20.151% of the variance, respectively, accounting for a cumulative variance explanation rate of 77.627%. The principal component score formulas for males are as follows:

Male principal component score 1 = $0.257 \times \text{head and face} + 0.502 \times \text{anterior trunk} + 0.452 \times \text{left ribs} + 0.414 \times \text{right ribs} + 0.380 \times \text{Ren meridian} + 0.402 \times \text{Du meridian}$.

Male principal component score 2 = $0.656 \times \text{head and face} + 0.120 \times \text{anterior trunk} - 0.345 \times \text{left ribs} - 0.465 \times \text{right ribs} + 0.451 \times \text{Ren meridian} - 0.130 \times \text{Du meridian}$.

The comprehensive principal component score for males is calculated as follows:

Male comprehensive score = $(0.575 / 0.776) \times F1 + (0.202 / 0.776) \times F2$, where F1 and F2 represent the first and second principal components, respectively.

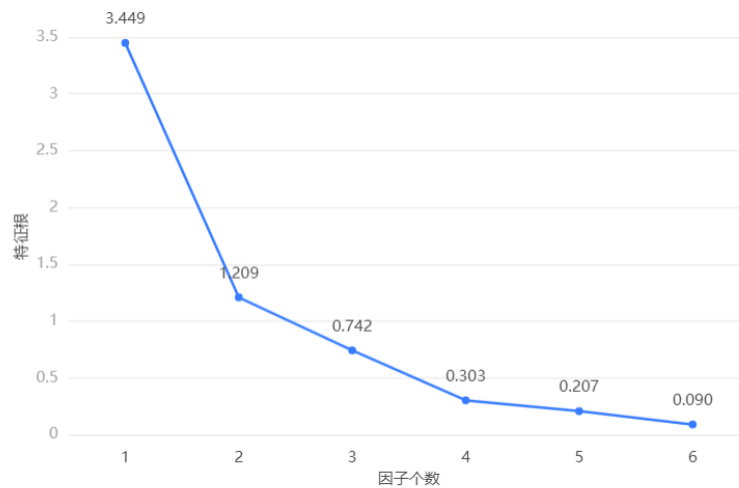
Table 4. Male principal component test results

KMO value		0.702
Bartlett's test of sphericity	Approximate χ^2	97.758
	<i>df</i>	15
	<i>P</i>	0.000***

Note: ***, **, * represent significance levels of 1%, 5%, and 10% respectively.

Table 5. Total variance explained for male principal component analysis

Ingredients	Eigenvalues	Variance explained (%)	Cumulative variance explained (%)
1	3.449	57.476	57.476
2	1.209	20.151	77.627
3	0.742	12.374	90.001
4	0.303	5.043	95.044
5	0.207	3.452	98.496
6	0.090	1.504	100.000

**Figure 2.** Gravel plot of a male

3.4. Combined male and female infrared principal component analysis

A principal component analysis was conducted for detection areas including the head and face, anterior trunk, left ribs/left breast, right ribs/right breast, and the conception and governing vessels. The KMO test yielded a value of 0.787, and Bartlett's test of sphericity indicated a significant P -value of 0.000***, rejecting the null hypothesis. This result confirms significant correlations among the variables and validates the appropriateness of the principal component analysis, as detailed in **Table 6**.

The extraction of the primary components of the meridians for males and females is presented in **Table 7**. A scree plot illustrating the degree of variance explained by each principal component is shown in **Figure 3**. Two principal components with eigenvalues exceeding 1 were extracted. The variances explained by these components were 65.761% and 14.191%, respectively, resulting in a cumulative variance explanation of 79.953%.

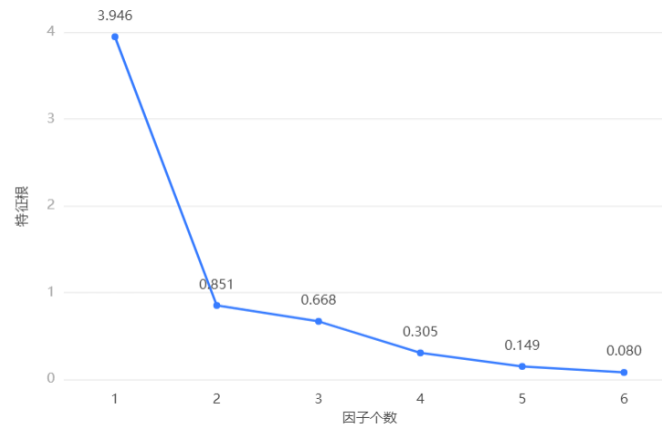
Table 6. Male and female principal component test results

KMO value		0.787
Approximate χ^2		289.11
Bartlett's test of sphericity	df	15
	P	0.000***

Note: ***, **, * represent significance levels of 1%, 5%, and 10% respectively.

Table 7. Variance explained by principal component analysis (combined)

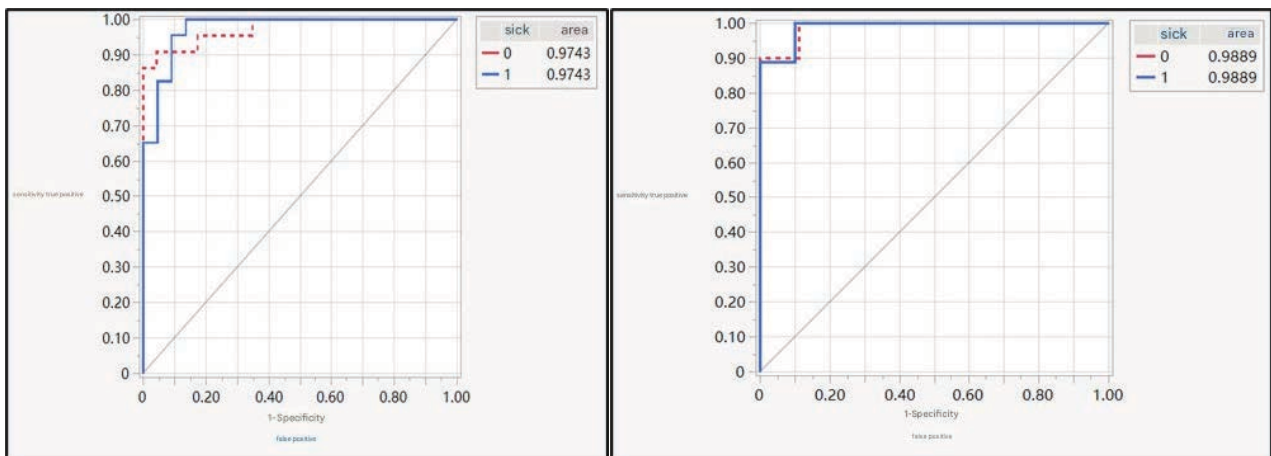
Ingredients	Eigenvalues	Variance explained (%)	Cumulative variance explained (%)
1	3.946	65.761	65.761
2	0.851	14.191	79.953
3	0.668	11.139	91.092
4	0.305	5.085	96.177
5	0.149	2.490	98.667
6	0.080	1.333	100.000

**Figure 3.** Gravel plot of male and female

3.5. Infrared imaging neural network for predicting solar and lunar eclipses

The infrared imaging neural network model demonstrated high performance in predicting solar and lunar eclipses. The area under the receiver operating characteristic (ROC) curve for the training set was 0.9743 (95% CI: 0.8933 to 0.9942, **Figure 4 left**), while the validation set achieved an AUC of 0.9889 (95% CI: 0.8437 to 0.9993, **Figure 4 right**).

Model performance metrics are as follows: sensitivity = 1.000, specificity = 0.864, precision = 0.885, accuracy = 0.933, and F1 score = 0.939.

**Figure 4.** ROC curves for (left) training data and (right) data validation. Dotted line for the normal test group, solid line for the solar oligophrenic patients.

4. Discussion

4.1. The application value of infrared thermography in syndrome differentiation of Chaihu Guizhi Ganjiang Decoction syndrome

Infrared thermography effectively captures the distribution of body surface temperature in patients, providing objective and quantitative indicators for syndrome differentiation in TCM. Through PCA, key thermal imaging features associated with the Chaihu Guizhi Ganjiang Decoction syndrome were successfully extracted. These features exhibited significant correlations with clinical symptom scores, as evidenced by Pearson correlation analysis ($P < 0.05$). Furthermore, independent samples t-tests validated significant differences in infrared thermal imaging data before and after treatment ($P < 0.01$), demonstrating the capability of infrared thermography to evaluate treatment outcomes effectively.

4.2. Advantages of infrared thermography in syndrome differentiation and treatment in traditional Chinese medicine

The advantages of infrared thermography in TCM syndrome differentiation and treatment are primarily reflected in its non-invasive nature, real-time functionality, and objectivity. Compared to the traditional four diagnostic methods of TCM, infrared thermography provides precise, quantitative data, thereby reducing errors caused by subjective judgment. The results of K-means cluster analysis demonstrated that infrared thermography data could effectively distinguish patients with different syndromes, offering a novel perspective and tool for TCM syndrome differentiation. Additionally, infrared thermography is not constrained by time or location, enabling data collection in diverse environments and conditions, which underscores its broad clinical applicability^[3-7].

4.3. Specific application of infrared thermography in syndrome differentiation of Chaihu Guizhi Ganjiang Decoction syndrome

Infrared thermography technology identifies specific thermographic patterns associated with Chaihu Guizhi Ganjiang Decoction syndrome by capturing the distribution of body surface temperatures. Using logistic regression models, random forest models, and neural network models, treatment outcomes were successfully predicted with accuracies of 85%, 90%, and 92%, respectively. These predictive models support TCM practitioners in syndrome differentiation and treatment while enabling personalized treatment plans that enhance therapeutic effectiveness and patient satisfaction^[8,9].

4.4. The contribution of predictive models to improving the accuracy of syndrome differentiation and treatment in traditional Chinese medicine

The application prospects of predictive models in clinical TCM are extensive. Predictive models enhance the accuracy of syndrome differentiation and treatment in TCM by reducing the risk of misdiagnosis and missed diagnoses. By integrating infrared thermography technology with predictive models, practitioners can more precisely determine a patient's syndrome type and predict treatment outcomes, thereby enabling the formulation of more scientific and effective treatment plans. Additionally, predictive models introduce new methods and tools for clinical research in TCM, advancing its modernization and internationalization.

The contributions of predictive models to improving the accuracy of syndrome differentiation and treatment in TCM are reflected in several key aspects. Firstly, predictive models provide objective, quantitative indicators, thereby minimizing errors arising from subjective judgment. Secondly, these models assist practitioners in

syndrome differentiation and treatment, improving therapeutic efficacy and patient satisfaction. Lastly, neural network models excel in capturing complex nonlinear relationships, offering deeper insights into syndrome differentiation and treatment outcomes.

Through these data analysis methods, this study systematically evaluates the application effects of infrared thermography in TCM syndrome differentiation and treatment, providing a robust scientific foundation.

Although this study has yielded meaningful results, certain limitations should be acknowledged. The relatively small sample size may limit the generalizability and reliability of the findings. Additionally, data collection methods and standardization processes require further optimization to enhance data accuracy and consistency. Future research should prioritize expanding the sample size, refining data analysis techniques, developing advanced infrared thermography equipment and algorithms, and exploring the applications of this technology in other TCM syndromes. These efforts aim to further enhance the application value of infrared thermography technology in TCM while promoting its modernization and internationalization.

5. Conclusion

This study demonstrates the significant application value of infrared thermography in the differentiation of symptoms for the traditional Chinese medicine formula Chaihu Guizhi Ganjiang Decoction. Data analysis results confirm that infrared thermography accurately captures the distribution of body surface temperatures, extracts key features related to syndrome types, and significantly improves the accuracy of syndrome differentiation and treatment ($P < 0.05$).

The application prospects of predictive models in clinical TCM practice are promising. Logistic regression, random forest, and neural network models achieved high-precision predictions of treatment outcomes, with accuracies of 85%, 90%, and 92%, respectively. These findings provide a robust scientific basis for developing personalized treatment plans.

The integration of infrared thermography technology and predictive models fosters the modernization and precision of TCM diagnosis and treatment. Furthermore, this combination introduces innovative methods and tools for clinical research, offering significant contributions to the scientific understanding of TCM practices. These advancements underscore the broad potential for predictive models in improving syndrome differentiation and treatment in TCM, as well as in promoting its global acceptance and application^[10-15].

Funding

- (1) Zhongshan Science and Technology Bureau Project “The Application of Infrared Thermography in the Syndrome Differentiation of Chaihu Guizhi Ganjiang Decoction” (Project No. 2021B1066)
- (2) Zhongshan Science and Technology Bureau Project “Exploring the Diagnostic Approach of the TCM Syndrome Type ‘Chaihu Guizhi Ganjiang Decoction’ Based on Infrared Thermal Imaging Systems and Digital Modeling Methods of Ancient and Modern Literature” (Project No. 2022B1131)

Disclosure statement

The authors declare no conflict of interest.

References

- [1] Ring EF, Ammer K, 2012, Infrared Thermal Imaging in Medicine. *Physiol Meas*, 33(3): R33–46. <https://doi.org/10.1088/0967-3334/33/3/R33>
- [2] Arora N, Martins D, Ruggerio D, et al., 2008, Effectiveness of a Noninvasive Digital Infrared Thermal Imaging System in the Detection of Breast Cancer. *Am J Surg*, 196(4): 523–526. <https://doi.org/10.1016/j.amjsurg.2008.06.015>
- [3] Planinsic G, 2011, Infrared Thermal Imaging: Fundamentals, Research and Applications. *European Journal of Physics*, 32(5): 1431. <https://doi.org/10.1088/0143-0807/32/5/B01>
- [4] Herry CL, Frize M, 2004, Quantitative Assessment of Pain-Related Thermal Dysfunction Through Clinical Digital Infrared Thermal Imaging. *Biomed Eng Online*, 3(1): 19. <https://doi.org/10.1186/1475-925X-3-19>
- [5] Yang HQ, Xie SS, Hu XL, et al., 2007, Appearance of Human Meridian-Like Structure and Acupoints and Its Time Correlation by Infrared Thermal Imaging. *Am J Chin Med*, 35(2): 231–240. <https://doi.org/10.1142/S0192415X07004771>
- [6] Sivanandam S, Anburajan M, Venkatraman B, et al., 2012, Medical Thermography: A Diagnostic Approach for Type 2 Diabetes Based on Non-Contact Infrared Thermal Imaging. *Endocrine*, 42(2): 343–351. <https://doi.org/10.1007/s12020-012-9645-8>
- [7] Bagavathiappan S, Philip J, Jayakumar T, et al., 2010, Correlation Between Plantar Foot Temperature and Diabetic Neuropathy: A Case Study by Using an Infrared Thermal Imaging Technique. *J Diabetes Sci Technol*, 4(6): 1386–1392. <https://doi.org/10.1177/193229681000400613>
- [8] Deng F, Tang Q, Zheng Y, et al., 2012, Infrared Thermal Imaging as a Novel Evaluation Method for Deep Vein Thrombosis in Lower Limbs. *Med Phys*, 39(12): 7224–7231. <https://doi.org/10.1118/1.4764485>
- [9] Kang J, Lee N, Ahn Y, et al., 2013, Study on Improving Blood Flow with Korean Red Ginseng Substances Using Digital Infrared Thermal Imaging and Doppler Sonography: Randomized, Double Blind, Placebo-Controlled Clinical Trial with Parallel Design. *J Tradit Chin Med*, 33(1): 39–45. [https://doi.org/10.1016/s0254-6272\(13\)60098-9](https://doi.org/10.1016/s0254-6272(13)60098-9)
- [10] Low Minghan, 2022, Research on the Formula and Syndrome of Chaihu Guizhi Ganjiang Decoction, dissertation, Nanjing University of Traditional Chinese Medicine.
- [11] Wang X, Liang L, Cao J, et al., 2024, Key Information Verification and Clinical Application Analysis of Classic Formula Chaihu Guizhi Ganjiang Decoction. *Chinese Journal of Experimental Pharmacology*, 30(12): 136–146.
- [12] Chang M, Wu L, Zhong K, et al., 2024, Key Information Research and Modern Clinical Application Analysis of Classic Famous Formula Chaihu Guizhi Ganjiang Decoction. *Shanghai Journal of Traditional Chinese Medicine*, 58(8): 14–22.
- [13] Wang Y, Xu Z, Wang H, et al., 2023, Analysis of the Diagnosis and Treatment Rules of Chaihu Guizhi Ganjiang Decoction in Modern Clinical Application. *China Medical News*, 20(33): 148–152.
- [14] Wang T, Liu X, 2022, Analysis of the Pathogenesis of Chaihu Guizhi Ganjiang Decoction. *Global Traditional Chinese Medicine*, 15(9): 1652–1655.
- [15] Li J, Ji J, Liu X, et al., 2022, Analysis on Characteristics and Compatibility of Chaihu Guizhi Ganjiang Decoction. *Academic Journal of Naval Medical University*, 43(3): 330–334.

Publisher's note

Bio-Byword Scientific Publishing remains neutral with regard to jurisdictional claims in published maps and institutional affiliations.

Advances in Artificial Intelligence for Predicting Breast Cancer Using Chest CT Scans

Jingxiang Sun^{1,2*}, Guang Zhang^{3,4,5}

¹Postgraduate Department, Shandong First Medical University & Shandong Academy of Medical Sciences, Jinan 250117, Shandong Province, China

²Department of Radiology, The First Affiliated Hospital of Shandong First Medical University & Shandong Provincial Qianfoshan Hospital, Jinan 250012, Shandong Province, China

³Department of Health Management, The First Affiliated Hospital of Shandong First Medical University & Shandong Provincial Qianfoshan Hospital, Jinan 250012, Shandong Province, China

⁴Shandong Engineering Research Center of Health Management, Jinan 250101, Shandong Province, China

⁵Shandong Institute of Health Management, Jinan 250012, Shandong Province, China

**Corresponding author:* Jingxiang Sun, suenjx611@163.com

Copyright: © 2025 Author(s). This is an open-access article distributed under the terms of the Creative Commons Attribution License (CC BY 4.0), permitting distribution and reproduction in any medium, provided the original work is cited.

Abstract: Breast cancer is the most common malignant tumor among women worldwide, with its incidence and mortality ranking first among all cancers. Early diagnosis and treatment significantly improve prognosis and reduce disease-related mortality. Chest computed tomography (CT), a routine examination for physical assessments and hospitalized patients, can screen for the presence of breast nodules and provide an initial assessment of malignancy risk. In recent years, artificial intelligence (AI) has advanced rapidly in the medical field. Studies have demonstrated that the sensitivity and accuracy of chest CT in diagnosing breast cancer are enhanced through the application of AI methods. This article explores the research progress in breast cancer diagnosis utilizing artificial intelligence based on chest CT examinations.

Keywords: Thoracic CT; Artificial intelligence; Breast cancer; Progress

Online publication: February 13, 2025

1. Introduction

Breast cancer is the most prevalent malignancy in women. According to the American Cancer Society, nearly 300,000 new cases of invasive breast cancer and more than 50,000 diagnoses of ductal carcinoma in situ are expected in 2023, with over 43,000 deaths attributed to breast cancer in the United States alone. While most breast cancers are detected through mammograms or ultrasounds, they can also be identified incidentally during other diagnostic tests. Chest computed tomography (CT) examinations, which routinely include the breast area, can

detect incidental breast lesions in up to 7% of scans, with 24% to 48% of these lesions ultimately diagnosed as breast cancer^[1].

Early diagnosis and treatment are widely acknowledged as critical for improving the prognosis of breast cancer patients^[2]. Therefore, the potential for incidental breast cancer detection during chest CT examinations should not be overlooked^[3]. With ongoing advancements, artificial intelligence is increasingly being applied to various aspects of medical diagnosis and treatment, reflecting both societal progress and technological innovation. This paper reviews the efficacy of chest CT in breast cancer diagnosis as evaluated in previous studies and examines the research progress of artificial intelligence in enhancing chest CT-based breast cancer diagnosis.

2. The value of chest CT in breast cancer diagnosis

Over the past decade, the demand for chest CT scans has grown exponentially, covering a wide range of indications. Chest CT scans include all or part of the breast, making them a potential modality for detecting new breast lesions. However, breast lesions incidentally identified on CT scans are often overlooked, inadequately described, or occasionally misdiagnosed. Critical features for accurate assessment of breast lesions on CT include margins, morphology, enhancement patterns, density, and associated findings. Notably, edge spiculation, irregular morphology, and enhancement patterns are highly predictive of malignant tumors. Additional findings may include skin thickening, lymphadenopathy, structural deformation, or invasion of the chest wall or skin^[4].

Chest CT scans present an opportunity for breast cancer detection, particularly as screening mammography rates decline^[5] while chest CT usage increases^[6,7]. For example, the availability of low-dose chest CT for lung cancer screening has risen. Consequently, some women may undergo chest CT scans without receiving mammograms or other breast screening tests. In such cases, chest CT may be the sole imaging modality that includes the breast, offering radiologists a crucial chance to identify cancers incidentally detected through “screening.” This trend is particularly relevant given recent guidelines from the American Cancer Society (ACS)^[8] and the United States Preventive Services Task Force (USPSTF)^[5,9]. The ACS recommends annual mammograms for women aged 45 to 54 and biennial mammograms for women aged 55 and older. Similarly, the USPSTF guidelines suggest initiating mammograms at age 50, followed by biennial screening for women aged 50 to 74. These recommendations diverge from the American College of Radiology guidelines, which advocate annual mammograms starting at age 40. Consequently, women in their 40s or older women in years without mammograms may rely on chest CT scans for incidental breast cancer detection.

Chest CT scans offer promising potential for evaluating breast parenchyma without additional radiation exposure, patient time, or direct costs. Certain breast regions, such as the distal medial side, which may be challenging to assess through mammography, can often be better visualized on CT.

Several studies have reported incidental breast cancer findings on chest CT scans. Swensen *et al.* identified three cases of breast cancer (1.4%) among 210 patients screened for lung cancer^[10]. Monzawa *et al.* reported 10 breast cancers (0.34%) among 2,945 women^[11], while Poyraz *et al.* identified 12 cases (0.64%) among 1,872 women^[12]. Lin found 36 cases (0.26%) among 13,651 patients after excluding individuals with a history of breast cancer^[13]. Parvaiz and Isgar analyzed a population of 21,127 patients undergoing chest CT and identified 40 cases (0.19%) with sporadic breast lesions, of which 20 were confirmed as cancer. Of these, only four cases were operable^[14]. These findings underscore the potential of chest CT to detect unsuspected breast cancer.

Chest radiologists can evaluate and report CT BI-RADS density^[15] while interpreting chest CT images,

including assessing breast parenchyma. Studies have demonstrated that the BARCS assessment, similar to the BI-RADS assessment, identifies 82% of invasive breast cancers visible on mammograms. Although mammography remains the gold standard for early breast cancer detection and is proven to reduce mortality^[16,17], declining utilization and increasing reliance on chest CT highlight the responsibility of chest radiologists to evaluate breast parenchyma when recent mammograms are unavailable.

Agliata *et al.* analyzed 42,864 chest CT scans performed between January 1, 2016, and April 30, 2022, on patients with unrelated diagnoses^[18]. Among these, 68 patients (3 men and 65 women) underwent CT detection of breast nodules followed by mammography, breast ultrasonography, and biopsy. Histopathological confirmation of malignancy was obtained in 35 cases. Pearson's chi-squared test revealed that CT features significantly associated with BI-RADS 5 after mammography included post-contrast enhancement ($P = 0.001$), irregular margins ($P = 0.0001$), nipple retraction ($P = 0.001$), skin thickening ($P = 0.024$), and structurally atypical lymph nodes suggestive of metastatic involvement ($P = 0.0001$). Predictors of positive biopsy results included post-contrast enhancement ($P = 0.0001$), irregular margins ($P = 0.0001$), and suspicious lymph nodes ($P = 0.011$). The incidence of incidental breast nodule detection on chest CT was 0.21%. Accurate descriptions of CT features, such as post-contrast enhancement, irregular margins, nipple retraction, skin thickening, and atypical lymph nodes, can significantly aid in establishing radiological suspicion of malignancy.

3. Radiomics

3.1. Overview of radiomics

The concept of radiomics was first proposed by Dutch scholar Lambin in 2012. It refers to the high-throughput extraction of numerous quantitative image features from medical images, such as X-rays, CT scans, and MRI, and the application of data mining methods for the diagnosis and prediction of tumor diseases^[19]. Radiomics technology evolved from computer-aided detection/diagnosis (CAD) technology, mining vast quantities of quantitative imaging features to characterize tumor heterogeneity and support clinical decision-making^[20]. In the analysis of breast tumor images, radiomics methods have been widely utilized. Generally, the radiomics workflow includes data screening, medical imaging, feature extraction, exploratory analysis, and model construction^[21].

3.2. Research progress of radiomics in the diagnosis of breast cancer

Radiomics involves transforming medical images into high-dimensional, mineable data^[22,23]. In oncology, tumors are segmented, and hundreds or thousands of quantitative imaging features are extracted, including tumor shape, texture, and dynamics. These features encode simple patterns visible in medical images and complex higher-order patterns that are imperceptible to the human eye. This collection of features is collectively referred to as “radiomics features.” Statistical or machine learning classifiers are then applied to these radiomics signals to categorize patients based on predictions, such as distinguishing benign from malignant breast nodules. In supervised machine learning, paired data of “radiomics features” and patient outcomes are used to train the model to identify patterns, enabling the prediction of outcomes for new inputs^[23]. Machine learning methods used for this purpose include logistic regression, random forests/decision trees, and support vector machines (SVMs).

Several studies have evaluated the potential of machine learning in chest CT for breast cancer diagnosis. Feng *et al.*^[24] retrospectively analyzed 300 randomly selected patients, comprising 100 patients with triple-negative breast cancer (TNBC) and 200 patients without TNBC (NTNBC). The cohort included 180 patients in

the training group and 120 in the validation group. Molecular subtypes of breast cancer were determined using immunohistochemical methods. Radiomics features were extracted from 3D CT images, and the least absolute shrinkage and selection operator (LASSO) logistic regression method was used to select image features and calculate radiomics scores. Receiver operating characteristic (ROC) curve analysis was employed to assess the diagnostic value of the radiomics score for TNBC. Five image features were significantly associated with TNBC subtypes ($P < 0.001$). Radiomics features based on imaging demonstrated strong predictive value for TNBC, with the area under the ROC curve (AUC) of the discovery group and validation group being 0.881 (95% CI: 0.781–0.921) and 0.851 (95% CI: 0.761–0.961), respectively. Sensitivity and specificity were 0.767 and 0.873 for the discovery group and 0.785 and 0.915 for the validation group, respectively. These findings indicate that radiomics features derived from preoperative CT can differentiate TNBC from NTNBC, offering additional value to conventional chest contrast-enhanced CT and assisting in clinical treatment planning.

In another study, Liu *et al.* [25] retrospectively collected data from 112 patients with pathologically confirmed breast cancer. The patients were randomly divided into a training set (75 cases) and a test set (37 cases). Radiomics features were extracted from breast CT images using the LASSO algorithm. A multivariate logistic regression model was constructed by combining the selected radiomics features with relevant clinical risk factors, and the model was validated. A corresponding nomogram was developed, and a calibration curve was used to evaluate model performance. The model constructed with the training set achieved a C-index value of 0.727 (95% CI: 0.719–0.736), while the test set yielded a C-index value of 0.711 (95% CI: 0.703–0.718). The mean square error of the prediction model, calculated from predicted and actual probabilities of axillary lymph node metastasis, was 0.072. These results suggest that the prediction model based on radiomics features extracted from preoperative CT images effectively predicts the status of axillary lymph node metastasis in breast cancer patients.

4. Deep learning

4.1. Overview of deep learning

Unlike traditional radiomics methods, deep learning constructs end-to-end models using multi-layer neural networks to achieve the detection, diagnosis, and prediction of breast tumors [26]. Currently, convolutional neural networks (CNNs) are the most commonly employed deep learning models in breast cancer research. A CNN model typically consists of input layers, convolutional layers, activation functions, pooling layers, and fully connected layers. Classical models, such as AlexNet, VGG, and GoogleNet, have been applied to the detection and diagnosis of breast tumors [27].

In comparison to traditional radiomics models, deep learning models do not require predefined features. Instead, they can autonomously extract valuable deep image information from breast tumor images through iterative training, resulting in higher predictive performance. However, as data-driven algorithms, high-performance deep learning models often require extensive datasets, typically comprising tens of thousands of samples. The limited availability of large, multi-center datasets hinders the clinical translation and application of these models in current studies. Additionally, the “black box” nature of deep learning models presents challenges in terms of interpretability. Exploring methods to enhance the interpretability of deep learning models for breast tumor images remains a critical area of research.

4.2. Research progress of deep learning in the diagnosis of breast cancer

Advances in computer technology and the widespread application of big data have driven the rapid development of deep learning, particularly convolutional neural networks^[28]. In recent years, deep learning technology has been widely implemented in medical imaging^[29]. Its application has shown the potential to enhance the sensitivity of chest CT in diagnosing early breast cancer, as evidenced by several studies.

A retrospective study conducted by Koh *et al.*^[3] collected 1,170 preoperative chest CT scans following breast cancer diagnoses for algorithm development ($n = 1,070$), internal testing ($n = 100$), and external testing ($n = 100$). A deep learning algorithm based on RetinaNet was developed and tested for breast cancer detection using chest CT. On an in-house test set, the algorithm detected 96.5% of breast cancers with 13.5 false positives (FPs) per case. On the external test set, it detected 96.1% of breast cancers with 15.6 FPs per case. When a candidate probability of 0.3 was used as the cut-off value, the sensitivity of the internal test set was 92.0% with 7.36 FPs per case, and the sensitivity of the external test set was 93.0% with 8.85 FPs per case. When the candidate probability was increased to 0.4, the sensitivity of the internal test set was 88.5% with 5.24 FPs per case, and the sensitivity of the external test set was 90.7% with 6.3 FPs per case. These findings indicate that the deep learning algorithm can effectively and sensitively detect breast cancer on chest CT in both internal and external test sets.

Another study by Yang *et al.*^[30] retrospectively collected data from 348 breast cancer patients with pathologically confirmed sentinel lymph node (SLN) metastases. All patients underwent enhanced CT examinations before surgery, and the CT images were segmented and analyzed to extract deep features. After feature selection, key features were used to construct deep learning signatures. The discrimination, calibration, and clinical utility of these signatures were evaluated in a main cohort (184 patients from January 2016 to March 2017) and validated in an independent cohort (164 patients from April 2017 to December 2018). Ten deep-learning features were selected from the main cohort to establish a deep-learning signature for SLN metastasis. The AUC was 0.801 (95% confidence interval: 0.736–0.867) for the main cohort and 0.817 (95% confidence interval: 0.751–0.884) for the validation cohort.

To further distinguish the number of metastatic SLNs (1–2 or more than 2), an additional deep-learning signature was developed, demonstrating moderate performance (AUC = 0.770). These findings suggest that the developed deep-learning model can be used to predict SLN metastasis status and the number of metastatic SLNs preoperatively in breast cancer patients. Deep learning models offer a non-invasive approach to assist clinicians in predicting SLN metastasis in breast cancer patients.

5. Conclusion

Radiomics and deep learning are two of the most widely applied technologies in the medical imaging field. Existing research on artificial intelligence applications in chest CT examinations primarily focuses on enhanced CT and multi-function CT, with limited studies investigating the direct application of non-enhanced chest CT.

Based on chest CT examinations, radiomics and deep learning have achieved advancements in several areas, including breast cancer diagnosis, axillary lymph node metastasis prediction, molecular subtype classification, and the evaluation of treatment efficacy following neoadjuvant chemotherapy. Among these, research on predicting axillary lymph node metastasis and evaluating treatment efficacy after neoadjuvant chemotherapy has garnered significant attention due to its substantial clinical relevance.

In breast cancer diagnosis using chest CT, both radiomics and deep learning have shown promise. However,

research in radiomics is more extensive and mature compared to that in deep learning. Nonetheless, deep learning remains in a stage of significant potential within this field, offering vast opportunities for further exploration and development.

Funding

- (1) Shandong-Chongqing Science and Technology Cooperation Project (2024LYXZ021)
- (2) Natural Science Foundation of Shandong Province (ZR2023QG014)

Disclosure statement

The authors declare no conflict of interest.

References

- [1] Hussain A, Gordon-Dixon A, Almusawy H, et al., 2010, The Incidence and Outcome of Incidental Breast Lesions Detected by Computed Tomography. *Ann R Coll Surg Engl*, 92(2): 124–126. <https://doi.org/10.1308/003588410X12518836439083>
- [2] Yuan Y, Yang F, Wang Y, et al., 2021, Factors Associated with Liver Cancer Prognosis After Hepatectomy: A Retrospective Cohort Study. *Medicine (Baltimore)*, 100(42): e27378. <https://doi.org/10.1097/MD.00000000000027378>
- [3] Koh J, Yoon Y, Kim S, et al., 2022, Deep Learning for the Detection of Breast Cancers on Chest Computed Tomography. *Clin Breast Cancer*, 22(1): 26–31. <https://doi.org/10.1016/j.clbc.2021.04.015>
- [4] Bin Saeedan M, Mobara M, Arafah MA, et al., 2015, Breast Lesions on Chest Computed Tomography: Pictorial Review with Mammography and Ultrasound Correlation. *Curr Probl Diagn Radiol*, 44(2): 144–154. <https://doi.org/10.1067/j.cpradiol.2014.09.002>
- [5] Sharpe RE Jr, Levin DC, Parker L, et al., 2013, The Effect of the Controversial US Preventive Services Task Force Recommendations on the Use of Screening Mammography. *J Am Coll Radiol*, 10(1): 21–24. <https://doi.org/10.1016/j.jacr.2012.07.008>
- [6] Broder J, Warshauer DM, 2006, Increasing Utilization of Computed Tomography in the Adult Emergency Department, 2000–2005. *Emerg Radiol*, 13(1): 25–30. <https://doi.org/10.1007/s10140-006-0493-9>
- [7] Eberth JM, Qiu R, Adams SA, et al., 2014, Lung Cancer Screening Using Low-Dose CT: The Current National Landscape. *Lung Cancer*, 85(3): 379–384. <https://doi.org/10.1016/j.lungcan.2014.07.002>
- [8] Oeffinger KC, Fontham ET, Etzioni R, et al., 2015, Breast Cancer Screening for Women at Average Risk: 2015 Guideline Update From the American Cancer Society. *JAMA*, 314(15): 1599–1614. <https://doi.org/10.1001/jama.2015.12783>. Erratum in *JAMA*, 315(13): 1406. <https://doi.org/10.1001/jama.2016.3404>
- [9] US Preventive Services Task Force, 2009, Screening for Breast Cancer: U.S. Preventive Services Task Force Recommendation Statement. *Ann Intern Med*, 151(10): 716–26, W-236. <https://doi.org/10.7326/0003-4819-151-10-200911170-00008>. Erratum in *Ann Intern Med*, 152(3): 199–200. Erratum in *Ann Intern Med*, 152(10): 688.
- [10] Swensen SJ, Jett JR, Sloan JA, et al., 2002, Screening for Lung Cancer with Low-Dose Spiral Computed Tomography. *Am J Respir Crit Care Med*, 165(4): 508–513. <https://doi.org/10.1164/ajrccm.165.4.2107006>
- [11] Monzawa S, Washio T, Yasuoka R, et al., 2013, Incidental Detection of Clinically Unexpected Breast Lesions by

Computed Tomography. *Acta Radiol*, 54(4): 374–379. <https://doi.org/10.1177/0284185113475607>

- [12] Poyraz N, Emlik GD, Keskin S, et al., 2015, Incidental Breast Lesions Detected on Computed Thorax Tomography. *J Breast Health*, 11(4): 163–167. <https://doi.org/10.5152/tjbh.2015.2656>
- [13] Lin YP, Hsu HH, Ko KH, et al., 2016, Differentiation of Malignant and Benign Incidental Breast Lesions Detected by Chest Multidetector-Row Computed Tomography: Added Value of Quantitative Enhancement Analysis. *PLoS One*, 11(4): e0154569. <https://doi.org/10.1371/journal.pone.0154569>
- [14] Parvaiz MA, Isgar B, 2013, Incidental Breast Lesions Detected on Diagnostic CT Scans: A 4-Year Prospective Study. *Breast J*, 19(4): 457–459. <https://doi.org/10.1111/tbj.12142>
- [15] Salvatore M, Margolies L, Kale M, et al., 2014, Breast Density: Comparison of Chest CT with Mammography. *Radiology*, 270(1): 67–73. <https://doi.org/10.1148/radiol.13130733>
- [16] Chetlen A, Mack J, Chan T, 2016, Breast Cancer Screening Controversies: Who, When, Why, and How? *Clin Imaging*, 40(2): 279–282. <https://doi.org/10.1016/j.clinimag.2015.05.017>
- [17] Webb ML, Cady B, Michaelson JS, et al., 2014, A Failure Analysis of Invasive Breast Cancer: Most Deaths from Disease Occur in Women Not Regularly Screened. *Cancer*, 120(18): 2839–2846. <https://doi.org/10.1002/cncr.28199>
- [18] Agliata MF, Calabrò N, Tricca S, et al., 2023, Mammary Nodules as Incidental Findings on Chest Computed Tomography: A Retrospective Analysis on Their Frequency and Predictive Value. *Radiol Med*, 128(8): 912–921. <https://doi.org/10.1007/s11547-023-01670-1>
- [19] Gu D, Su K, Zhao H, 2020, A Case-Based Ensemble Learning System for Explainable Breast Cancer Recurrence Prediction. *Artif Intell Med*, 107: 101858. <https://doi.org/10.1016/j.artmed.2020.101858>
- [20] Lambin P, Rios-Velazquez E, Leijenaar R, et al., 2012, Radiomics: Extracting More Information from Medical Images Using Advanced Feature Analysis. *Eur J Cancer*, 48(4): 441–446. <https://doi.org/10.1016/j.ejca.2011.11.036>
- [21] Valdora F, Houssami N, Rossi F, et al., 2018, Rapid Review: Radiomics and Breast Cancer. *Breast Cancer Res Treat*, 169(2): 217–229. <https://doi.org/10.1007/s10549-018-4675-4>
- [22] Gillies RJ, Kinahan PE, Hricak H, 2016, Radiomics: Images Are More than Pictures, They Are Data. *Radiology*, 278(2): 563–577. <https://doi.org/10.1148/radiol.2015151169>
- [23] Avanzo M, Stancanella J, El Naqa I, 2017, Beyond Imaging: The Promise of Radiomics. *Phys Med*, 38: 122–139. <https://doi.org/10.1016/j.ejmp.2017.05.071>
- [24] Feng Q, Hu Q, Liu Y, et al., 2020, Diagnosis of Triple Negative Breast Cancer Based on Radiomics Signatures Extracted from Preoperative Contrast-Enhanced Chest Computed Tomography. *BMC Cancer*, 20(1): 579. <https://doi.org/10.1186/s12885-020-07053-3>
- [25] Liu Q, Liu W, Yang J, et al., 2020, Pre-Academic Prediction of Axillary Lymph Node Metastasis in Breast Cancer by CT Imaging Group. *China Medical Equipment*, 35(9): 88–92.
- [26] Sechopoulos I, Teuwen J, Mann R, 2021, Artificial Intelligence for Breast Cancer Detection in Mammography and Digital Breast Tomosynthesis: State of the Art. *Semin Cancer Biol*, 72: 214–225. <https://doi.org/10.1016/j.semcancer.2020.06.002>
- [27] Mahmood T, Arsalan M, Owais M, et al., 2020, Artificial Intelligence-Based Mitosis Detection in Breast Cancer Histopathology Images Using Faster R-CNN and Deep CNNs. *J Clin Med*, 9(3): 749. <https://doi.org/10.3390/jcm9030749>
- [28] Mazurowski MA, Buda M, Saha A, et al., 2019, Deep Learning in Radiology: An Overview of the Concepts and a Survey of the State of the Art with Focus on MRI. *J Magn Reson Imaging*, 49(4): 939–954. <https://doi.org/10.1002/jmri.26534>

- [29] Chartrand G, Cheng PM, Vorontsov E, et al., 2017, Deep Learning: A Primer for Radiologists. *Radiographics*, 37(7): 2113–2131. <https://doi.org/10.1148/rg.2017170077>
- [30] Yang X, Wu L, Ye W, et al., 2020, Deep Learning Signature Based on Staging CT for Preoperative Prediction of Sentinel Lymph Node Metastasis in Breast Cancer. *Acad Radiol*, 27(9): 1226–1233. <https://doi.org/10.1016/j.acra.2019.11.007>

Publisher's note

Bio-Byword Scientific Publishing remains neutral with regard to jurisdictional claims in published maps and institutional affiliations.

Advances in Radiomics for Individualized and Precision-Based Diagnosis and Treatment of Lung Cancer

Tongtong Liu[†], Fang Wang[†], Shuai Qie, Xuefeng Wang, Kuan Liu, Yang Li, Hongyun Shi*

Department of Radiotherapy, Affiliated Hospital of Hebei University, Baoding 071000, Hebei Province, China

[†]These authors contributed equally to this work and shared first authorship.

*Corresponding author: Hongyun Shi, hyshi2015@163.com

Copyright: © 2025 Author(s). This is an open-access article distributed under the terms of the Creative Commons Attribution License (CC BY 4.0), permitting distribution and reproduction in any medium, provided the original work is cited.

Abstract: Lung cancer is among the most prevalent cancers and has the highest mortality rate globally. The diagnosis, pathohistological classification, and molecular testing of lung cancer primarily rely on tissue biopsy or surgical resection. These methods are invasive and associated with limitations, including sample quantity and quality, as well as patient tolerance. Radiomics, an emerging technology, enables the extraction of high-throughput quantitative information from medical images, providing radiomic features applicable to clinical diagnosis and treatment. Significant advancements have been made in the application of radiomics to the diagnosis, molecular detection, efficacy prediction, and prognosis of lung cancer. This review examines the progress in radiomics for individualized and precise diagnosis and treatment of lung cancer in recent years.

Keywords: Lung cancer; Non-small cell lung cancer; Small cell lung cancer; Radiomics

Online publication: February 13, 2025

1. Introduction

Lung cancer is one of the most common cancers globally and accounts for the highest mortality among all malignancies ^[1]. In 2020, an estimated 2.2 million new cases were reported, resulting in 1.8 million deaths, which represented 21% of all cancer-related fatalities ^[2]. Non-small cell lung cancer (NSCLC) accounts for 80–85% of cases ^[3], while small cell lung cancer (SCLC) comprises 10–15% ^[4]. Due to the non-specific nature of lung cancer symptoms, more than 70% of patients present with advanced disease (IASLC stage III or IV) at diagnosis ^[5]. According to the American Association for Cancer Research (AACR), as of July 2021, the five-year survival rate for lung cancer was 21.7% ^[6].

Early-stage lung cancer treatments include surgical resection, stereotactic body radiation therapy (SBRT), and percutaneous ablation. Conversely, the primary treatment options for advanced unresectable NSCLC are

radiotherapy, chemotherapy, targeted therapy, and immunotherapy. Current diagnostic methods for lung cancer, including pathological and radiomic characterization and the detection of driver genes and immune receptors (e.g., programmed cell death ligand 1 [PD-L1]), are largely dependent on histological sampling via percutaneous transthoracic needle biopsy (PTNB), bronchoscopic biopsy, or surgical resection^[7]. However, these techniques are constrained by the localized nature of tissue sampling, which may not adequately represent the tumor's heterogeneity^[8]. Moreover, as the expression of driver genes and immune receptors can change over time, repeated biopsies may be required. Tissue biopsy procedures are further influenced by patient tolerance, the risk of complications, and the quantity and quality of the obtained samples.

Medical imaging has become an indispensable tool in modern medicine due to its convenience, speed, and reproducibility. Radiomics, a relatively mature medical image informatics technology, employs artificial intelligence to extract high-throughput quantitative data from imaging modalities such as computed tomography (CT), magnetic resonance imaging (MRI), and positron emission tomography-computed tomography (PET/CT)^[9]. This technology enables the mining of imaging features related to tumor heterogeneity, aiming to develop an individualized and interpretable analytical tool suitable for clinical use^[10]. It is hypothesized that various medical imaging modalities can provide quantitative data correlating with tumor pathophysiology, gene and protein expression, and treatment outcomes, including the efficacy and prognosis of radiotherapy and other therapies^[11].

A growing body of research in radiomics focuses on predicting tumor histology, driver mutations, treatment response, recurrence, and prognosis. These studies contribute to the advancement of precise and personalized diagnosis and treatment. This review highlights recent progress in radiomics, particularly its applications in the individualized and precise diagnosis and management of lung cancer.

2. Radiomics in lung cancer diagnosis

In contemporary clinical practice, the diagnosis of lung cancer remains reliant on puncture biopsy. While puncture biopsy is considered the gold standard for tumor diagnosis, it is an invasive procedure that may yield tissue samples that are not representative of the tumor's overall characteristics^[8]. Additionally, the procedure is associated with potential risks of complications. Therefore, it is imperative to develop new, highly precise methods for accurately diagnosing tumors and determining the degree of tumor differentiation (DTD), lymph node metastasis (LNM), and pathological types^[12].

Numerous studies have demonstrated the significant clinical value of radiomics in addressing these diagnostic challenges. Hendrix *et al.*^[13] and Dennie *et al.*^[14], in their respective studies, extracted texture features from CT images of malignant and benign pulmonary nodules and utilized them to develop high-sensitivity and high-specificity image-based modeling techniques. Their findings validated the effectiveness of such models in classifying pulmonary nodules.

Fan *et al.*^[15] conducted a retrospective analysis aimed at predicting the pathological subtypes of lung nodules in 160 patients with lung adenocarcinoma using radiomics. The study concluded that radiomic features could differentiate between invasive adenocarcinomas and non-invasive lesions, demonstrating a high predictive capability for invasive adenocarcinomas. Similarly, Wang *et al.*^[16] constructed a predictive model using three algorithms: Random Forest, Support Vector Machine, and Logistic Regression. The objective was to predict mediastinal lymph node metastasis in patients with NSCLC. The CT radiomic model developed using the Random Forest algorithm exhibited a high degree of accuracy, with an area under the curve (AUC) value of 0.909.

In another study, Zhu *et al.* ^[17] collected CT images from 129 lung cancer patients and developed a radiomics model to distinguish between lung adenocarcinoma (ADC) and lung squamous cell carcinoma (SCC). The AUCs for the training and validation sets were 0.905 and 0.893, respectively, with sensitivities of 83.00% and 82.80% and specificities of 92.90% and 90.00%. These results demonstrate that radiomics is a highly effective method for identifying the pathological types of lung cancer.

In conclusion, substantial evidence from multiple studies indicates that radiomics is an effective approach for predicting the degree of tumor differentiation, lymph node metastasis, and pathological types in lung cancer patients.

3. Radiomics in the detection of EGFR-mutated genes

Targeted therapy has become a pivotal component in the management of patients with NSCLC. Given that the *Epidermal Growth Factor Receptor (EGFR)* is a frequently utilized target gene in NSCLC, determining the mutation status and subtype of *EGFR* is crucial for the effective implementation of targeted therapy. Molecular testing remains the primary method for identifying *EGFR* mutation status. However, this approach has limitations due to the temporal and spatial heterogeneity of tumors, rendering it unsuitable for certain patients ^[18].

Radiomics has made significant progress in predicting *EGFR* mutations. In a study by Mei *et al.* ^[19], the CT imaging features of 296 NSCLC patients were analyzed and combined with clinical features to construct a predictive model. This model achieved AUC values of 0.655 for the *EGFR* exon 19 deletion mutation, 0.675 for the *EGFR* exon 21 L858R mutation, and 0.664 for the overall mutation status. These findings suggest that imaging characteristics may play a critical role in predicting *EGFR* status and indicate the potential of radiomic features as biomarkers for identifying *EGFR* mutation status and subtypes.

Cheng *et al.* ^[20] developed a gradient-enhanced decision tree model based on the ground-glass appearance of CT images in early-stage lung adenocarcinoma. The model identified *EGFR* mutation status with an AUC value of 0.822. This model was validated in patients with lung adenocarcinoma undergoing targeted therapy, demonstrating a significant improvement in the remission rate of *EGFR*-mutated patients, increasing from 25.9% to 53.8%.

In another study, Clay *et al.* ^[21] incorporated CT images of lung tissue with a 10-mm peri-tumor circumference into their analysis. The predictive model developed in this study achieved an AUC value of 0.72 for identifying *EGFR* mutation status.

In conclusion, substantial evidence demonstrates that CT-based radiomics has excellent predictive efficacy in determining the *EGFR* mutation status of NSCLC patients, thereby offering significant potential for enhancing targeted therapy strategies.

4. Radiomics in the assessment of lung cancer treatment efficacy

The current clinical treatments for lung cancer include chemotherapy, radiotherapy, targeted therapy, immunotherapy, and other modalities. However, the prognosis of individual patients may vary significantly depending on the treatment regimen employed. Moreover, there is a lack of reliable methods for accurately predicting and assessing treatment response ^[22]. In recent years, the use of imaging techniques, such as CT, PET/CT, and others, to predict the efficacy of lung cancer treatments has garnered increasing attention. The ability to predict therapeutic efficacy and prognostic outcomes using these techniques could substantially enhance their

clinical applications.

In a study by Yang *et al.* ^[23], a predictive model was developed using radiomic features extracted from pre-treatment chest CT images. This model successfully predicted the response of NSCLC to first-line chemotherapy, targeted therapy, or a combination of both, achieving an AUC of 0.746 (95% confidence interval [CI], 0.646–0.846). Zhang *et al.* ^[24] conducted a retrospective study of 122 NSCLC patients with EGFR mutation-positive status to investigate the efficacy of combining CT radiomics with cytokeratin 19 fragment levels in predicting the outcomes of epidermal growth factor receptor tyrosine kinase inhibitors (EGFR-TKIs) therapy. The AUCs for the clinical model, the radiomics model, and the combined model in the training set were 0.686, 0.800, and 0.836, respectively; the AUCs in the validation set were 0.666, 0.774, and 0.837, respectively.

Regarding immunotherapy, the prediction of treatment response is currently based on the expression of biomarkers within the tumor immune microenvironment, such as PD-L1. Tian *et al.* ^[25] analyzed CT images from 143 NSCLC patients and constructed a CT radiomic nomogram by integrating clinical factors with radiomic features. This model demonstrated high efficacy in assessing PD-1 expression in NSCLC patients, with an AUC of 0.92.

To predict the efficacy of stereotactic body radiation therapy (SBRT) for NSCLC, Wang *et al.* ^[26] developed and validated a nomogram based on radiomic features extracted from pre-treatment CT images. The model exhibited high predictive performance, with an AUC value of 0.808 for the training set and 0.741 for the validation set.

The evidence from these studies demonstrates that radiomic features can effectively forecast treatment response in patients with NSCLC. This capability can assist clinicians in modifying, intensifying, or altering treatment plans at the earliest opportunity, thereby improving patient outcomes.

5. Radiomics in lung cancer regression

In the context of lung cancer regression, radiomics-based studies have proven to facilitate more precise survival predictions for lung cancer patients and support clinicians in selecting personalized treatment strategies. Several studies have demonstrated the efficacy of intra-tumor radiomic features in predicting overall survival (OS), tumor recurrence prognosis, and time to progression in lung cancer patients.

Sawayanagi *et al.* ^[27] developed a predictive model using clinical features derived from pre-treatment CT scans and radiomic features of the primary tumor. The predicted OS time (mean: 37.8 months) was found to closely align with the observed OS time (33.7 months), demonstrating the model's accuracy. Niu *et al.* ^[28] proposed a multi-omics model incorporating CT images, dosimetric features, and clinical characteristics of lung cancer patients. This model significantly enhanced the precision of radiation pneumonitis (RP) prediction, achieving AUC values of 0.94 and 0.92 in the test and validation sets, respectively. The study also revealed that patients with RP exhibited a longer OS compared to those without RP, particularly those with mild RP. The median OS was 31 months in the non-RP group and 49 months in the RP group (hazard ratio [HR] = 0.53, $P = 0.0022$). Among RP subgroups, the median OS was 57 months for patients with mild RP and 25 months for those with severe RP (HR = 3.72, $P < 0.0001$).

Huang *et al.* ^[29] utilized machine learning to analyze pre-treatment FDG-PET and lung cancer CT scans. Their integrated PET+CT model demonstrated high predictive accuracy for disease progression in NSCLC patients, achieving an accuracy of 0.790 and an AUC of 0.876. Zheng *et al.* ^[30] conducted a multicenter trial to predict

progression-free survival (PFS) using CT scan results for SCLC. The study also evaluated the incremental value of radiomic features alongside clinical risk factors for individual PFS estimation. Results indicated that radiomic features were significantly associated with PFS (HR = 4.531, 95% CI: 3.524–5.825, $P < 0.001$). Additionally, the radiomic nomogram demonstrated superior predictive performance for PFS (C-index 0.799) compared to the clinical nomogram (C-index 0.629).

Collectively, these studies underscore the efficacy of radiomics in predicting survival outcomes for patients with various forms of lung cancer. This approach holds significant promise for guiding the development of personalized treatment strategies, ultimately improving patient care and prognosis.

6. Limitations and future prospects

In the diagnosis and treatment of tumors, achieving accurate diagnosis and staging, administering standardized and individualized treatments, and predicting treatment response, recurrence, and prognosis are of paramount importance. Radiomics, an emerging medical imaging technology, enables the generation of descriptive data, the development of predictive models, and the correlation of quantitative imaging features with phenotypic or gene-protein characteristics. It contributes significantly to the detection, diagnosis, staging, treatment response prediction, and prognosis assessment of lung cancer, thereby playing an increasingly vital role in clinical decision-making.

However, several limitations persist in current radiomics research:

- (1) Study design: Most studies in the field involve relatively small sample sizes and are retrospective, single-center investigations. These studies often lack external validation datasets and incorporate a limited range of clinical factors and radiomic features.
- (2) Equipment dependence: High-quality, standardized imaging data are crucial for radiomics. Variations in imaging equipment and techniques across different institutions can affect the reliability and reproducibility of radiomic features, leading to inconsistent results.
- (3) Standardization challenges: The radiomics process currently lacks standardized databases, research protocols, image reconstruction algorithms, pre-processing methods, and feature extraction algorithms. Additionally, the stability and reproducibility of studies require significant improvement to enable widespread clinical application.
- (4) Resource requirements: The implementation of radiomics and artificial intelligence (AI) demands substantial investment in technology, expertise, and training. These requirements may pose challenges, particularly for smaller healthcare institutions or those with limited resources.

Addressing these challenges and limitations is critical to fully realizing the potential of radiomics in optimizing lung cancer diagnosis and treatment. Overcoming these obstacles is essential to advancing personalized medicine and enhancing clinical outcomes in lung cancer management.

Disclosure statement

The authors declare no conflict of interest.

References

- [1] Xu Y, Hosny A, Zeleznik R, et al., 2019, Deep Learning Predicts Lung Cancer Treatment Response from Serial Medical Imaging. *Clin Cancer Res*, 25(11): 3266–3275. <https://doi.org/10.1158/1078-0432.CCR-18-2495>
- [2] Sung H, Ferlay J, Siegel RL, et al., 2021, Global Cancer Statistics 2020: GLOBOCAN Estimates of Incidence and Mortality Worldwide for 36 Cancers in 185 Countries. *CA Cancer J Clin*, 71(3): 209–249. <https://doi.org/10.3322/caac.21660>
- [3] Cancer Research UK, 2019, Types of Lung Cancer, viewed August 23, 2024. <https://www.cancerresearchuk.org/about-cancer/lung-cancer/stages-typesgrades/types>
- [4] Rudin CM, Brambilla E, Faivre-Finn C, et al., 2021, Small-Cell Lung Cancer. *Nat Rev Dis Primers*, 7(1): 3. <https://doi.org/10.1038/s41572-020-00235-0>
- [5] Yin X, Liao H, Yun H, et al., 2022, Artificial Intelligence-Based Prediction of Clinical Outcome in Immunotherapy and Targeted Therapy of Lung Cancer. *Semin Cancer Biol*, 86(Pt 2): 146–159. <https://doi.org/10.1016/j.semcancer.2022.08.002>
- [6] AACR Cancer Progress Report, 2024, Cancer Progress Report, viewed August 23, 2024, <https://cancerprogressreport.aacr.org/progress/>
- [7] Lantuejoul S, Sound-Tsao M, Cooper WA, et al., 2020, PD-L1 Testing for Lung Cancer in 2019: Perspective From the IASLC Pathology Committee. *J Thorac Oncol*, 15(4): 499–519. <https://doi.org/10.1016/j.jtho.2019.12.107>
- [8] Hu M, Wu L, Zhang X, et al., 2023, Comparative Evaluation of 2 Different Percutaneous Techniques of Simultaneous Needle Biopsy With Microwave Ablation of Suspected Malignant Pulmonary Nodules. *Technol Cancer Res Treat*, 22: 15330338231168458. <https://doi.org/10.1177/15330338231168458>
- [9] Kumar V, Gu Y, Basu S, et al., 2012, Radiomics: The Process and the Challenges. *Magn Reson Imaging*, 30(9): 1234–1248. <https://doi.org/10.1016/j.mri.2012.06.010>
- [10] Hatt M, Tixier F, Visvikis D, et al., 2017, Radiomics in PET/CT: More Than Meets the Eye? *J Nucl Med*, 58(3): 365–366. <https://doi.org/10.2967/jnumed.116.184655>
- [11] Lambin P, Rios-Velazquez E, Leijenaar R, et al., 2012, Radiomics: Extracting More Information from Medical Images Using Advanced Feature Analysis. *Eur J Cancer*, 48(4): 441–446. <https://doi.org/10.1016/j.ejca.2011.11.036>
- [12] Park YY, Park ES, Kim SB, et al., 2012, Development and Validation of a Prognostic Gene-Expression Signature for Lung Adenocarcinoma. *PLoS One*, 7(9): e44225. <https://doi.org/10.1371/journal.pone.0044225>
- [13] Hendrix N, Veenstra DL, Cheng M, et al., 2022, Assessing the Economic Value of Clinical Artificial Intelligence: Challenges and Opportunities. *Value Health*, 25(3): 331–339. <https://doi.org/10.1016/j.jval.2021.08.015>
- [14] Dennie C, Bayanati H, Souza CA, et al., 2021, Role of the Thoracic Radiologist in the Evaluation and Management of Solid and Subsolid Lung Nodules. *Thorac Surg Clin*, 31(3): 283–292. <https://doi.org/10.1016/j.thorsurg.2021.04.004>
- [15] Fan L, Fang M, Li Z, et al., 2019, Radiomics Signature: A Biomarker for the Preoperative Discrimination of Lung Invasive Adenocarcinoma Manifesting as a Ground-Glass Nodule. *Eur Radiol*, 29(2): 889–897. <https://doi.org/10.1007/s00330-018-5530-z>
- [16] Wang Y, Wu Y, Wang L, et al., 2023, Value of CT Radiomics Models Constructed by Three Algorithms to the Prediction of Mediastinal Lymph Node Metastasis in Non-Small-Cell Lung Cancer Patients. *Journal of Chinese Practical Diagnosis and Therapy*, 37(11): 1081–1086.
- [17] Zhu X, Dong D, Chen Z, et al., 2018, Radiomic Signature as a Diagnostic Factor for Histologic Subtype Classification of Non-Small Cell Lung Cancer. *Eur Radiol*, 28(7): 2772–2778. <https://doi.org/10.1007/s00330-017-5221-1>
- [18] Lambin P, Leijenaar RTH, Deist TM, et al., 2017, Radiomics: The Bridge Between Medical Imaging and Personalized

Medicine. *Nat Rev Clin Oncol*, 14(12): 749–762. <https://doi.org/10.1038/nrclinonc.2017.141>

- [19] Lu CF, Liao CY, Chao HS, et al., 2023, A Radiomics-Based Deep Learning Approach to Predict Progression Free-Survival After Tyrosine Kinase Inhibitor Therapy in Non-Small Cell Lung Cancer. *Cancer Imaging*, 23(1): 9. <https://doi.org/10.1186/s40644-023-00522-5>
- [20] Cheng B, Deng H, Zhao Y, et al., 2022, Predicting EGFR Mutation Status in Lung Adenocarcinoma Presenting as Ground-Glass Opacity: Utilizing Radiomics Model in Clinical Translation. *Eur Radiol*, 32(9): 5869–5879. <https://doi.org/10.1007/s00330-022-08673-y>
- [21] Clay R, Kipp BR, Jenkins S, et al., 2017, Computer-Aided Nodule Assessment and Risk Yield (CANARY) May Facilitate Non-Invasive Prediction of EGFR Mutation Status in Lung Adenocarcinomas. *Sci Rep*, 7(1): 17620. <https://doi.org/10.1038/s41598-017-17659-6>
- [22] Chang R, Qi S, Wu Y, et al., 2022, Deep Multiple Instance Learning for Predicting Chemotherapy Response in Non-Small Cell Lung Cancer Using Pretreatment CT Images. *Sci Rep*, 12: 19829. <https://doi.org/10.1038/s41598-022-24278-3>
- [23] Yang F, Zhang J, Zhou L, et al., 2022, CT-Based Radiomics Signatures can Predict the Tumor Response of Non-Small Cell Lung Cancer Patients Treated with First-Line Chemotherapy and Targeted Therapy. *Eur Radiol*, 32(3): 1538–1547. <https://doi.org/10.1007/s00330-021-08277-y>
- [24] Zhang C, Ding Z, Chen P, 2023, The Value of CT Radiomics Combined with Cytokeratin-19 Fragment in Predicting the Effectiveness of EGFR-TKIs for Non-Small Cell Lung Cancer with EGFR Mutation. *Radiologic Practice*, 38(12): 1532–1538.
- [25] Tian Q, Feng F, Chen Q, et al., 2023, CT Radiomics Nomogram for Evaluating Programmed Death Receptor 1 Expression of Non-Small Cell Lung Cancer. *Chinese Journal of Medical Imaging Technology*, 39(4): 543–548.
- [26] Wang H, Wang H, Wang X, et al., 2023, The Value of Nomogram Model Based on CT Radiomics in Predicting the Efficacy of Stereotactic Body Radiotherapy for Lung Tumors. *Journal of Modern Oncology*, 31(5): 898–904.
- [27] Sawayanagi S, Yamashita H, Nozawa Y, et al., 2022, Establishment of a Prediction Model for Overall Survival after Stereotactic Body Radiation Therapy for Primary Non-Small Cell Lung Cancer Using Radiomics Analysis. *Cancers (Basel)*, 14(16): 3859. <https://doi.org/10.3390/cancers14163859>
- [28] Niu L, Chu X, Yang X, et al., 2023, A Multiomics Approach-Based Prediction of Radiation Pneumonia in Lung Cancer Patients: Impact on Survival Outcome. *J Cancer Res Clin Oncol*, 149(11): 8923–8934. <https://doi.org/10.1007/s00432-023-04827-7>
- [29] Huang B, Sollee J, Luo YH, et al., 2022, Prediction of Lung Malignancy Progression and Survival with Machine Learning Based on Pre-Treatment FDG-PET/CT. *EBioMedicine*, 82: 104127. <https://doi.org/10.1016/j.ebiom.2022.104127>
- [30] Zheng X, Liu K, Li C, et al., 2023, A CT-Based Radiomics Nomogram for Predicting the Progression-Free Survival in Small Cell Lung Cancer: A Multicenter Cohort Study. *Radiol Med*, 128(11): 1386–1397. <https://doi.org/10.1007/s11547-023-01702-w>

Publisher's note

Bio-Byword Scientific Publishing remains neutral with regard to jurisdictional claims in published maps and institutional affiliations.

The High Expression of *EXOSC3* in OSCC is Associated with Poor Prognosis and Immune Infiltration

Yucunxi Liu, Jianguo Liu*

Special Key Laboratory of Oral Diseases Research, School of Stomatology, Zunyi Medical University, Zunyi 563000, Guizhou Province, China

*Corresponding author: Jianguo Liu, 852235104@qq.com

Copyright: © 2025 Author(s). This is an open-access article distributed under the terms of the Creative Commons Attribution License (CC BY 4.0), permitting distribution and reproduction in any medium, provided the original work is cited.

Abstract: Oral squamous cell carcinoma (OSCC) is the most common malignant tumor in the oral and maxillofacial region, primarily affecting the tongue, gingiva, oral cavity, buccal mucosa, and floor of the mouth. It exhibits high rates of recurrence and metastasis, contributing to a poor prognosis for patients. Identifying molecular markers associated with OSCC holds significant value for advancing its diagnosis, treatment, and prognosis. *Exosome Component 3 (EXOSC3)* is a protein-coding gene involved in the auto-degradation of E3 ubiquitin ligase COP 1 and rRNA processing in the nucleus and cytoplasmic sol. This gene plays a crucial role in diseases such as colon cancer and non-small cell lung cancer. Bioinformatics analysis revealed that *EXOSC3* expression is significantly elevated in OSCC and is associated with poor patient prognosis. Gene Ontology (GO) and Kyoto Encyclopedia of Genes and Genomes (KEGG) enrichment analyses indicate that *EXOSC3* is strongly linked to the cytokine-cytokine receptor interaction, Toll-like receptor signaling pathway, and JAK-STAT signaling pathway. Moreover, immune infiltration analysis demonstrated a significant association between *EXOSC3* expression and immune cell subset infiltration, as well as immune checkpoint expression, underscoring its importance in OSCC. However, further research is required to elucidate the specific role of *EXOSC3* in OSCC diagnosis and treatment. A comprehensive investigation into the mechanisms of *EXOSC3* in OSCC may reveal new potential targets for improving the diagnosis and treatment of this malignancy.

Keywords: *EXOSC3*; Oral squamous cell carcinoma; Immune microenvironment; Immune checkpoint

Online publication: February 13, 2025

1. Introduction

Oral squamous cell carcinoma (OSCC) is a malignant tumor originating from the epithelium of the oral mucosa, accounting for over 90% of all oral cancers ^[1]. Various factors, including smoking, alcohol consumption, viral infections, environmental influences, and genetic predispositions, are associated with OSCC development ^[2]. The unique anatomical characteristics of the oral and maxillofacial region, characterized by abundant blood supply and lymphatic networks, render it susceptible to lymph node metastasis, a key factor influencing prognosis. Additionally, the complex structural nature of the maxillofacial region causes significant damage to aesthetics and

functional abilities, such as speech, thereby severely impacting the quality of life of affected individuals^[3]. Despite advancements in treatment modalities, including radiotherapy, chemotherapy, surgery, and immunotherapy, the prognosis for patients in advanced stages remains suboptimal^[4]. Thus, exploring novel diagnostic and therapeutic targets is essential for addressing the underlying mechanisms of OSCC development.

Exosome Component 3 (EXOSC3) is a protein-coding gene implicated in the auto-degradation of E3 ubiquitin ligase COP 1 and rRNA processing within the nucleus and cytoplasmic sol. Clinically, *EXOSC3* is associated with diseases such as cerebellar ataxia type 1B and non-syndromic cerebellar ataxia, as well as the development of various tumors. For instance, MYD88 regulates *EXOSC3* to influence colon cancer progression^[5]. In non-small cell lung cancer, functional variants of *EXOSC3* are associated with patient prognosis and survival^[6]. However, studies investigating the role of *EXOSC3* in OSCC remain limited. Therefore, a detailed exploration of its function in OSCC may provide new insights into potential therapeutic targets.

This study utilizes bioinformatics analysis of transcriptome data from The Cancer Genome Atlas (TCGA) database to examine differences in *EXOSC3* expression between OSCC and adjacent tissues. The impact of these expression differences on OSCC patient prognosis is assessed through survival curve analysis. Co-expression analyses within the TCGA-OSCC cohort are conducted to identify potential functional networks involving *EXOSC3*. Additionally, Gene Ontology (GO) and Kyoto Encyclopedia of Genes and Genomes (KEGG) analyses are employed to explore the pathways through which *EXOSC3* may influence OSCC progression. Immune infiltration and drug sensitivity analyses further evaluate the potential impact of *EXOSC3* on immunotherapy and chemotherapy responses.

2. Materials and methods

2.1. Sample data and clinical information download

Transcriptome data and clinical information for OSCC patients were downloaded from TCGA, comprising data from 346 tumor tissues and 32 normal tissues^[7].

2.2. ROC analysis

To evaluate the diagnostic performance of *EXOSC3* in the TCGA-OSCC cohort, the “pROC” R package was used to analyze the expression levels and clinical information of OSCC cases. The sensitivity of *EXOSC3* in OSCC was assessed, and the area under the curve (AUC) was calculated.

2.3. Survival analysis

The impact of *EXOSC3* expression levels on OSCC patient prognosis was investigated by excluding cases with missing clinical information. Patients were categorized into high- and low-expression groups based on *EXOSC3* expression levels. Survival analysis and visualization were performed using the “survival” R package.

2.4. Co-expression analysis

To identify co-expressed genes associated with *EXOSC3* in the TCGA-OSCC cohort, correlation analysis was conducted using the “limma” R package. Pearson’s correlation test was employed to calculate correlation coefficients, with a significance threshold of $P < 0.001$. The results were visualized using scatter plots.

2.5. Differential expression analysis

To identify differentially expressed genes (DEGs) associated with *EXOSC3*, OSCC patients were divided into

high- and low-expression groups based on the median expression level of *EXOSC3*. Differential analysis was performed using the “limma” R package, with selection criteria of $|\log\text{FC}| > 1$ and $P < 0.05$. The top 50 DEGs were visualized using a heatmap^[8].

2.6. Functional enrichment analysis

The potential roles of *EXOSC3* in OSCC were explored through GO and KEGG enrichment analyses of DEGs associated with *EXOSC3*. The analyses were conducted using the “clusterProfiler” R package, with a significance threshold of $P < 0.05$. The results were visualized using the “ggplot2” R package^[9].

2.7. Immune infiltration analysis

The impact of *EXOSC3* on immune cell subsets in OSCC was assessed using the CIBERSORT algorithm to calculate immune cell scores and evaluate immune infiltration. Spearman correlation analysis was employed, with a significance threshold of $P < 0.05$, to determine the relationship between *EXOSC3* expression and immune cell subsets^[10].

2.8. Immune checkpoint analysis

To investigate the role of *EXOSC3* in immunotherapy, Pearson correlation analysis was conducted on 47 immune checkpoint genes, with a significance threshold of $P < 0.001$.

2.9. Drug sensitivity analysis

The effect of *EXOSC3* on chemotherapy drug sensitivity in the TCGA-OSCC cohort was evaluated using the “pRRophetic” R package to analyze the IC_{50} values of chemotherapy drugs for each sample. Patients were divided into high- and low-expression groups based on the median *EXOSC3* expression level, and differences in IC_{50} values were analyzed using the Wilcoxon test. The results were visualized using the “limma” R package.

2.10. Statistical analysis

All statistical analyses were conducted using R (v4.3.2, R Foundation for Statistical Computing). A P -value of < 0.05 was considered statistically significant.

3. Results

3.1. Abnormal expression of *EXOSC3* in OSCC and its association with poor prognosis

Transcriptome data and relevant clinical information from the TCGA-OSCC cohort were analyzed. Using the “limma” R package, it was found that *EXOSC3* expression was significantly elevated in OSCC tissues compared to normal tissues (**Figure 1A**). To confirm this finding, only cases with paired data were analyzed, revealing consistent results; *EXOSC3* expression was significantly higher in paired OSCC tissues compared to paired normal tissues (**Figure 1B**).

To further explore the role of *EXOSC3* in OSCC, an ROC curve was plotted for the TCGA-OSCC cohort. The area under the curve (AUC) was 0.870, with a 95% confidence interval of 0.816–0.922, indicating that *EXOSC3* exhibits good diagnostic efficacy for OSCC (**Figure 1C**). Kaplan-Meier survival analysis revealed that patients with high *EXOSC3* expression had significantly poorer overall survival (**Figure 1D**). Additionally, higher *EXOSC3* expression levels were positively associated with more advanced tumor stages, including the T stage.

3.2. Gene co-expression analysis of EXOSC3 in OSCC

Given the observed association between elevated EXOSC3 expression and poor prognosis in OSCC, gene co-expression analysis was performed using the “limma” R package. Six genes were identified as strongly correlated with EXOSC3: *APTX*, *CLTA*, *RPS6*, *MELK*, *DNAJA1*, and *STOML2* (Figures 2A–F).

3.3. Functional analysis of EXOSC3 in OSCC

To investigate the functional roles of EXOSC3 in OSCC, samples were categorized into high and low expression groups based on the median EXOSC3 expression level. Differential expression analysis using the “limma” R package identified DEGs associated with EXOSC3. The top 50 DEGs were visualized using a heatmap (Figure 3A).

GO enrichment analysis revealed that EXOSC3 was involved in various cellular biological processes, including the humoral immune response, activation of natural killer cells in immune responses, negative regulation of activated T cell proliferation, and natural killer cell activation (Figures 3B and C). KEGG enrichment analysis identified its association with key pathways such as cytokine-cytokine receptor interaction, natural killer cell-mediated cytotoxicity, the Toll-like receptor signaling pathway, and the JAK-STAT signaling pathway. These pathways are implicated in tumorigenesis and progression (Figures 3D and E). These findings suggest that EXOSC3 may play a pivotal role in OSCC.

3.4. Association of EXOSC3 with the immune microenvironment in OSCC

Enrichment analysis indicated that EXOSC3 is closely linked to immune cell activity, particularly involving natural killer cells and T cells. To further explore this relationship, the association between EXOSC3 and the immune microenvironment in OSCC was assessed. Significant differences in stromal scores were observed between high and low EXOSC3 expression groups, suggesting that EXOSC3 expression levels may influence stromal cell content in the tumor microenvironment (Figure 4A).

Immune cell infiltration was analyzed using the CIBERSORT algorithm. Significant differences were observed in immune cell subsets, including T cells CD8, T cells CD4 memory activated, T cells follicular helper, macrophages M0, and macrophages M1, between high and low EXOSC3 expression groups (Figure 4B). Spearman correlation analysis further revealed significant correlations of EXOSC3 with macrophages M1, T cells CD8, T cells CD4 memory activated, T cells follicular helper, monocytes, and macrophages M0 (Figures 4C–F).

3.5. Impact of EXOSC3 expression on tumor-related treatments

The role of EXOSC3 in immunotherapy was evaluated by examining its correlation with 47 immune checkpoint genes. Positive correlations were identified with *CD40*, *TNFRSF25*, *CD70*, *LAG3*, *PDCD1*, *IDO1*, *HAVCR2*, *CD274*, *PDCD1LG2*, and *CTLA4*, highlighting the potential role of EXOSC3 in immune regulation and immunotherapy (Figures 5A and B).

To assess its impact on chemotherapy sensitivity, data from the Cancer Genome Project (CGP) database were analyzed. A significant correlation was found between EXOSC3 expression levels and sensitivity to various chemotherapy drugs, including 5-Fluorouracil, AKT inhibitor VIII, Bexarotene, and Bleomycin (Figures 5C–F).

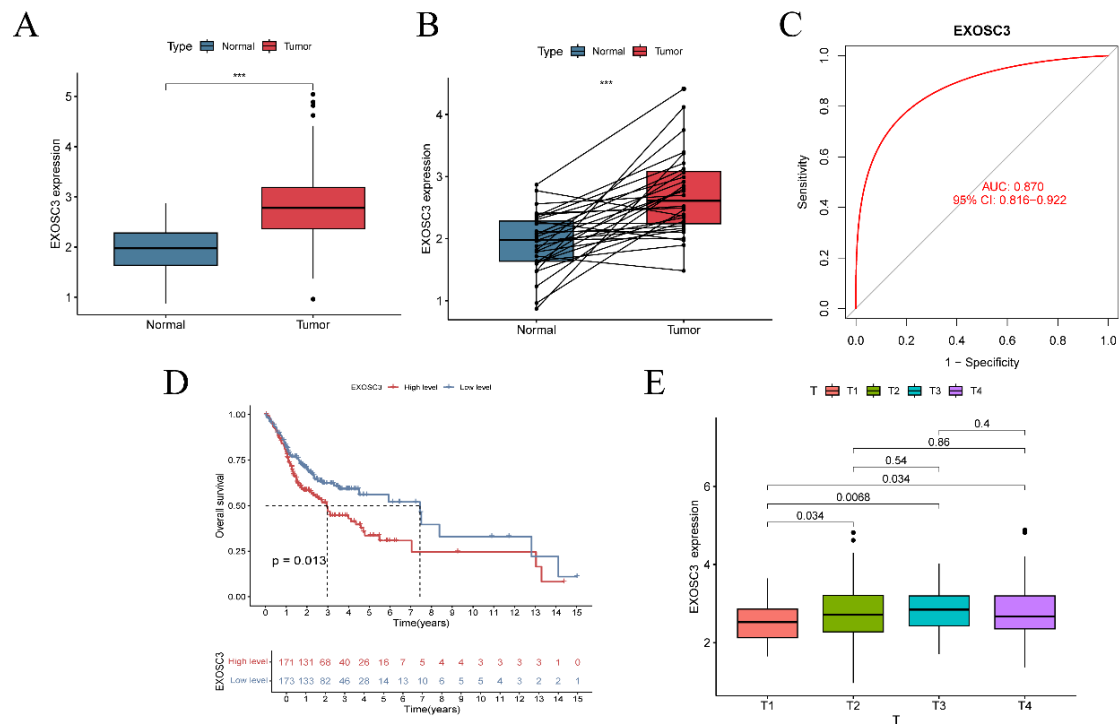


Figure 1. High expression of *EXOSC3* in OSCC is associated with poor prognosis. (A) In the TCGA-OSCC cohort, *EXOSC3* expression was significantly higher in OSCC tissues compared to adjacent normal tissues ($***P < 0.001$). (B) Paired analysis of adjacent normal tissues and OSCC tissues also demonstrated significantly increased *EXOSC3* expression in OSCC ($***P < 0.001$). (C) Receiver operating characteristic curve for *EXOSC3* in the TCGA-OSCC cohort, indicating its diagnostic efficacy. (D) Kaplan-Meier survival curve illustrating overall survival differences between high-expression and low-expression groups of *EXOSC3*. (E) Correlation between T stage and *EXOSC3* expression in patients from the TCGA-OSCC cohort.

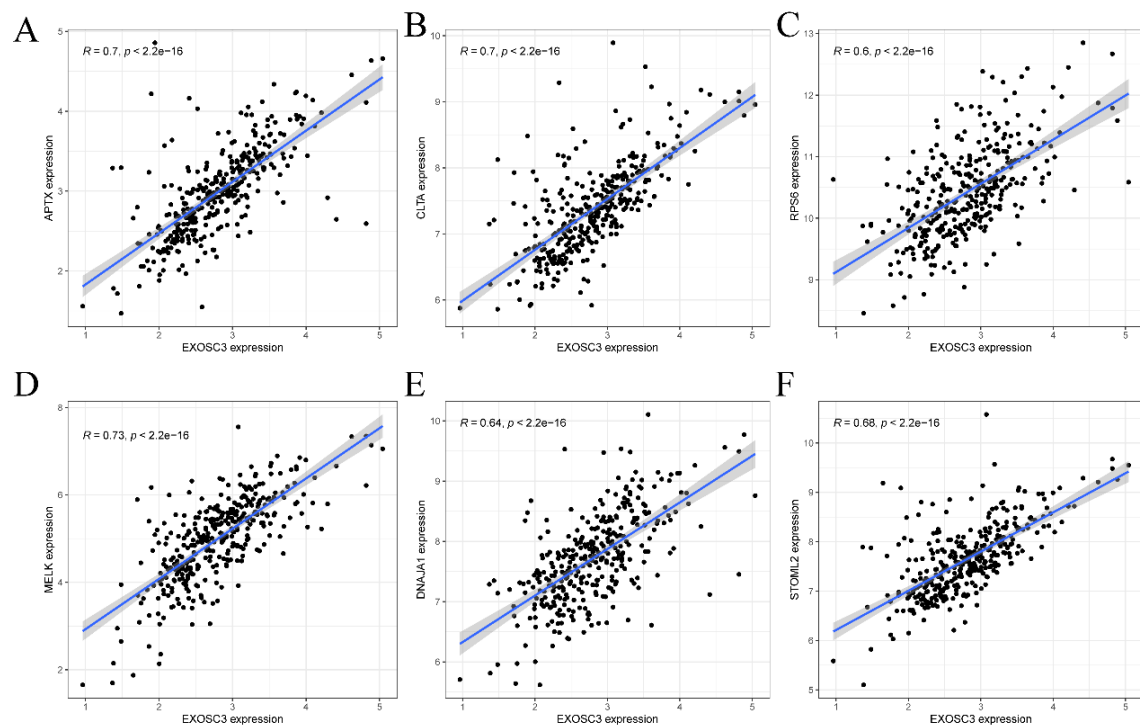


Figure 2. Gene co-expression of *EXOSC3* in OSCC. (A–F) Identification of six genes co-expressed with *EXOSC3* in the TCGA-OSCC cohort.

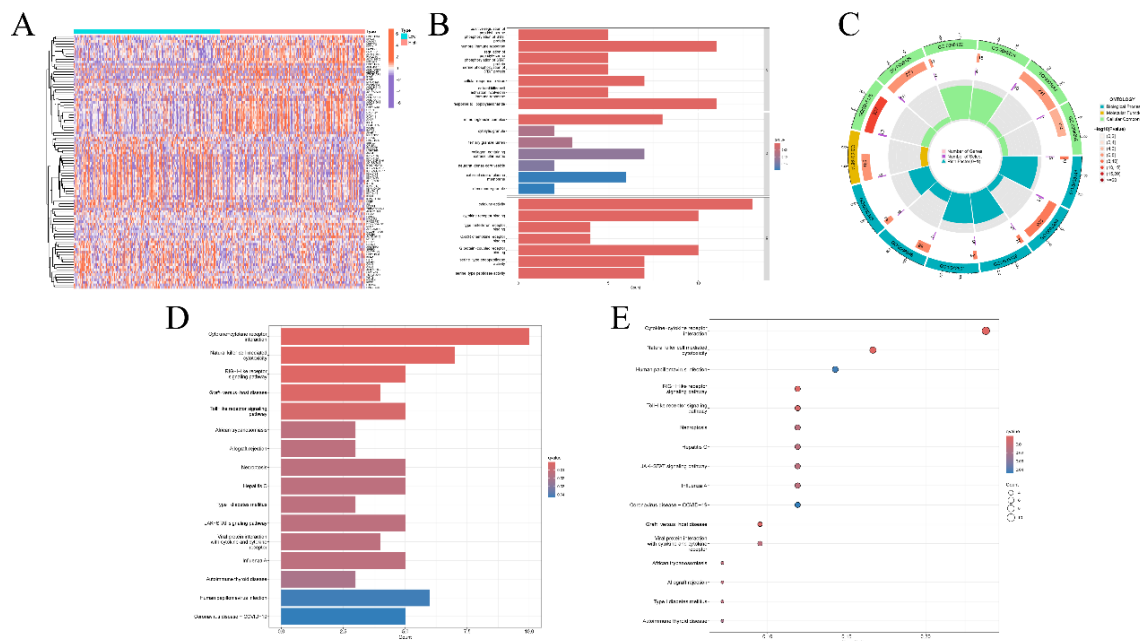


Figure 3. Functional role of *EXOSC3* in OSCC. (A) Heatmap of differentially expressed genes associated with *EXOSC3* in the TCGA-OSCC cohort. (B–C) Results of Gene Ontology enrichment analysis. (D–E) Results of Kyoto Encyclopedia of Genes and Genomes enrichment analysis.

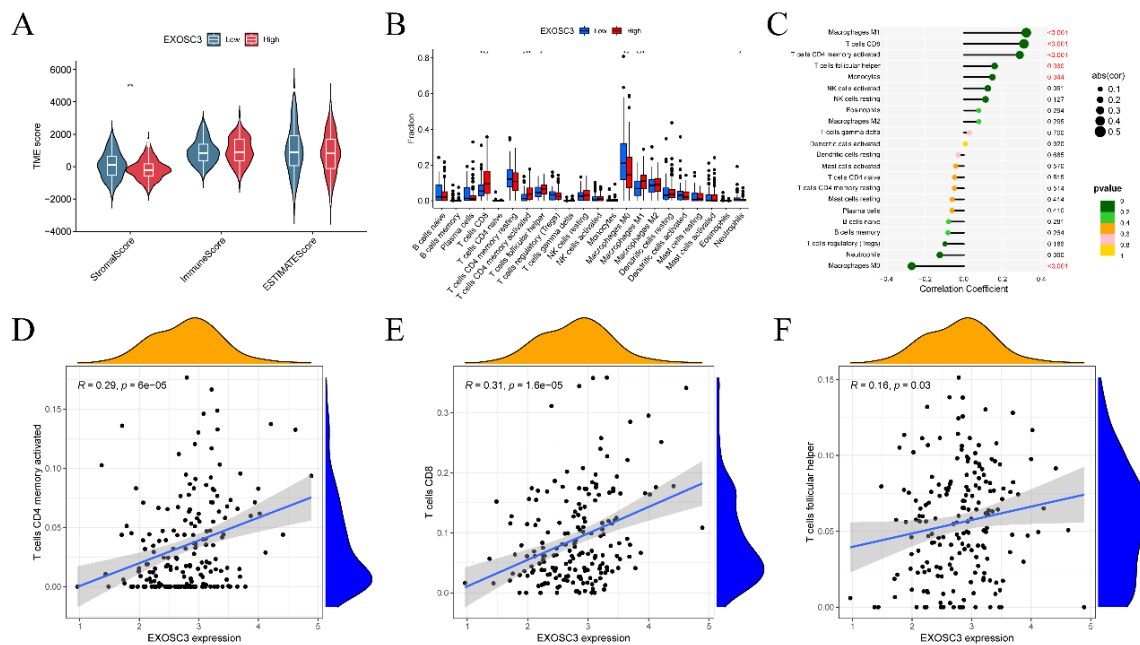


Figure 4. The role of *EXOSC3* in the immune microenvironment. (A) Assessment of *EXOSC3* in the immune microenvironment of OSCC. (B) Differences in various immune cell populations between high and low *EXOSC3* expression groups in OSCC. (C–F) Correlations between *EXOSC3* expression and specific immune cell populations.

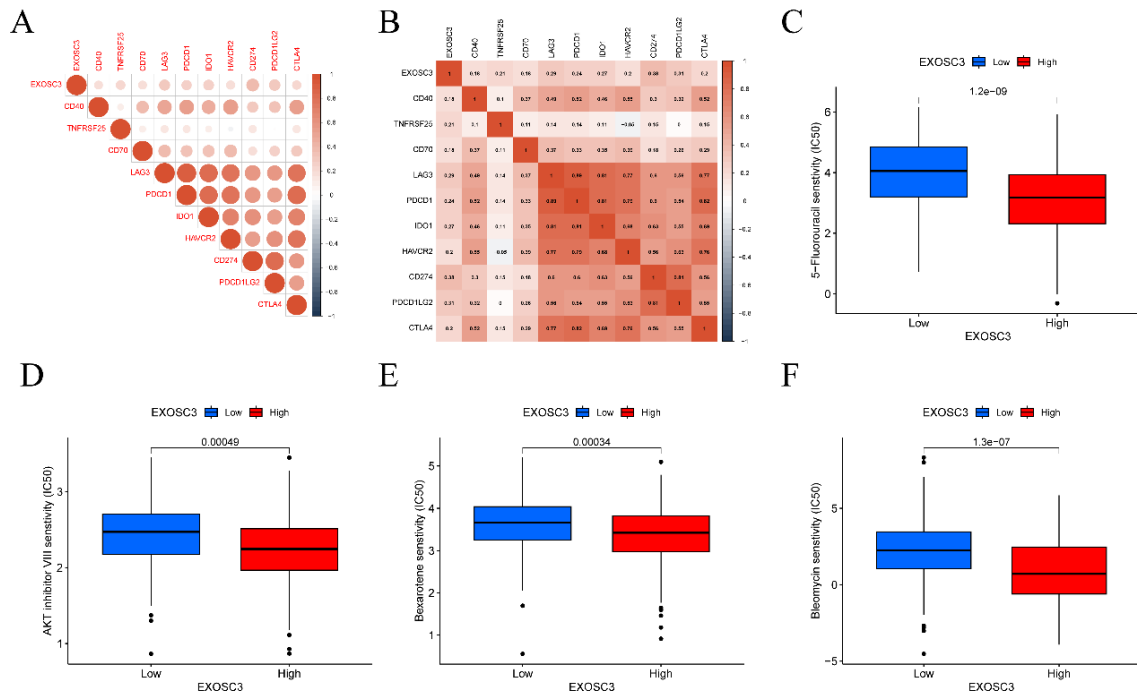


Figure 5. Correlation of *EXOSC3* expression levels with immune checkpoints and chemotherapy drugs in OSCC. (A–B) Analysis of correlations between *EXOSC3* expression and immune checkpoint genes. (C) Association between *EXOSC3* expression and sensitivity to 5-Fluorouracil. (D) Association between *EXOSC3* expression and sensitivity to AKT inhibitor VIII. (E) Association between *EXOSC3* expression and sensitivity to Bexarotene. (F) Association between *EXOSC3* expression and sensitivity to Bleomycin.

4. Discussion

OSCC is a prevalent type of squamous cell carcinoma in the head and neck region, predominantly originating from the stratified squamous epithelium of the oral mucosa and accounting for up to 90% of oral cancers^[11]. Commonly affected areas include the tongue, buccal mucosa, gingiva, and floor of the mouth. Due to the unique anatomical characteristics of the oral and maxillofacial region, including a rich blood supply and lymphatic drainage, OSCC often presents with a poor prognosis^[12]. Despite advances in radiotherapy, chemotherapy, surgery, immunotherapy, and combination therapies, the 5-year survival rate for OSCC under conventional treatment models remains suboptimal due to high recurrence and metastasis rates^[13]. Consequently, there is an urgent need to identify novel diagnostic and therapeutic targets to improve early detection and treatment outcomes.

EXOSC3 is a protein-coding gene encoding a non-catalytic component of human exosomes. This complex exhibits 3'-5' exoribonuclease activity, playing a crucial role in RNA processing and degradation^[14]. Its primary physiological functions include RNA binding and exoribonuclease activity. *EXOSC3* is also implicated in diseases such as spinocerebellar ataxia type 1B and non-syndromic spinocerebellar ataxia. In cancer development, *EXOSC3* has been shown to play a significant role. Protein sequencing studies have linked *EXOSC3* to pancreatic cancer, and in gastric cancer, *EXOSC3* significantly influences treatment outcomes based on risk scores^[15]. Furthermore, *EXOSC3* is considered a potential molecular biomarker for lung cancer in Chinese populations^[16]. However, limited research exists on the role of *EXOSC3* in OSCC, necessitating further investigation into its potential functions.

Bioinformatics analysis of TCGA-OSCC cohort data revealed that *EXOSC3* is significantly overexpressed in OSCC tissues, a finding corroborated in paired OSCC samples. To determine whether this overexpression influences diagnostic and prognostic outcomes, ROC analysis and Kaplan-Meier survival curve analysis were conducted. The ROC curve demonstrated an AUC of 0.870, indicating high diagnostic efficacy in the TCGA-OSCC cohort. Similarly, Kaplan-Meier survival analysis showed that patients with high *EXOSC3* expression exhibited poorer prognosis compared to those with low expression. Clinical data analysis further revealed that increased *EXOSC3* expression correlated with advanced T stage. These findings suggest that *EXOSC3* overexpression is associated with poor prognosis and higher clinical stages in OSCC.

To explore the functional implications of *EXOSC3*, gene co-expression analysis was conducted using TCGA-OSCC cohort data. Six genes—*APTX*, *CLTA*, *RPS6*, *MELK*, *DNAJ1*, and *STOML2*—were identified as positively correlated with *EXOSC3*. These genes have established roles in tumor biology: *APTX* serves as a prognostic marker for cancer post-kidney transplantation^[17], *CLTA* promotes hepatocellular carcinoma progression via small extracellular vesicles^[18], and *RPS6* contributes to drug resistance in gastric cancer through *NRF2*. Additionally, *MELK* regulates *DLAT* in mitochondrial mediation of liver cancer, *DNAJ1* activates the mutant p53/NF-κB pathway to promote breast cancer proliferation and metastasis, and *STOML2* facilitates colorectal cancer progression via the MAPK signaling pathway and interaction with *PHB*. The co-expression of these tumor-associated genes with *EXOSC3* suggests that *EXOSC3* may exert its oncogenic effects through these pathways.

To further elucidate the potential pathways involved, GO and KEGG enrichment analyses were performed. GO enrichment analysis identified cellular immune activities associated with *EXOSC3*, including the humoral immune response, natural killer cell activation in immune response, negative regulation of activated T cell proliferation, and natural killer cell activation. KEGG enrichment analysis highlighted several key pathways, such as cytokine-cytokine receptor interaction, natural killer cell-mediated cytotoxicity, Toll-like receptor signaling, and JAK-STAT signaling. The Toll-like receptor signaling pathway has been implicated in OSCC pathogenesis^[19], while the JAK-STAT pathway has been shown to promote OSCC progression and invasion^[20].

The relationship between *EXOSC3* and immune infiltration in OSCC was analyzed to verify its role in the tumor immune microenvironment. Significant differences in stromal scores were observed between high and low *EXOSC3* expression groups, suggesting a potential impact of *EXOSC3* on stromal cell content in the tumor microenvironment. Immune cell infiltration analysis revealed associations between *EXOSC3* and specific immune cells, particularly T cells CD8 and T cells CD4 memory activated, which are known to influence tumorigenesis and progression.

In terms of therapeutic implications, several immune checkpoint genes, including *CD40*, *TNFRSF25*, *CD70*, *LAG3*, *PDCD1*, *IDO1*, *HAVCR2*, *CD274*, *PDCD1LG2*, and *CTLA4*, were positively correlated with *EXOSC3* expression. This suggests a potential role for *EXOSC3* in immunotherapy efficacy for OSCC. However, further experimental validation is necessary to determine whether *EXOSC3* can serve as a biomarker for immunotherapy. While surgery remains the primary treatment modality for OSCC, chemotherapy is an essential adjunct. In this study, lower *EXOSC3* expression levels were associated with higher sensitivity to chemotherapy agents such as 5-Fluorouracil, AKT inhibitor VIII, Bexarotene, and Bleomycin. These findings may expand the range of therapeutic options and guide the development of new treatment strategies.

5. Conclusion

In summary, *EXOSC3* is significantly overexpressed in OSCC tissues, and its elevated expression is closely associated with poor patient prognosis and the advancement of clinical stages. *EXOSC3* may exert its effects through interactions with multiple co-expressed genes and critical biological pathways. Furthermore, its high expression is linked to alterations in the tumor immune microenvironment and immune cell infiltration. These findings highlight the potential of *EXOSC3* as a promising target for novel therapeutic approaches, including immune checkpoint therapy and chemotherapy.

Disclosure statement

The authors declare no conflict of interest.

References

- [1] Bugshan A, Farooq I, 2020, Oral Squamous Cell Carcinoma: Metastasis, Potentially Associated Malignant Disorders, Etiology and Recent Advancements in Diagnosis. *F1000Res*, 9: 229. <https://doi.org/10.12688/f1000research.22941.1>
- [2] Chai A, Lim KP, Cheong SC, 2020, Translational Genomics and Recent Advances in Oral Squamous Cell Carcinoma. *Semin Cancer Biol*, 61: 71–83. <https://doi.org/10.1016/j.semcancer.2019.09.011>
- [3] Ma X, Yang R, Li H, et al., 2024, Role of Exosomes in the Communication and Treatment Between OSCC and Normal Cells. *Heliyon*, 10(7): e28148. <https://doi.org/10.1016/j.heliyon.2024.e28148>
- [4] Ramqvist T, Dalianis T, 2011, An Epidemic of Oropharyngeal Squamous Cell Carcinoma (OSCC) Due to Human Papillomavirus (HPV) Infection and Aspects of Treatment and Prevention. *Anticancer Res*, 31(5): 1515–1519.
- [5] Eggens VR, Barth PG, Niermeijer JM, et al., 2014, EXOSC3 Mutations in Pontocerebellar Hypoplasia Type 1: Novel Mutations and Genotype-Phenotype Correlations. *Orphanet J Rare Dis*, 9: 23. <https://doi.org/10.1186/1750-1172-9-23>
- [6] Lu G, Liu H, Wang H, et al., 2024, Potentially Functional Variants of INPP5D and EXOSC3 in Immunity B Cell-Related Genes are Associated with Non-Small Cell Lung Cancer Survival. *Front Immunol*, 15: 1440454. <https://doi.org/10.3389/fimmu.2024.1440454>
- [7] Tomczak K, Czerwinska P, Wiznerowicz M, 2015, The Cancer Genome Atlas (TCGA): An Immeasurable Source of Knowledge. *Contemp Oncol (Pozn)*, 19(1A): A68–A77. <https://doi.org/10.5114/wo.2014.47136>
- [8] Ritchie ME, Phipson B, Wu D, et al., 2015, Limma Powers Differential Expression Analyses for RNA-Sequencing and Microarray Studies. *Nucleic Acids Res*, 43(7): e47. <https://doi.org/10.1093/nar/gkv007>
- [9] Xu S, Hu E, Cai Y, et al., 2024, Using clusterProfiler to Characterize Multiomics Data. *Nat Protoc*, 19(11): 3292–3320. <https://doi.org/10.1038/s41596-024-01020-z>
- [10] Chen B, Khodadoust MS, Liu CL, et al., 2018, Profiling Tumor Infiltrating Immune Cells with CIBERSORT. *Methods Mol Biol*, 1711: 243–259. https://doi.org/10.1007/978-1-4939-7493-1_12
- [11] Oyeyemi BF, Kaur US, Paramraj A, et al., 2023, Microbiome Analysis of Saliva from Oral Squamous Cell Carcinoma (OSCC) Patients and Tobacco Abusers with Potential Biomarkers for Oral Cancer Screening. *Heliyon*, 9(11): e21773. <https://doi.org/10.1016/j.heliyon.2023.e21773>
- [12] Liu B, Si W, Wei B, et al., 2023, PTP4A1 Promotes Oral Squamous Cell Carcinoma (OSCC) Metastasis Through Altered Mitochondrial Metabolic Reprogramming. *Cell Death Discov*, 9(1): 360. <https://doi.org/10.1038/s41420-023-01657-x>
- [13] Mumtaz M, Bijnsdorp IV, Bottger F, et al., 2022, Secreted Protein Markers in Oral Squamous Cell Carcinoma (OSCC).

Clin Proteomics, 19(1): 4. <https://doi.org/10.1186/s12014-022-09341-5>

- [14] Szeto CH, Rubin S, Sidlow R, 2023, Homozygous EXOSC3 c.395A>C Variants in Pontocerebellar Hypoplasia Type 1B: A Sibling Pair with Childhood Lethal Presentation and Literature Review. *Cureus*, 15(5): e39226. <https://doi.org/10.7759/cureus.39226>
- [15] Bauer L, Hapfelmeier A, Blank S, et al., 2018, A Novel Pretherapeutic Gene Expression-Based Risk Score for Treatment Guidance in Gastric Cancer. *Ann Oncol*, 29(1): 127–132. <https://doi.org/10.1093/annonc/mdx685>
- [16] Xie Y, Wu H, Hu W, et al., 2022, Identification of Hub Genes of Lung Adenocarcinoma Based on Weighted Gene Co-Expression Network in Chinese Population. *Pathol Oncol Res*, 28: 1610455. <https://doi.org/10.3389/pore.2022.1610455>
- [17] Fu Q, Yang F, Liao M, et al., 2019, Rap GTPase Interactor: A Potential Marker for Cancer Prognosis Following Kidney Transplantation. *Front Oncol*, 9: 737. <https://doi.org/10.3389/fonc.2019.00737>
- [18] Xu Y, Yao Y, Yu L, et al., 2023, Clathrin Light Chain A Facilitates Small Extracellular Vesicle Uptake to Promote Hepatocellular Carcinoma Progression. *Hepatol Int*, 17(6): 1490–1499. <https://doi.org/10.1007/s12072-023-10562-5>
- [19] Di Lorenzo A, Bolli E, Tarone L, et al., 2020, Toll-Like Receptor 2 at the Crossroad Between Cancer Cells, the Immune System, and the Microbiota. *Int J Mol Sci*, 21(24): 9418. <https://doi.org/10.3390/ijms21249418>
- [20] Shao F, Pang X, Baeg GH, 2021, Targeting the JAK/STAT Signaling Pathway for Breast Cancer. *Curr Med Chem*, 28(25): 5137–5151. <https://doi.org/10.2174/0929867328666201207202012>

Publisher's note

Bio-Byword Scientific Publishing remains neutral with regard to jurisdictional claims in published maps and institutional affiliations.

Comparative Effectiveness of Medical Radiation Protection Spray and Triethanolamine Cream in Preventing and Treating Radiodermatitis in Breast Cancer Patients

Yuge Ran¹, Chan Liu¹, Lanhui Yuan¹, Huibin Yang¹, Lei Su¹, Kunjie Wang², Qianqian Han³, Xiaoxi Wu⁴,
Hongyun Shi^{1*}

¹Department of Radiotherapy, Affiliated Hospital of Hebei University, Baoding 071000, Hebei Province, China

²Department of Oncology, Affiliated Hospital of Hebei University, Baoding 071000, Hebei Province, China

³Department of General Surgery, Affiliated Hospital of Hebei University, Baoding 071000, Hebei Province, China

⁴Department of Nutrition, Affiliated Hospital of Hebei University, Baoding 071000, Hebei Province, China

*Corresponding author: Hongyun Shi, hyshi2015@163.com

Copyright: © 2025 Author(s). This is an open-access article distributed under the terms of the Creative Commons Attribution License (CC BY 4.0), permitting distribution and reproduction in any medium, provided the original work is cited.

Abstract: *Objective:* This study investigates the preventive and therapeutic effects of medical radiation protection spray (Bergmann) compared to triethanolamine cream in patients undergoing radiotherapy following breast cancer surgery. *Methods:* Ninety patients with breast cancer who received postoperative radiotherapy between July 2018 and July 2021 were randomly divided into the Bergmann treatment (experimental) group and the triethanolamine cream treatment (control) group, with 45 patients in each group. Radiodermatitis severity was assessed using the RTOG radiodermatitis grading standards. *Results:* The radiation dose required to develop grade I radiodermatitis was significantly higher in the experimental group compared to the control group, at $(36.13 \pm 1.17 \text{ Gy})$ and $(25.38 \pm 0.63 \text{ Gy})$, respectively. At a radiation dose of 30 Gy, the proportion of grade I radiodermatitis cases in the experimental group was significantly lower than in the control group ($P = 0.002$). At radiation doses of 40 Gy and 50 Gy, the proportion of grade II radiodermatitis cases in the experimental group was also significantly lower than in the control group ($P < 0.001$). No cases of grade III or higher radiodermatitis were observed in the experimental group, while three cases of grade III radiodermatitis occurred in the control group, although the difference was not statistically significant. No patients in the experimental group discontinued treatment due to radiodermatitis or mucosal reactions, whereas two patients in the control group interrupted treatment due to these reactions but eventually completed therapy. *Conclusion:* Bergmann spray effectively prevents radiodermatitis in patients undergoing radiotherapy after breast cancer surgery and is more effective than triethanolamine cream in treating skin lesions. Its ease of use improves the quality of life for patients undergoing radiotherapy and ensures successful treatment completion. Bergmann is suitable for clinical promotion and application.

Keywords: Breast cancer surgery; Radiodermatitis; Triethanolamine cream; Medical radiation protection spray

Online publication: February 13, 2025

1. Introduction

Breast cancer is a malignant tumor originating in the glandular epithelial tissue of the breast. According to the 2018 GLOBOCAN global statistical report ^[1], the incidence and mortality rates of lung cancer are the highest among all tumors. While the incidence of breast cancer is comparable to that of lung cancer, its prognosis is generally more favorable. However, most patients require radiotherapy following radical surgery.

Radiotherapy is a critical component of comprehensive breast cancer treatment but is often accompanied by side effects. Among these, radiodermatitis is the most common side effect observed in patients undergoing radiotherapy after radical surgery. Radiodermatitis typically manifests as localized redness, swelling, blisters, and other burn-like changes within the irradiated skin area ^[2]. Severe radiodermatitis can cause significant pain, prolong hospitalization, increase medical costs, and adversely affect treatment outcomes.

This study aims to compare the efficacy of medical radiation protection spray (Bergmann) with triethanolamine cream in preventing and treating radiodermatitis during radiotherapy in breast cancer patients after radical surgery ^[3]. The objective is to provide patients with a superior option for managing radiodermatitis effectively.

2. Materials and methods

2.1. General information

A total of 90 patients diagnosed with breast cancer and treated with radical surgery at our hospital between July 2018 and July 2021 were included in the study. The patients were divided into an experimental group and a control group, with 45 patients in each group. The experimental group received Bergmann spray applied to the skin in the radiation field twice daily from the initiation of radiotherapy. When grade I skin reactions occurred, the application frequency was increased to four times daily. The control group received triethanolamine cream applied to the skin in the radiation field three times daily after the occurrence of grade I radiodermatitis following radiotherapy.

In the experimental group, patient ages ranged from 37 to 61 years, with a median age of 52 years, while in the control group, ages ranged from 37 to 69 years, with a median age of 53 years.

2.2. Treatment method

All patients were treated using an Elekta medical linear accelerator. The chest wall was irradiated with 6 MeV electron beams in conventional divisions. The chest wall irradiation field was defined as follows:

- (1) Upper limit: Lower edge of the clavicle
- (2) Lower limit: 2 cm below the contralateral breast fold
- (3) Medial limit: Body midline
- (4) Lateral limit: Midaxillary line

The radiotherapy dose was administered as DT50Gy/2Gy/25f over 5 weeks.

Patients in the experimental group used medical radiation protection spray prophylactically from the initiation of radiotherapy, applying it as follows:

- (1) Prophylactic application: Once 30 minutes before and 10 minutes after radiotherapy, spray the site twice daily.
- (2) With redness and swelling: Spray 2–3 times per application, 3 times daily.
- (3) With skin ulceration: After debridement, spray 2–3 times per application, 4 times daily.

After completing radiotherapy, the spray was continued for an additional 7–10 days.

For the control group, once grade I radiodermatitis developed during radiotherapy, triethanolamine cream was applied locally to the radiation field three times daily. Residual cream was removed from the skin before radiotherapy sessions.

Radiotherapy doses corresponding to the onset of grade I–IV radiodermatitis were observed and recorded for all patients, along with the duration and resolution time for each grade of skin reaction.

2.3. Radiodermatitis grading standards

Radiodermatitis was graded according to the RTOG acute radiodermatitis grading standards ^[4,5]:

- (1) Grade 0: No noticeable skin changes.
- (2) Grade I: Mild erythema or dry skin reaction.
- (3) Grade II: Scattered erythema, moist skin reaction, or moderate edema in skin folds.
- (4) Grade III: Confluent moist skin reaction with a diameter >1.5 cm.
- (5) Grade IV: Skin ulceration, necrosis, or hemorrhage.

2.4. Statistical methods

Statistical analysis was performed using SPSS 22.0. The doses corresponding to skin reactions at all levels were described using the mean \pm standard deviation (SD). The χ^2 test was employed to compare categorical data, with a significance level of $P < 0.05$.

3. Results

3.1. Radiation dose for grade I radiodermatitis in the two groups

The radiation dose required to induce grade I radiodermatitis was significantly higher in the experimental group compared to the control group, with doses of 36.13 ± 1.17 Gy and 25.38 ± 0.63 Gy, respectively. This indicates that Bergmann spray effectively prevents radiodermatitis and delays its onset (see **Table 1**).

Table 1. Radiation dose for grade I radiodermatitis in the two groups of patients (mean \pm SD, Gy)

Group	Number of cases	Dose for grade I radiodermatitis
Experimental group	45	36.13 ± 1.17
Control group	45	25.38 ± 0.63
<i>P</i> value		< 0.001

3.2. Incidence of grade I radiodermatitis at different radiation doses

At a radiation dose of 30 Gy, the proportion of patients with grade I skin reactions was significantly lower in the experimental group compared to the control group ($P = 0.002$), demonstrating a statistically significant difference. However, at doses of 10, 20, 40, and 50 Gy, no statistically significant differences were observed between the two groups ($P > 0.05$).

3.3. Incidence of grade II radiodermatitis at different radiation doses

At radiation doses of 40 Gy and 50 Gy, the proportion of patients with grade II radiodermatitis in the experimental

group was significantly lower than in the control group ($P < 0.001$). At doses of 10, 20, and 30 Gy, the differences in grade II radiodermatitis incidence between the two groups were not statistically significant ($P > 0.05$) (**Table 2**).

Table 2. Comparison of grade II radiodermatitis incidence between the two groups

Group	Number of cases	Grade II radiodermatitis [n (%)]	Below grade II radiodermatitis [n (%)]
Experimental group	45	7 (15.6%)	38 (84.4%)
Control group	45	11 (24.4%)	34 (75.6%)
<i>P</i> value		0.292	

3.4. Incidence of grade III skin reactions

No cases of grade III or higher radiodermatitis were observed in the experimental group, whereas 3 cases of grade III radiodermatitis occurred in the control group. The difference between the two groups was not statistically significant ($P > 0.05$).

3.5. Treatment interruptions due to severe radiodermatitis

No patients in the experimental group required treatment interruptions due to severe radiodermatitis or mucosal reactions. In the control group, 2 patients experienced interruptions due to severe radiodermatitis, but treatment was ultimately completed. The difference between the two groups was not statistically significant ($P > 0.05$).

4. Discussion

The role and significance of radiotherapy in tumor treatment have become increasingly prominent, establishing it as one of the primary methods for managing malignant tumors. Radiotherapy delivers a specific dose of radiation to tumors, damaging the DNA of tumor cells to inhibit their growth and induce cell death^[6]. This damage includes direct effects of radiation and indirect effects caused by the ionization of water^[7], leading to the formation of free radicals. However, normal cells within the radiation field are inevitably exposed to damage. While normal tissues possess self-repair capabilities, repeated radiation exposure can disrupt the balance between tissue damage and repair. Radiodermatitis is one of the most common tissue injuries caused by radiotherapy^[8]. Statistics indicate that the incidence of skin damage among cancer patients undergoing radiotherapy is 91.4%, with 58.1% experiencing severe damage that necessitates treatment interruption. Each day of treatment delay reduces the local control rate by 1–3%, exacerbating patient discomfort, and psychological distress, and negatively impacting treatment outcomes and quality of life.

The mechanism underlying radiodermatitis is complex, involving various pathophysiological reactions, microenvironmental regulation, and both treatment-related and patient-related factors^[9]. Treatment-related risk factors include the type of radiation source, radiation dose, frequency of exposure, location and area of the irradiated field, and the presence of overlapping radiation fields^[10]. Furthermore, the use of radiosensitizing drugs and concurrent radiotherapy and chemotherapy increases the likelihood of radiodermatitis. Patient-specific factors also contribute to radiodermatitis^[11], such as obesity, the presence of skin folds, nutritional status, smoking, ultraviolet exposure, individual sensitivity to radiation, and comorbidities such as autoimmune diseases. Rare genetic mutations have also been implicated^[12–14], with current research suggesting that mutations in the *Ataxia-Telangiectasia Mutated (ATM)* genes increase susceptibility to severe radiodermatitis^[15].

Radiotherapy remains a crucial treatment modality for breast cancer. However, it is essential to concurrently enhance understanding of its side effects and develop strategies to mitigate radiotherapy-related complications. Bergmann, the experimental drug used in this study, primarily comprises superoxide dismutase and its stabilizer. This formulation effectively and promptly removes harmful free radicals generated during radiotherapy, interrupts the free radical reaction chain, and promotes the active repair of human tissues^[8]. The main component, ThSD, enhances bioavailability and efficiently neutralizes O₂^[-] produced by ionization in local skin and mucosal tissues. This delays the onset of radiation-induced damage, mitigates its severity, and supports the continuity of radiotherapy. Additionally, the stabilizer D-DT stabilizes the protein and cell membrane structures, provides deep hydration, and resists absorption by the body, thereby protecting skin and mucosal cells from damage. Bergmann's bionic buffer system creates a catalytic environment conducive to healing, facilitating the repair of skin and mucosal tissues.

The findings of this study demonstrate that Bergmann exerts a protective effect on the skin of breast cancer patients undergoing radiotherapy, effectively reducing the incidence and severity of radiation-induced skin damage. It increases the radiation tolerance of skin in the irradiated field, aids in repairing radiation-induced skin injuries, and ensures the smooth progress of radiotherapy. This contributes to reduced pain and hospitalization costs for patients undergoing radiotherapy. Additionally, Bergmann's ease of use supports its clinical applicability and warrants further promotion.

Funding

This work was supported by the Baoding City Self-Financed Fund Project (Project No. 2241ZF339).

Disclosure statement

The authors declare no conflict of interest.

References

- [1] Bray F, Ferlay J, Soerjomataram I, et al., 2018, Global Cancer Statistics 2018: GLOBOCAN Estimates of Incidence and Mortality Worldwide for 36 Cancers in 185 Countries. *CA Cancer J Clin*, 68(6): 394–424. <https://doi.org/10.3322/caac.21492>. Erratum in *CA Cancer J Clin*, 70(4): 313. <https://doi.org/10.3322/caac.21609>
- [2] Zhang X, Li H, Li Q, et al., 2018, Application of Red Light Phototherapy in the Treatment of Radioactive Dermatitis in Patients with Head and Neck Cancer. *World J Surg Oncol*, 16(1): 222. <https://doi.org/10.1186/s12957-018-1522-3>
- [3] Zenda S, Yamaguchi T, Yokota T, et al., 2018, Topical Steroid Versus Placebo for the Prevention of Radiation Dermatitis in Head and Neck Cancer Patients Receiving Chemoradiotherapy: The Study Protocol of J-SUPPORT 1602 (TOPICS Study), a Randomized Double-Blinded Phase 3 Trial. *BMC Cancer*, 18(1): 873. <https://doi.org/10.1186/s12885-018-4763-1>
- [4] Pixberg C, Koch R, Eich HT, et al., 2016, Acute Toxicity Grade 3 and 4 After Irradiation in Children and Adolescents: Results From the IPPARCA Collaboration. *Int J Radiat Oncol Biol Phys*, 94(4): 792–799. <https://doi.org/10.1016/j.ijrobp.2015.12.353>
- [5] Narvaez C, Doemer C, Idel C, et al., 2018, Radiotherapy Related Skin Toxicity (RAREST-01): Mepitel® Film Versus Standard Care in Patients with Locally Advanced Head-and-Neck Cancer. *BMC Cancer*, 18(1): 197. <https://doi.org/10.1186/s12957-018-1522-3>

org/10.1186/s12885-018-4119-x

- [6] Pasquier D, Le Tinier F, Bennadji R, et al., 2019, Intensity-Modulated Radiation Therapy with Simultaneous Integrated Boost for Locally Advanced Breast Cancer: A Prospective Study on Toxicity and Quality of Life. *Sci Rep*, 9(1): 2759. <https://doi.org/10.1038/s41598-019-39469-8>
- [7] Liochev SI, 2013, Reactive Oxygen Species and the Free Radical Theory of Aging. *Free Radic Biol Med*, 60: 1–4. <https://doi.org/10.1016/j.freeradbiomed.2013.02.011>
- [8] Zenda S, Ota Y, Tachibana H, et al., 2016, A Prospective Picture Collection Study for a Grading Atlas of Radiation Dermatitis for Clinical Trials in Head-and-Neck Cancer Patients. *J Radiat Res*, 57(3): 301–306. <https://doi.org/10.1093/jrr/rrv092>
- [9] Méry B, Vallard A, Trone JC, et al., 2015, Correlation Between Anthropometric Parameters and Acute Skin Toxicity in Breast Cancer Radiotherapy Patients: A Pilot Assessment Study. *Br J Radiol*, 88(1055): 20150414. <https://doi.org/10.1259/bjr.20150414>
- [10] Blanchecotte J, Ruffier-Loubière A, Reynaud-Bougnoix A, et al., 2015, Toxicité Aiguë Cutanée de L'irradiation Mammaire Avec Modulation D'intensité Avec Technique de Champ Dans le Champ (Optimisation Avec Pré-Segmentation) [Acute Skin Toxicity in Breast Intensity Modulated Radiotherapy Using Field in Field Technique]. *Cancer Radiother*, 19(2): 82–88. <https://doi.org/10.1016/j.canrad.2014.10.007>
- [11] De Langhe S, Mulliez T, Veldeman L, et al., 2014, Factors Modifying the Risk for Developing Acute Skin Toxicity After Whole-Breast Intensity Modulated Radiotherapy. *BMC Cancer*, 14: 711. <https://doi.org/10.1186/1471-2407-14-711>
- [12] Kawamura K, Qi F, Meng Q, et al., 2019, Nucleolar Protein Nucleolin Functions in Replication Stress-Induced DNA Damage Responses. *J Radiat Res*, 60(3): 281–288. <https://doi.org/10.1093/jrr/rry114>
- [13] Vulin A, Sedkaoui M, Moratille S, et al., 2018, Severe PATCHED1 Deficiency in Cancer-Prone Gorlin Patient Cells Results in Intrinsic Radiosensitivity. *Int J Radiat Oncol Biol Phys*, 102(2): 417–425. <https://doi.org/10.1016/j.ijrobp.2018.05.057>
- [14] Qiao Y, Hu CX, Song DA, et al., 2017, High Throughput-Targeted Sequencing Panel for Exploring Radiosensitivity Associated Genes in Esophageal Squamous Cell Carcinoma. *Zhonghua Zhong Liu Za Zhi*, 39(8): 584–588. <https://doi.org/10.3760/cma.j.issn.0253-3766.2017.08.005>
- [15] Liu Z, Yu D, Xu J, et al., 2018, Human Umbilical Cord Mesenchymal Stem Cells Improve Irradiation-Induced Skin Ulcers Healing of Rat Models. *Biomed Pharmacother*, 101: 729–736. <https://doi.org/10.1016/j.biopha.2018.02.093>

Publisher's note

Bio-Byword Scientific Publishing remains neutral with regard to jurisdictional claims in published maps and institutional affiliations.

Research Progress on the Mechanism of Action of Traditional Chinese Medicine Extracts in the Prevention and Treatment of Periodontitis

Tian Ke, Rao Lu, Tang Jing*

Special Key Laboratory of Oral Diseases Research, School of Stomatology, Zunyi Medical University, Zunyi 563000, Guizhou Province, China

*Corresponding author: Tang Jing, htkw890104@163.com

Copyright: © 2025 Author(s). This is an open-access article distributed under the terms of the Creative Commons Attribution License (CC BY 4.0), permitting distribution and reproduction in any medium, provided the original work is cited.

Abstract: Periodontitis is an inflammatory infectious disease affecting the periodontal supporting tissues and is the primary cause of tooth loosening and tooth loss in adults. Clinically, supragingival scaling, subgingival scaling, root planing, and other basic periodontal treatments, often combined with antibiotic therapy, are commonly employed with moderate efficacy. However, the increasing prevalence of antibiotic resistance and associated adverse reactions has become a growing concern. Recent studies have demonstrated the significant impact of traditional Chinese medicine (TCM) extracts in both the prevention and treatment of periodontitis, exhibiting remarkable effectiveness. This review explores the role and mechanisms of TCM extracts in the prevention and treatment of periodontitis, providing a reference for further elucidation of their mechanisms and a theoretical basis for the development of Chinese herbal medicine-based care products.

Keywords: Traditional Chinese medicine extracts; Prevention and treatment of periodontitis; Mechanism of action

Online publication: February 13, 2025

1. Introduction

Periodontitis is a multifactorial and complex disease resulting from an imbalance between pathogenic microorganisms in dental plaque and the host immune system ^[1]. The primary clinical manifestations of periodontitis include gingival redness, swelling, bleeding, formation of periodontal pockets, alveolar bone resorption, and tooth mobility. In severe cases, these symptoms can lead to tooth loss, making periodontitis a leading cause of impaired chewing function in adults ^[2].

Standard treatment for periodontitis typically involves a combination of basic periodontal therapies and drug interventions. However, as a chronic inflammatory condition, prolonged use of pharmacological treatments can result in adverse effects such as bacterial resistance, gastrointestinal discomfort, allergic reactions, and potential

damage to liver and kidney functions ^[3].

In recent years, traditional Chinese medicine (TCM) has gained considerable attention for its role in the prevention and treatment of periodontitis. Compared to antibiotics, TCM offers antibacterial, anti-inflammatory, and immune-regulatory properties, which can help reduce the recurrence and complications associated with periodontal diseases ^[4]. Advances in the isolation, purification, and analysis of active components in TCM have enabled the identification and pharmacological evaluation of these components. Numerous studies have confirmed the significant efficacy of various TCM extracts in the prevention and treatment of periodontitis ^[5].

This review summarizes the effects and mechanisms of TCM extracts in the prevention and treatment of periodontitis, providing a foundation for further research into the mechanisms of TCM in managing periodontitis and a theoretical basis for the development of herbal-based care products.

2. Research on the effects and mechanisms of traditional Chinese medicine extracts in the prevention and treatment of periodontitis

2.1. Flavonoids

2.1.1. *Rhodiola rosea* flavonoids

Rhodiola rosea flavonoids have been shown to reduce the gingival index (GI) and sulcus bleeding index (SBI), downregulate the expression levels of interleukin-6 (IL-6), interleukin-18 (IL-18), matrix metalloproteinase-2 (MMP-2), and matrix metalloproteinase-9 (MMP-9) in the serum of rats with periodontitis, thereby alleviating periodontal inflammation ^[6,7].

2.1.2. Naringin

Naringin inhibits autophagy in mouse embryonic osteoblast precursor cells (MC3T3-E1) mediated by the protein kinase B (AKT)/mammalian target of rapamycin (mTOR) pathway, promotes osteogenic differentiation and mineralization, and alleviates periodontitis ^[8]. Additionally, naringin upregulates the expression of lncRNA MEG3 in periodontitis-derived periodontal ligament stem cells (PDLSCs), inhibits the Wnt/ β -catenin pathway, and promotes osteogenic differentiation ^[9].

2.1.3. Icariin (ICA)

ICA activates the EphB4-EphrinB2 signaling pathway, promoting the osteogenic differentiation of MC3T3-E1 cells ^[10].

2.1.4. Isoliquiritigenin (ISL)

ISL inhibits the nuclear factor- κ B (NF- κ B)/NLR family pyrin domain containing 3 (NLRP3)/gasdermin D (GSDMD) pathway, reduces Pg-LPS/ATP-induced pyroptosis in human gingival fibroblasts (hGFs), and alleviates periodontitis ^[11].

2.1.5. Puerarin

Puerarin exhibits anti-periodontitis effects by reducing alveolar bone resorption and inhibiting the differentiation of mouse monocyte macrophage leukemia cells (RAW264.7) into osteoclasts. It suppresses p38 MAPK phosphorylation and alleviates periodontal inflammation ^[12]. Furthermore, puerarin inhibits the interleukin-23/

helper T cell 17 (Th17) inflammatory axis and upregulates osteoprotegerin (OPG) expression, reducing alveolar bone resorption^[13]. It also promotes the proliferation of new osteoblasts, mitigates periodontal inflammation in rats with periodontitis, and inhibits alveolar bone resorption^[14]. Additionally, puerarin downregulates the Notch signaling pathway, preventing the differentiation of RAW264.7 cells into osteoclasts^[15].

2.1.6. Eriodictyol

Eriodictyol reduces inflammation in rats with periodontitis and promotes the osteogenic differentiation of human periodontal ligament stem cells (hPDLSCs) by activating the Yes-associated protein (YAP)/transcriptional co-activator with PDZ-binding motif (TAZ) signaling pathway^[16].

2.1.7. Soy isoflavones (SIF)

Soy isoflavones alleviate periodontal inflammation and inhibit alveolar bone resorption. They suppress the Slit homolog 2 (Slit2)/ p38 mitogen-activated protein kinase (p38 MAPK) signaling pathway, thereby reducing alveolar bone resorption and periodontal inflammation in rats with periodontitis^[17]. Genistein (GEN), a major subclass of soy isoflavones, also inhibits alveolar bone resorption and alleviates periodontal inflammation^[18,19].

2.1.8. Hyperoside (Hyp)

Hyperoside inhibits the Toll-like receptor 4 (TLR4)/myeloid differentiation factor 88 (MyD88)/NF-κB pathway, reduces the number of osteoclasts in periodontal tissues, and suppresses the periodontitis response in rats^[20].

2.1.9. Baicalin

Baicalin possesses antibacterial properties, promotes immunity, alleviates alveolar bone resorption, and inhibits periodontitis. Gong *et al.*^[21] found that baicalin inhibits *Porphyromonas gingivalis*, *Fusobacterium nucleatum*, and *Aggregatibacter actinomycetemcomitans*. It reduces the number of osteoclasts in periodontal tissues, prevents alveolar bone resorption, and counters systemic inflammatory responses. Further research indicates that baicalin downregulates the mTOR signaling pathway, inhibits macrophage polarization to M1, and promotes immune responses, thereby mitigating periodontitis in mice^[22]. In periodontal ligament cells (PDLs) induced by interleukin-1β (IL-1β), human oral keratinocytes (HOKs), and hPDLSCs, baicalin suppresses matrix metalloproteinase-1 (MMP-1)/tissue inhibitor of metalloproteinase 1 (TIMP-1), negatively regulates TLR signaling, inhibits the Janus kinase 2 (JAK2)/signal transducer and activator of transcription 3 (STAT3) pathway, promotes cell proliferation and migration, reduces apoptosis, and alleviates periodontal inflammation^[23]. Clinically, baicalin combined with metronidazole is effective in treating periodontitis of the stomach-fire and kidney-deficiency type, reducing oxidative stress and improving periodontal conditions^[24].

2.1.11. Luteolin

Luteolin blocks the NF-κB and NLRP3/IL-1β signaling pathways in gingival tissues of rats with periodontitis, thereby preventing periodontal tissue destruction and promoting alveolar bone remodeling^[25].

2.1.12. Astragalus extract

Astragalus extract contains total flavonoids from astragalus (TFA) and astragaloside IV (AS-IV). The combination of TFA and gingival mesenchymal stem cells (GMSCs) effectively treats periodontal inflammation^[26]. AS-IV

inhibits the TLR4/MyD88/NF- κ B pathway and promotes periodontal tissue remodeling in rats with periodontitis ^[27].

2.1.13. Quercetin (Quer)

Quercetin promotes osteogenesis, inhibits alveolar bone resorption, and reduces periodontal inflammation. In a cigarette smoke-related periodontitis (CSR) model of human periodontal ligament cells (hPDLs) induced by cigarette smoke extract (CSE) and lipopolysaccharide (LPS), quercetin enhances the expression of alkaline phosphatase (ALP), runt-related transcription factor 2 (RUNX2), and collagen type I (COL1), promoting osteogenesis ^[28]. Additionally, quercetin inhibits the JAK/STAT pathway, promotes hPDL migration, and alleviates smoking-related periodontal lesions ^[29]. It further alleviates alveolar bone resorption and reduces periodontal inflammation through the Nrf2, NF- κ B/NLRP3, and microRNA-21a-5p/PDCD4/NF- κ B pathways ^[30]. In rats with diabetic periodontitis, quercetin liposomes lower blood glucose levels, reduce advanced glycation end products (AGEs), and alleviate periodontal inflammation and alveolar bone resorption ^[31].

2.1.14. Kaempferol

Kaempferol reduces the levels of phosphorylated extracellular signal-regulated kinase (p-ERK), phosphorylated p38 MAPK (p-p38), and phosphorylated c-Jun N-terminal kinase (p-JNK) in the MAPK signaling pathway, thus inhibiting periodontitis and osteoclast formation, differentiation, and proliferation ^[32].

2.1.15. Nobiletin

Nobiletin significantly inhibits periodontal inflammation by blocking the chemokine CCL2/CCR2 signaling axis, reducing inflammatory damage in rats with periodontitis ^[33,34].

2.2. Polyphenols

2.2.1. Proanthocyanidins (PA)

Proanthocyanidins (PA) are natural pigments widely present in plants, with the highest concentration found in grape seeds ^[35]. Grape seed proanthocyanidin extract (GSPE) inhibits the TLR4/NF- κ B signaling pathway, thereby alleviating periodontal inflammation in rats with diabetic periodontitis ^[36]. Additionally, PA restores lysine lactylation in periodontal ligament stem cells (PDLSCs) under inflammatory conditions and promotes their osteogenesis through the Wnt/ β -catenin pathway ^[37].

2.2.2. Protocatechuic acid

Protocatechuic acid, the primary metabolite of anthocyanins, upregulates silent information regulator 1 (SIRT1), inhibits the thioredoxin-interacting protein (TXNIP)-NLRP3 axis, and alleviates inflammatory damage in human periodontal ligament fibroblasts (hPDLFs) induced by LPS ^[38].

2.2.3. Ellagic acid

Ellagic acid reduces the adhesion ability of *Porphyromonas gingivalis* and *Fusobacterium nucleatum*, thereby exhibiting antibacterial effects ^[39]. Moreover, ellagic acid downregulates the expression of IL-6, C-reactive protein (CRP), and vascular endothelial growth factor-A (VEGF-A), while upregulating interleukin-10 (IL-10), thus inhibiting periodontal inflammation and reducing alveolar bone resorption ^[40].

2.2.4. Curcumin (Cur)

Curcumin (Cur) induces the expression of early growth response factor 1 (EGR1), activates the Wnt/ β -catenin signaling pathway, and promotes osteogenic differentiation in hPDLSCs, as well as the proliferation and osteogenesis of PDLSC-extracellular vesicles (EVs) ^[41]. In rats with periodontitis, Cur regulates the solute carrier family 7 member 11 (SLC7A11)/glutathione peroxidase 4 (GPX4) axis, increases antioxidant glutathione (GSH) levels, inhibits ferroptosis, and mitigates periodontal inflammation ^[42]. Furthermore, in hGFs and hPDLSCs induced by LPS, Cur inhibits the NF- κ B pathway, suppresses cyclooxygenase-2 (COX-2) expression, and alleviates periodontal inflammation ^[43].

2.2.5. Farrerol

Farrerol suppresses the mTOR/STAT3 signaling pathway, reduces the distance between the cemento-enamel junction (CEJ) and alveolar bone crest (ABC), decreases levels of IL-1 β , IL-6, and tumor necrosis factor- α (TNF- α), and alleviates periodontal inflammation and alveolar bone resorption in rats with periodontitis ^[44].

2.2.6. Resveratrol (RSV)

Resveratrol (RSV) exhibits anti-inflammatory properties, promotes osteogenesis, and suppresses alveolar bone resorption. Pterostilbene (4'-MR), a derivative of RSV, inhibits the NF- κ B pathway, reduces inflammation in hGFs induced by LPS under high-glucose culture conditions, and alleviates periodontal inflammation in rats with diabetic periodontitis ^[45]. RSV also activates the SLC7A11/GPX4 pathway, downregulates the NF- κ B pathway, inhibits ferroptosis in osteocytes, and mitigates diabetic periodontitis ^[46]. In hGFs induced by LPS, RSV inhibits the phosphatidylinositol 3-kinase (PI3K)/AKT signaling pathway and alleviates the periodontal inflammatory response ^[47]. Additionally, RSV activates the extracellular signal-regulated kinase (ERK)/Wnt/ β -catenin signaling pathway, induces apoptosis of activated T cells, modulates immune responses, and alleviates periodontal inflammation ^[48]. Both *in vivo* and *in vitro* studies have demonstrated that RSV activates the nuclear factor-E2-related factor 2 (Nrf2)/heme oxygenase-1 (HO-1) pathway, inhibits the NF- κ B pathway, reduces inflammation in hPDLSCs induced by LPS, promotes osteogenesis, and mitigates alveolar bone resorption in rats with periodontitis ^[49]. Moreover, RSV suppresses the osteoprotegerin (OPG)/receptor activator of nuclear factor- κ B ligand (RANKL)/receptor activator of nuclear factor- κ B (RANK) signaling pathway in periodontal tissues, reducing alveolar bone resorption ^[50].

2.2.7. Pomegranate peel polyphenols

Pomegranate peel polyphenols reduce gingival bleeding and the risk of periodontal disease progression ^[51]. Punicalagin, a bioactive compound found in pomegranate peel polyphenols, inhibits the growth and adhesion of *Porphyromonas gingivalis* and *Fusobacterium nucleatum*, thereby alleviating periodontal inflammation ^[52].

2.3. Polysaccharides

2.3.1. Lycium barbarum glycopeptide

Lycium barbarum glycopeptide enhances the phosphorylation of ERK, thereby promoting osteogenic repair and regeneration in rats with periodontitis ^[53].

2.3.2. Morinda officinalis polysaccharide

Morinda officinalis polysaccharide upregulates SIRT1, reduces the expression and acetylation of NLRP3,

and inhibits periodontal inflammation in hPDLFs stimulated by LPS ^[54]. Furthermore, *Morinda officinalis* polysaccharide suppresses the expression of fibronectin (FN) and fibronectin-containing extra domain A (FN-EDA) in hPDLFs, thereby alleviating periodontal inflammation ^[55].

2.4. Glycosides

2.4.1. Ginsenosides

Ginsenosides exhibit antibacterial effects, inhibit biofilm formation, suppress periodontal inflammation and alveolar bone resorption, promote osteogenesis, and reduce osteoclast formation. Ginsenoside Rd (GSRd) inhibits the growth, virulence, and biofilm formation of *Porphyromonas gingivalis*, reduces osteoclast formation, and thereby mitigates the pathogenicity of periodontal bacteria, periodontal inflammation, and bone resorption ^[56]. Ginsenosides (Re, Ra8, and Rf) bind to the epidermal growth factor receptor (EGFR), enhance the expression of HO-1, promote the osteogenic differentiation of periodontal ligament cells (PDLs), and inhibit alveolar bone resorption and periodontal inflammation ^[57]. Furthermore, ginsenoside Rg1 promotes the phosphorylation of AMP-activated protein kinase (AMPK), inhibits the dynamin-related protein 1 (Drp1)/NLRP3 signaling pathway, downregulates the expression of Caspase-1 and gasdermin D N-terminal fragment (GSDMD-NT), and alleviates pyroptosis and inflammatory injury ^[58]. Ginsenoside Rb3 suppresses the ERK/NF- κ B, mitogen-activated protein kinase (MAPK)/AKT/NF- κ B, and STAT3 signaling pathways, reduces osteoclast formation, alleviates gingivitis and alveolar bone resorption, and inhibits periodontal inflammation ^[59]. Additionally, ginsenoside Rg6 exhibits antibacterial activity against *Porphyromonas gingivalis*. Rg6 also reduces the expression of IL-6, TNF- α , IL-1 β , and monocyte chemoattractant protein-1 (MCP-1) in hPDLs induced by Pg-LPS. Simultaneously, it increases the expression of catalase (CAT), superoxide dismutase (SOD), alkaline phosphatase (ALP), and osteocalcin (OCN), thereby exhibiting anti-periodontitis, antioxidative, and osteogenic effects ^[60].

2.4.2. Salidroside

Salidroside and *Scrophularia ningpoensis* exhibit significant inhibitory effects on the biofilm formation of *Porphyromonas gingivalis* and *Fusobacterium nucleatum* and demonstrate bactericidal activity ^[61].

2.5. Terpenoids

2.5.1. Ursolic acid

Ursolic acid activates the AMPK/SIRT1 signaling pathway, reduces alveolar bone resorption, and promotes the repair and reconstruction of alveolar bone ^[62].

2.5.2. Carvacrol

Carvacrol hydrogel significantly reduces alveolar bone resorption and improves periodontal inflammation ^[63].

2.5.3. Isodon excisa

A decoction of *Isodon excisa* inhibits the release of IL-1 β , IL-6, and TNF- α in the gingival tissues and serum of rats with periodontitis, alleviating periodontal inflammation and tissue destruction ^[64].

2.5.4. Genipin

Genipin increases the expression of Nrf2 and HO-1 in hPDLs, alleviates oxidative stress, and reduces damage to

periodontal tissues in rats with periodontitis ^[65].

2.5.5. Glycyrrhizin

Glycyrrhizin mitigates periodontal inflammation by activating liver X receptor alpha (LXR α) and inhibiting the COX-2/NF- κ B pathway ^[66].

2.6. Alkaloids

2.6.1. Berberine (BBR)

Berberine hydrochloride exhibits antibacterial activity, inhibits periodontal inflammation, promotes osteogenesis, and alleviates alveolar bone resorption. BBR significantly suppresses the occurrence and development of *Aggregatibacter actinomycetemcomitans*, *Porphyromonas gingivalis*, and periodontitis ^[67]. In rats with periodontitis associated with type 2 diabetes mellitus (T2DM), BBR demonstrates therapeutic effects by blocking the NF- κ B pathway and inhibiting M1 polarization of macrophages ^[68]. Additionally, BBR binds to the EGFR on the cell membranes of hPDLSCs, mediating and activating the extracellular signal-regulated kinase (ERK)-FOS pathway, thereby promoting osteogenesis ^[5]. BBR-loaded hydrogel facilitates the phosphorylation of PI3K/AKT, contributing to anti-periodontal inflammation and osteogenesis ^[69]. Furthermore, BBR enhances the expression of G protein-coupled receptor 30 (GPR30) and blocks the p38 MAPK/NF- κ B signaling pathway, thereby inhibiting alveolar bone resorption and periodontal inflammation, ultimately contributing to the treatment of periodontitis in rats ^[70].

2.6.2. Emodin

Emodin inhibits the NLRP3 inflammasome and upregulates microRNA-218 expression, thus suppressing periodontal inflammation and bone resorption in rats ^[71]. In clinical applications, emodin effectively treats moderate to severe chronic periodontitis by downregulating NF- κ B and suppressing the expression of IL-1 β , IL-4, and IL-6 ^[72].

2.7. Other compounds

2.7.1. Forsythin

Forsythin inhibits the phosphorylation of p38 MAPK, alleviating periodontal inflammation and osteoclast activation, and improving periodontitis symptoms ^[73].

2.7.2. Moringa oleifera leaf extract

Moringa oleifera leaf extract suppresses periodontal inflammation and alveolar bone resorption. It inhibits the phosphorylation of p38 α /mitogen-activated protein kinase 14 (MAPK14) and enhances the expression of osteoprotegerin (OPG)/receptor activator of nuclear factor- κ B ligand (RANKL), interleukin-1 receptor antagonist (IL-1Ra), and IL-10, thereby inhibiting periodontitis ^[74]. Cryptochlorogenic acid and orientin, constituents of *Moringa oleifera* leaf extract, exhibit specific effects. Cryptochlorogenic acid inhibits the p38 MAPK signaling pathway, resulting in anti-inflammatory and anti-bone-resorption effects ^[75]. Furthermore, it blocks the NF- κ B/Jumonji domain-containing protein 3 (JMJD3) signaling axis, inhibits M1 polarization of macrophages, promotes cell survival, and suppresses periodontal inflammation ^[76]. Orientin reduces the expression of autophagy protein LC3-II, thereby inhibiting periodontal inflammation and alveolar bone resorption through autophagy modulation ^[77].

2.7.3. Tripterygium wilfordii polyglycoside

Tripterygium wilfordii polyglycoside decreases the sulcus bleeding index (SBI), periodontal probing depth (PD), and clinical attachment loss (CAL) while alleviating periodontal inflammation and alveolar bone resorption [78].

2.7.4. Eupatol

Eupatol inhibits the growth of *Porphyromonas gingivalis* and *Fusobacterium nucleatum*, blocks activation of the NF- κ B signaling pathway, and suppresses the secretion of TNF- α , IL-1 β , and prostaglandin E2 (PGE2) in hGFs induced by LPS, thereby reducing periodontal inflammation [79].

2.7.5. Allicin

Allicin inhibits the TLR4/MyD88 signaling pathway and reduces the levels of fasting plasma glucose (FPG), IL-6, and TNF- α , thereby mitigating periodontal inflammation in obese rats with periodontitis [80].

2.7.6. Cannabidiol (CBD)

CBD inhibits the TLR4/NF- κ B pathway, thereby alleviating periodontal inflammation in rats and hPDLs induced by LPS [81]. CBD also reduces CAL, lowers tissue inflammation, inhibits the growth of *Porphyromonas gingivalis*, and demonstrates significant therapeutic effects on experimental periodontitis in mice. Moreover, CBD promotes the proliferation and migration of hGFs under inflammatory conditions and suppresses periodontal inflammation [82].

3. Conclusion

Periodontitis is a chronic, progressive disease resulting from an imbalance in oral microecology. Its pathogenesis centers on the interaction between periodontal pathogenic bacteria and the host immune system, leading to the destruction of periodontal supporting tissues and, in severe cases, tooth loosening and loss [1,2]. Clinically, basic periodontal treatment is commonly employed, often combined with antibiotics to significantly alleviate the symptoms of periodontitis [4].

In recent years, the understanding of TCM has advanced significantly, with numerous studies demonstrating its unique advantages in the prevention and treatment of periodontitis. This review highlights that TCM extracts, including flavonoids, polyphenols, polysaccharides, glycosides, naphthoquinones, terpenes, alkaloids, and other compounds, exert therapeutic effects through pathways such as MAPK (ERK, ERK1/2, p38, JNK), mTOR, Wnt/ β -catenin, SLC7A11/GPX4, NF- κ B, EphB4-EphrinB2, YAP/TAZ, Slit2/p38MAPK, JAK2/STAT3, CCL2/CCR2, SIRT1/TXNIP/NLRP3, AMPK/Drp1/NLRP3, and Nrf2/HO-1. These compounds inhibit autophagy and ferroptosis, promote cell proliferation, and reduce oxidative stress. As a result, they suppress the growth of periodontal pathogenic bacteria, mitigate periodontal inflammation and alveolar bone resorption, promote the repair and reconstruction of alveolar bone, enhance periodontal tissue regeneration, and modulate the host immune response.

Nevertheless, the clinical application of TCM extracts warrants further research and validation. With the growing understanding of the molecular mechanisms underlying the effects of TCM in the prevention and treatment of periodontitis, the influence of TCM active ingredients on specific targets and intracellular effector factors will provide a solid theoretical foundation for their broader application in managing periodontitis.

Funding

The present study was supported in part by the Natural Science and Technology Foundation of Guizhou Province (QiankeheJichu-ZK[2022]Yiban606), National Natural Science Foundation of China (82160181), Science and Technology Foundation of Guizhou Health and Health Committee (gzwkj2024-455), and Zunyi Oral Disease Immune Prevention and Medical Biomaterials Research and Development Innovation Talent Team (Zunyi Science Talent [2022] No.1).

Disclosure statement

The authors declare no conflict of interest.

References

- [1] Kwon T, Lamster IB, Levin L, 2021, Current Concepts in the Management of Periodontitis. *Int Dent J*, 71(6): 462-476. <https://doi.org/10.1111/idj.12630>
- [2] Eke PI, Borgnakke WS, Genco RJ, 2020, Recent Epidemiologic Trends in Periodontitis in the USA. *Periodontol 2000*, 82(1): 257–267. <https://doi.org/10.1111/prd.12323>
- [3] Makeeva IM, Daurova FY, Byakova SF, et al., 2016, Sensitivity of Microbial Associations of Periodontal Lesions to Antibacterial Agents. *Stomatologiya*, 95(3): 26–30. <https://doi.org/10.17116/stomat201695326-30>
- [4] Zhou Z, Tang J, 2017, Research Progress of Chinese Herbal Medicine Extracts and Prescriptions in the Treatment of Periodontitis. *Medical Recapitulate*, 23(11): 2245–2248.
- [5] Liu J, Zhao X, Pei D, et al., 2018, The Promotion Function of Berberine for Osteogenic Differentiation of Human Periodontal Ligament Stem Cells via ERK-FOS Pathway Mediated by EGFR. *Sci Rep*, 8(1): 2848. <https://doi.org/10.1038/s41598-018-21116-3>
- [6] Wang H, Liu X, Kong C, et al., 2020, Effect of Rhodopsin Flavonoid on Expression of IL-6 and IL-18 in Serum of Experimental Periodontitis Rats. *Chinese Journal of Laboratory Diagnosis*, 24(4): 664–666.
- [7] Wang H, 2020, Effect of Hylotelephium Purpureum Gel on Expression of MMP-2, MMP-9 in Periodontal Tissues and Serum of Experimental Periodontitis Rats, dissertation, Jilin University.
- [8] Wu Z, 2023, Effect and Mechanism of Naringin Mediating Autophagy to Promote Alveolar Bone Osteogenesis Through Akt/mTOR Pathway, dissertation, Xinjiang Medical University.
- [9] Li S, Yao Y, Zhao G, 2023, Naringin Promotes Osteogenic Differentiation of Inflammatory Periodontal Stem Cells by Regulating lncRNA MEG3/Wnt/ β -Catenin Signaling Pathway. *Cellular & Molecular Immunology*, 39(1): 59–64.
- [10] Yang H, 2023, Research on EphB4-EphrinB2 Signaling Pathway Regulated by Icariin in Promoting Osteogenic Differentiation of MC3T3-E1 Cells, dissertation, Jinzhou Medical University.
- [11] Lv X, 2022, Isoliquiritigenin Alleviates P. gingivalis-LPS/ATP-Induced Pyroptosis by Inhibiting NF- κ B/NLRP3/GSDMD Signals in HGFs, dissertation, Qingdao University.
- [12] Wang J, Qin H, 2021, Effect of Puerarin on the Improvement of Symptoms and Periodontal Tissue Growth in Mice with Chronic Periodontitis Based on the Pathway of p38 Mitogen-Activated Protein Kinase. *Journal of Oral and Maxillofacial Surgery*, 31(4): 207–211.
- [13] Zhang L, Liu Y, Wu Y, et al., 2020, Effects of Puerarin on Alveolar Bone Resorption and OPG/RANKL/RANK Pathway in Rats with Periodontitis Based on IL-23/Th17 Inflammatory Axis. *Journal of Oral Science Research*, 36(9): 844–849.
- [14] Zhan L, Ma R, Wan N, et al., 2022, Effects of Puerarin on Th17/Treg Cell Immune Homeostasis and the Expression of

Related Transcription Factors in Rats with Periodontitis. *Journal of Kunming Medical University*, 43(11): 36–43.

- [15] Liu C, Yan Y, Mo L, et al., 2024, Puerarin Inhibits the Differentiation of Raw264.7 Cells into Osteoclasts Through the Notch Signaling Pathway. *Chinese Journal of Tissue Engineering Research*, 28(35): 5636–5641.
- [16] Zhao Y, Yao N, Geng Q, et al., 2024, The Effect of Eriodictyol on Osteogenic Differentiation of Periodontitis Periodontal Ligament Stem Cells by Regulating the YAP/TAZ Signaling Pathway. *Hebei Medicine*, 30(7): 1105–1114.
- [17] Dai Z, Guo Y, Liu Y, et al., 2024, Impacts of Soy Isoflavones Inhibiting Slit2/MAPK Signaling Pathway on Alveolar Bone Resorption and Inflammatory Response in Periodontitis Rats. *Cellular & Molecular Immunology*, 40(6): 1131–1136.
- [18] Thangavel P, Puga-Olguín A, Rodríguez-Landa JF, et al., 2019, Genistein as Potential Therapeutic Candidate for Menopausal Symptoms and Other Related Diseases. *Molecules*, 24(21): 3892. <https://doi.org/10.3390/molecules24213892>
- [19] Zhang X, Hou S, Peng Y, et al., 2023, Effect of Genistein on Periodontal Tissues in Mice with Periodontitis. *Chinese Journal of Geriatric Dentistry*, 21(3): 153–156 + 192.
- [20] Zhang J, Jia C, He B, et al., 2023, Hyperoside Inhibits TLR4/MyD88/NF-κB Signaling Pathway to Reduce Periodontal Tissue Damage in Rats with Periodontitis. *Shaanxi Medical Journal*, 52(11): 1463–1467 + 1472.
- [21] Gong Y, Wang C, Wu Z, et al., 2021, Antibacterial Effect of Baicalin and Its Anti-Inflammatory and Osteogenic Ability on Experimental Periodontitis in Rats. *Journal of Xinjiang Medical University*, 44(4): 415–420.
- [22] Zhou Y, Chen Z, Liu Y, et al., 2021, EGCG and Baicalin Inhibit M1 Polarization of Macrophages in Mice Periodontitis Through mTOR Synergistically. *Journal of Oral Science Research*, 37(7): 622–627.
- [23] Wang Q, Feng B, Gao Y, 2023, Effect and Mechanism of Baicalin on the Proliferation and Migration of Human Periodontal Ligament Stem Cells Induced by Lipopolysaccharide. *China Pharmacy*, 34(10): 1216–1222.
- [24] Xia L, Xu D, Zhang B, et al., 2023, Effect of Baicalin Combined with Metronidazole on Periodontal Index and Inflammatory Factors in Patients with Gastric Fire and Kidney Deficiency Type Periodontitis. *China Practical Medical*, 18(16): 11–16.
- [25] Casili G, Ardizzone A, Lanza M, et al., 2020, Treatment with Luteolin Improves Lipopolysaccharide-Induced Periodontal Diseases in Rats. *Biomedicines*, 8(10): 442. <https://doi.org/10.3390/biomedicines8100442>
- [26] Li Y, Xing H, Wang Y, et al., 2020, Effects of Luteolin on NLRP3/IL-1β Signal Pathway and Bone Remodeling in Periodontitis Rats. *Journal of Oral Science Research*, 36(12): 1117–1122.
- [27] Zhang J, Yang H, 2022, Effect of Gingival Mesenchymal Stem Cells Combined with Total Flavonoids of Astragalus on Periodontitis Rats. *The Chinese Journal of Clinical Pharmacology*, 38(24): 3020–3024.
- [28] Wang D, Liu Y, Shao L, et al., 2023, The Impacts of Astragaloside IV on Periodontal Tissue Remodeling in Orthodontic Rats with Periodontitis by Inhibiting TLR4/MyD88/NF-κB Signaling Pathway. *Journal of Practical Stomatology*, 39(6): 722–729.
- [29] Yu J, 2023, Study on the Role of Quercetin-Regulated Autophagy in the Inhibition of Osteogenic Differentiation of Human Periodontal Ligament Cells by Cigarette Smoke Extract, dissertation, Chongqing Medical University.
- [30] Shen Y, Qi X, Feng Y, et al., 2024, A Preliminary Study of Quercetin in the Prevention of Periodontal Lesions in Smokers Through JAK/STAT Signal Pathway. *Journal of Modern Stomatology*, 38(2): 100–107.
- [31] Wei Y, Fu J, Wu W, et al., 2021, Quercetin Prevents Oxidative Stress-Induced Injury of Periodontal Ligament Cells and Alveolar Bone Loss in Periodontitis. *Drug Des Devel Ther*, 15: 3509–3522. <https://doi.org/10.2147/DDDT.S315249>
- [32] Zhang W, Jia L, Zhao B, et al., 2021, Quercetin Reverses TNF-α Induced Osteogenic Damage to Human Periodontal Ligament Stem Cells by Suppressing the NF-κB/NLRP3 Inflammasome Pathway. *Int J Mol Med*, 47(4): 39. <https://doi.org/10.3892/ijmm.2021.4740>

- [33] Yang SY, Hu Y, Zhao R, et al., 2024, Quercetin-Loaded Mesoporous Nano-Delivery System Remodels Osteoimmune Microenvironment to Regenerate Alveolar Bone in Periodontitis via the miR-21a-5p/PDCD4/NF- κ B Pathway. *J Nanobiotechnology*, 22(1): 94. <https://doi.org/10.1186/s12951-024-02352-4>
- [34] Guo X, Li S, Liang X, et al., 2021, Effect of Quercetin on Periodontal Tissues and Serum AGEs Level in Rats with Diabetic Periodontitis. *Journal of Oral Science Research*, 37(7): 628–631.
- [35] Xiao M, 2023, In Vitro Study on Anti-Inflammatory and Anti-Osteoclastic Effects of Kaempferol on Periodontitis Through MAPK Signaling Pathway, dissertation, Nanchang University.
- [36] Hosokawa Y, Hosokawa I, Ozaki K, et al., 2021, Nobiletin Inhibits Inflammatory Reaction in Interleukin-1 β -Stimulated Human Periodontal Ligament Cells. *Pharmaceutics*, 13(5): 667. <https://doi.org/10.3390/pharmaceutics13050667>
- [37] Yu J, Yu M, Li N, 2023, The Impact of Nobiletin on the Inflammatory Injury in Rats with Periodontitis by Regulating the CCL2–CCR2 Signaling Axis. *Hebei Medicine*, 29(12): 1937–1941.
- [38] Cui L, Wu N, Xu J, et al., 2021, Effect of Proanthocyanidins on Related Inflammatory Factors in Diabetic Rats with Periodontitis. *Journal of Nongken Medicine*, 43(1): 6–10.
- [39] Zhu X, 2022, Effect of Grape Seed Proanthocyanidins on Periodontal Tissue of Experimental Diabetic Periodontitis Rats, dissertation, Shihezi University.
- [40] Wu Y, Wang X, Zhang Y, et al., 2024, Proanthocyanidins Ameliorate LPS-Inhibited Osteogenesis of PDLSCs by Restoring Lysine Lactylation. *Int J Mol Sci*, 25(5): 2947. <https://doi.org/10.3390/ijms25052947>
- [41] Ma T, Shi J, Zhang L, et al., 2022, Protective Effect and Mechanism of Protocatechuic Acid on Lipopolysaccharide-Induced Inflammatory Reaction in Human Periodontal Ligament Fibroblasts. *Guangxi Medical Journal*, 44(2): 172–178 + 197.
- [42] Nu E, Ju R, A R, et al., 2023, Antibacterial Effect of Ellagic Acid on *Porphyromonas gingivalis* and *Fusobacterium nucleatum* In Vitro. *Beijing Journal of Stomatology*, 31(6): 400–404.
- [43] Yu M, 2024, Experimental Study of Ellagic Acid in the Treatment of Chronic Periodontitis, dissertation, Xinjiang Medical University.
- [44] Shi W, Ling D, Zhang F, et al., 2021, Curcumin Promotes Osteogenic Differentiation of Human Periodontal Ligament Stem Cells by Inducing EGR1 Expression. *Arch Oral Biol*, 121: 104958. <https://doi.org/10.1016/j.archoralbio.2020.104958>
- [45] Lan Q, Cao J, Bi X, et al., 2023, Curcumin-Primed Periodontal Ligament Stem Cells-Derived Extracellular Vesicles Improve Osteogenic Ability Through the Wnt/ β -Catenin Pathway. *Front Cell Dev Biol*, 11: 1225449. <https://doi.org/10.3389/fcell.2023.1225449>
- [46] Wang Y, Lin H, Huang W, et al., 2023, Curcumin Attenuates Periodontal Injury via Inhibiting Ferroptosis of Ligature-Induced Periodontitis in Mice. *Int J Mol Sci*, 24(12): 9835. <https://doi.org/10.3390/ijms24129835>
- [47] Diomede F, Fonticoli L, Guarnieri S, et al., 2021, The Effect of Liposomal Curcumin as an Anti-Inflammatory Strategy on Lipopolysaccharide e from *Porphyromonas gingivalis* Treated Endothelial Committed Neural Crest Derived Stem Cells: Morphological and Molecular Mechanisms. *Int J Mol Sci*, 22(14): 7534. <https://doi.org/10.3390/ijms22147534>
- [48] Tang X, Li Q, Gao Y, et al., 2023, Effects of Farrerol on Periodontal Tissue Injury and mTOR/STAT3 Signaling Pathway in Rats with Ligation Periodontitis. *Journal of Chinese Pharmaceutical Sciences*, 58(24): 2252–2258.
- [49] Sun Y, 2023, 4'-Methoxyresveratrol Inhibits the Inflammatory Response of Human Gingival Fibroblasts Stimulated by LPS with High Concentration Glucose and Its Mechanism, dissertation, Shandong University.
- [50] Li Y, Huang Z, Pan S, et al., 2023, Resveratrol Alleviates Diabetic Periodontitis-Induced Alveolar Osteocyte Ferroptosis

Possibly via Regulation of SLC7A11/GPX4. *Nutrients*, 15(9): 2115. <https://doi.org/10.3390/nu15092115>

- [51] Wang Y, Li S, Li J, et al., 2022, Resveratrol Inhibits Human Gingival Fibroblast Inflammation Induced by Lipopolysaccharide Through PI3K/AKT Signaling Pathway. *Journal of North Sichuan Medical College*, 37(5): 561–566.
- [52] Jiang H, Ni J, Hu L, et al., 2023, Resveratrol May Reduce the Degree of Periodontitis by Regulating ERK Pathway in Gingival-Derived MSCs. *Int J Mol Sci*, 24(14): 11294. <https://doi.org/10.3390/ijms241411294>
- [53] Ma Y, Qian Y, Chen Y, et al., 2024, Resveratrol Modulates the Inflammatory Response in hPDLSCs via the NRF2/HO-1 and NF- κ B Pathways and Promotes Osteogenic Differentiation. *J Periodontal Res*, 59(1): 162–173. <https://doi.org/10.1111/jre.13200>
- [54] Wei X, 2023, Effect of Leucetrol on OPG/RANKL/RANK Signaling Pathway in Rats with Periodontitis. *Fujian Journal of Medicine*, 45(5): 102–105.
- [55] Eltay EG, Gismalla BG, Mukhtar MM, et al., 2021, Punica granatum Peel Extract as Adjunct Irrigation to Nonsurgical Treatment of Chronic Gingivitis. *Complement Ther Clin Pract*, 43: 101383. <https://doi.org/10.1016/j.ctcp.2021.101383>
- [56] A R, 2023, Effects of Punicalagin on the Growth and Adhesion of Periodontal Pathogens Under Different Conditions, dissertation, Xinjiang Medical University.
- [57] Liu C, 2022, Experimental Study on the Treatment of Lycium barbarum Polysaccharide-Glycoprotein in Periodontitis, dissertation, University of Electronic Science and Technology of China.
- [58] Cai H, Wang Z, Zhang Z, et al., 2023, Morinda officinalis Polysaccharides Inhibit the Expression and Activity of NOD-like Receptor Thermal Protein Domain Associated Protein 3 in Inflammatory Periodontal Ligament Cells by Upregulating Silent Information Regulator Sirtuin 1. *West China Journal of Stomatology*, 41(6): 662–670.
- [59] Zhang Z, Dai J, Cai H, et al., 2024, Effects of Morinda officinalis Polysaccharides on FN and FN-EDA of Periodontal Ligament Fibroblasts in Inflammatory Microenvironment. *Shanghai Journal of Stomatology*, 33(2): 123–129.
- [60] Zhou S, Ji Y, Yao H, et al., 2022, Application of Ginsenoside Rd in Periodontitis With Inhibitory Effects on Pathogenicity, Inflammation, and Bone Resorption. *Front Cell Infect Microbiol*, 12: 813953. <https://doi.org/10.3389/fcimb.2022.813953>
- [61] Kim EN, Kaygusuz O, Lee HS, et al., 2021, Simultaneous Quantitative Analysis of Ginsenosides Isolated from the Fruit of *Panax ginseng* C.A. Meyer and Regulation of HO-1 Expression through EGFR Signaling Has Anti-Inflammatory and Osteogenic Induction Effects in HPDL Cells. *Molecules*, 26(7): 2092. <https://doi.org/10.3390/molecules26072092>
- [62] Chu K, Zhang Z, Chu Y, et al., 2023, Ginsenoside Rg1 Alleviates Lipopolysaccharide-Induced Pyroptosis in Human Periodontal Ligament Cells via Inhibiting Drp1-Mediated Mitochondrial Fission. *Arch Oral Biol*, 147: 105632. <https://doi.org/10.1016/j.archoralbio.2023.105632>
- [63] Sun M, Ji Y, Zhou S, et al., 2023, Ginsenoside Rb3 Inhibits Osteoclastogenesis via ERK/NF- κ B Signaling Pathway In Vitro and In Vivo. *Oral Dis*, 29(8): 3460–3471. <https://doi.org/10.1111/odi.14352>
- [64] Sun M, Ji Y, Li Z, et al., 2020, Ginsenoside Rb3 Inhibits Pro-Inflammatory Cytokines via MAPK/AKT/NF- κ B Pathways and Attenuates Rat Alveolar Bone Resorption in Response to *Porphyromonas gingivalis* LPS. *Molecules*, 25(20): 4815. <https://doi.org/10.3390/molecules25204815>
- [65] Zhang Y, Shi H, 2024, Ginsenoside Rb3 Alleviates the Formation of Osteoclasts Induced by Periodontal Ligament Fibroblasts in the Periodontitis Microenvironment Through the STAT3 Pathway. *Cell Biol Int*, 48(9): 1343–1353. <https://doi.org/10.1002/cbin.12201>
- [66] Lee WJ, Kim EN, Trang NM, et al., 2023, Ameliorative Effect of Ginsenoside Rg6 in Periodontal Tissue Inflammation and Recovering Damaged Alveolar Bone. *Molecules*, 29(1): 46. <https://doi.org/10.3390/molecules29010046>

- [67] Shen X, 2023, The Effect of Traditional Chinese Medicine Radix Scrophulariae and Salidroside on Dominant Bacteria of Periodontitis and Peri-Implantitis, dissertation, Hubei University of Medicine.
- [68] Wang Y, Li D, Zhao F, et al., 2023, Effects of Ursolic Acid on Alveolar Bone Resorption in Periodontitis Rats by Regulating AMPK/SIRT1 Pathway. *Shaanxi Medical Journal*, 52(5): 517–522.
- [69] Zhou L, Teng N, Gao T, et al., 2024, Protective Effect of Carvacrol Hydrogel on the Alveolar Bone in Rats with Periodontitis. *West China Journal of Stomatology*, 42(5): 593–608.
- [70] Yang L, Feng T, Li S, 2021, Therapeutic Effect of Rabdosia excisa Decoction on Experimental Periodontitis in Rats. *Journal of Shanxi College of Traditional Chinese Medicine*, 22(5): 332–335 + 340.
- [71] Deng Y, 2023, Genipin Regulates Mitochondrial Dysfunction Through Nrf2 to Relieve Oxidative Stress Damage in Periodontitis, dissertation, Jilin University.
- [72] Zhang N, Hou X, Zhang W, et al., 2021, Glycyrrhizin Plays a Role in the Treatment of Periodontitis by Regulating the COX-2/NF- κ B Signaling Pathway. *Journal of Molecular Diagnosis and Therapy*, 13(9): 1469–1472.
- [73] Zhu Y, Kang J, Zhao J, et al., 2023, Effects of Berberine on Inflammatory Genes and Alveolar Bone Resorption in Mice with Periodontitis. *Biological Chemical Engineering*, 9(6): 85–88.
- [74] Xia S, Jing R, Shi M, et al., 2024, BBR Affects Macrophage Polarization via Inhibition of NF- κ B Pathway to Protect Against T2DM-Associated Periodontitis. *J Periodontal Res*, 59(4): 728–737. <https://doi.org/10.1111/jre.13246>
- [75] Wang C, Liu C, Liang C, et al., 2023, Role of Berberine Thermosensitive Hydrogel in Periodontitis via PI3K/AKT Pathway In Vitro. *Int J Mol Sci*, 24(7): 6364. <https://doi.org/10.3390/ijms24076364>. Erratum in *Int J Mol Sci*, 25(10): 5104. <https://doi.org/10.3390/ijms25105104>
- [76] Gu L, Ke Y, Gan J, et al., 2021, Berberine Suppresses Bone Loss and Inflammation in Ligature-Induced Periodontitis Through Promotion of the G Protein-Coupled Estrogen Receptor-Mediated Inactivation of the p38MAPK/NF- κ B Pathway. *Arch Oral Biol*, 122: 104992. <https://doi.org/10.1016/j.archoralbio.2020.104992>
- [77] Liu S, Huang X, Sun W, 2024, Influences of Emodin on Bone Mineral Density and Inflammatory Response in Rats with Chronic Periodontitis by Up-regulating miR-218 Expression. *Current Medicine*, 52(4): 594–601.
- [78] Chai H, Liang S, Niu Y, et al., 2020, Down-regulation of NF- κ B in Periodontal Tissue Cells is One of the Mechanisms of Emodin in the Treatment of Moderate and Severe Chronic Periodontitis. *Journal of Practical Stomatology*, 36(3): 517–520.
- [79] Su J, Zhu Y, Zhang W, 2021, Effects of Phillyrin on p38 MAPK/c-Fos Signal Pathway and Osteoclast Activation in Periodontitis Rats. *Journal of Oral Science Research*, 37(1): 33–38.
- [80] Wang F, Long S, Zhang J, 2021, Moringa oleifera Lam. Leaf Extract Safely Inhibits Periodontitis by Regulating the Expression of p38 α /MAPK14-OPG/RANKL. *Arch Oral Biol*, 132: 105280. <https://doi.org/10.1016/j.archoralbio.2021.105280>
- [81] Yuan H, 2022, Mechanism of Cryptochlorogenic Acid from Moringa oleifera Leaf on Inhibiting Periodontitis and Alveolar Bone Resorption, dissertation, Nanchang University.
- [82] Fang H, 2023, Cryptochlorogenic Acid Through NF- κ B/JMJD3 Signal Axis Mediated Macrophage Polarization in the Treatment of Periodontitis, dissertation, Nanchang University.
- [83] Lan Y, 2023, Mechanism of Orientin on Inhibiting Periodontal Inflammation and Osteoclast Differentiation via Autophagy, dissertation, Nanchang University.
- [84] Ren B, Yao H, 2022, Effect of Tripterygium wilfordii Polyglycosides on Experimental Periodontitis in Rats. *Journal of Modern Stomatology*, 36(1): 10–14.
- [85] Chen H, Wang L, Lin Q, et al., 2023, Study on the Antibacterial and Anti-inflammatory Effects of Conyza blinii Lévl.

Ethanol Extract on Chronic Periodontitis In Vitro. Chinese Medicine Guide, 29(2): 28–34.

- [86] Xie L, Li X, Huang X, et al., 2023, Effects of Allicin on Insulin Resistance and Free Fatty Acid Levels in Obese Rats with Periodontitis. Shanghai Journal of Stomatology, 32(4): 375–379.
- [87] Chen H, Liu Y, Yu S, et al., 2023, Cannabidiol Attenuates Periodontal Inflammation Through Inhibiting TLR4/NF- κ B Pathway. J Periodontal Res, 58(4): 697–707. <https://doi.org/10.1111/jre.13118>
- [88] Qi M, Qi X, Zhou X, et al., 2023, Therapeutic Effect of Cannabidiol Combined with Minocycline on Periodontitis. International Journal of Stomatology, 51(4): 392–400.

Publisher's note

Bio-Byword Scientific Publishing remains neutral with regard to jurisdictional claims in published maps and institutional affiliations.

Symptom Experiences and Coping Patterns in Pancreatic Cancer Patients During Chemotherapy: A Qualitative Study

Xin Tian¹, Ping Chen², Wen Zhou³, Peiyang Mao¹, Jian Li¹, Cheng Lei⁴, Xiaojing Xue⁵, Changlin Li², Yuxian Nie³, Feng Gao⁵, Jie Li⁵, Gang Feng⁵, Xiaobo Du⁵, Qiuling Shi^{1,3*}, Jingyu Zhang^{3*}

¹School of Public Health, Chongqing Medical University, Chongqing 401331, China

²Department of Oncology, Chengdu Seventh People's Hospital (Affiliated Cancer Hospital of Chengdu Medical College), Chengdu 610000, Sichuan Province, China

³State Key Laboratory of Ultrasound in Medicine and Engineering, College of Biomedical Engineering, Chongqing Medical University, Chongqing 400000, China

⁴Sichuan Cancer Hospital & Institute, Sichuan Cancer Center, Affiliate Cancer Hospital of University of Electronic Science and Technology of China, Chengdu 610000, Sichuan Province, China

⁵Department of Oncology, Mianyang Central Hospital, School of Medicine, University of Electronic Science and Technology of China, Mianyang 621000, Sichuan Province, China

*Corresponding authors: Qiuling Shi, qshi@cqmu.edu.cn; Jingyu Zhang, zhangjingyu0304@cqmu.edu.cn

Copyright: © 2025 Author(s). This is an open-access article distributed under the terms of the Creative Commons Attribution License (CC BY 4.0), permitting distribution and reproduction in any medium, provided the original work is cited.

Abstract: *Objective:* To explore symptom experiences and self-coping patterns during the early and late stages of chemotherapy in these patients to provide a basis for developing targeted symptom management strategies. *Methods:* A total of 27 patients with pancreatic cancer undergoing chemotherapy at two medical institutions were recruited between November 2023 and August 2024. Semi-structured interviews were conducted in person or over the phone. Data were analyzed using traditional content and thematic analyses. *Results:* Three themes were identified: symptom experience, self-coping patterns, and existing obstacles. During the early stages of chemotherapy, patients reported a higher frequency of unpleasant symptoms and recognized these symptoms earlier in the treatment course. Patients in the early stages primarily relied on external support to cope with symptoms, while those in the later stages adopted self-care strategies. Several challenges related to unpleasant symptoms were observed, which appeared to correlate with the self-coping patterns employed. *Conclusion:* Patients with pancreatic cancer undergoing chemotherapy experience a complex and diverse range of symptoms, with varying coping patterns at different stages of treatment. Symptom management during chemotherapy presents significant challenges. Healthcare providers should improve the ongoing monitoring of symptoms post-chemotherapy. By linking patients' symptom experiences and self-coping patterns at different stages of chemotherapy to their specific challenges, personalized symptom management strategies can be developed to enhance care quality.

Keywords: Pancreatic cancer; Chemotherapy; Symptom experience; Self-coping; Existing obstacles

Online publication: February 13, 2025

1. Introduction

Pancreatic cancer is a highly lethal disease and currently ranks as the sixth leading cause of mortality worldwide ^[1]. The global 5-year survival rate is approximately 10% ^[2]. Systemic chemotherapy, encompassing neoadjuvant, adjuvant, and radical chemotherapy, remains the cornerstone of pancreatic cancer treatment. These systemic treatments significantly improve tumor-related clinical outcomes, including curative effects, overall survival, and progression-free survival ^[3-6].

However, chemotherapeutic agents often induce a range of adverse physiological effects due to their toxic side effects. A meta-analysis indicates that hematological, gastrointestinal, and constitutional symptoms have the highest incidence rates ^[7]. A study investigating two first-line chemotherapy regimens identified severe side effects, including anorexia, fatigue, nausea, diarrhea, and constipation ^[8]. Furthermore, reports show that advanced pancreatic cancer patients undergoing chemotherapy exhibit a higher incidence of severe symptoms, particularly fatigue (56.9%), anxiety (50.4%), and nausea (9.8%) ^[9].

Recent studies on the symptom burden experienced by pancreatic cancer patients have primarily focused on symptoms during the natural course of the disease or postoperative recovery ^[10,11]. Limited research exists on the symptom burden associated with different cycles of chemotherapy. Additionally, existing assessment tools often feature an excessive number of items, poor readability, and lack of specificity for pancreatic cancer patients, restricting their ability to report symptoms effectively ^[12].

In China's healthcare system, due to limited medical resources, most patients undergo chemotherapy during daytime outpatient visits. Patients receive infusion therapy at the hospital and return home the same day for rest and recovery. While healthcare providers monitor patients' conditions during hospital-based therapy, the severity of symptoms experienced at home remains inadequately assessed ^[13]. Furthermore, poor communication and interaction between physicians and patients outside of hospital settings often lead to insufficient symptom management during intervals between chemotherapy sessions ^[14].

Patients' self-coping strategies for managing therapy-related symptoms are critical for reducing symptom burden and maintaining normal functional status and quality of life (QOL) during home-based recovery periods ^[15]. Previous observations have indicated that the symptom burden of cancer patients varies across chemotherapy cycles ^[16]. However, the specific symptom burden and self-coping patterns of pancreatic cancer patients at different stages of chemotherapy remain unclear.

The Symptom Experience in Time (SET) theory suggests that when patients recognize the onset of unpleasant symptoms, they engage in self-assessment and subsequently pursue either self-care or external assistance to facilitate effective symptom management ^[15]. By integrating symptom-related theories, such as the theory of unpleasant symptoms and the symptom management model, the SET theory incorporates temporal dimensions to provide valuable guidance for understanding symptom experiences and corresponding coping patterns.

Therefore, this study aimed to explore differences in symptom experiences and self-coping patterns during the early and late stages of chemotherapy among patients with pancreatic cancer. The findings are intended to serve as a foundation for implementing personalized clinical symptom assessment methods and improving phased symptom management interventions.

2. Materials and Methods

2.1. Study design

This study utilized a descriptive qualitative research approach, incorporating semi-structured personal interviews

to investigate the symptom experiences and self-coping patterns of patients with pancreatic cancer undergoing chemotherapy. The research combined thematic analysis with traditional content analysis methodologies. This approach was particularly advantageous, as thematic analysis provided a structured framework to explore patients' symptom experiences and their perceptions throughout the treatment process ^[17]. Traditional content analysis complemented this by objectively examining the textual data derived from thematic analysis. The study adhered to the Standards for Reporting Qualitative Research (SRQR) checklist to enhance transparency and ensure methodological rigor.

2.2. Participants and settings

A purposive sampling method, guided by the principle of maximum variation sampling, was employed to recruit 27 patients undergoing chemotherapy for pancreatic cancer at two tertiary hospitals in Southwest China between November 2023 and August 2024. The inclusion criteria were as follows: (1) patients aged 18 years or older; (2) confirmation of pancreatic malignancy through imaging and pathology, with patients undergoing chemotherapy; and (3) patients possessing clear consciousness and normal communication abilities. For this study, chemotherapy cycles were classified as early-stage (three or fewer cycles) or late-stage (more than three cycles) ^[18]. Ethical approval was obtained from the ethics committees of Mianyang Central Hospital (No: S202203501) and Chengdu Seventh People's Hospital (No: QT202300101). All participants provided written or electronic informed consent prior to inclusion.

2.3. Data collection

Patients meeting the inclusion criteria were identified in the oncology outpatient or inpatient departments. The study's purpose and procedures were thoroughly explained, and informed consent was obtained along with demographic and clinical information. Interviews were conducted face-to-face or telephonically at times convenient for the participants. Based on the SET theoretical framework, a formal interview outline (**Table 1**) was developed following discussions between two specialist physicians and two specialized nurses. Preliminary interviews with two patients further informed the outline's design.

Table 1. Outline of the interview

Number	Question
1	What symptoms did you experience during chemotherapy?
2	Could you describe the severity of these symptoms? Kindly elucidate your specific experiences in detail.
3	Have you noticed any disparity in the perception of these symptoms at various time points?
4	What effects have these symptoms had on you?
5	How do you typically cope with these symptoms? Do you ask for help positively?
6	What challenges or needs do you encounter during chemotherapy?

The interviews were conducted independently by researchers with over 12 months of clinical research experience and systematic training in qualitative research. Audio recordings and data collection were facilitated using electronic tablets. The sequence of questions during interviews was adjusted flexibly to ensure an engaging and accessible process. Data saturation was deemed achieved when no new themes emerged during the preliminary analysis and after interviewing two additional participants. At this point, the study was concluded.

2.4. Data analysis

Data transcription and analysis commenced immediately after the first interview. Within 24 hours of each interview, two researchers (Xin Tian and Peiyang Mao) transcribed the audio recordings into standard text, supplemented the transcripts with interview notes, and conducted verbatim verification. The first author utilized traditional content and thematic analyses as guiding frameworks for the data analysis.

Patient identities were anonymized using identifiers (P1–P27), and text encoding was conducted independently by researchers based on the study's thematic focus. The initial coding clusters were developed using the SET theoretical framework. Discrepancies in coding were resolved through team discussions to achieve consensus, and adjustments were made until a uniform agreement was reached. Subsequently, the findings were integrated and iteratively refined to delineate primary themes and subthemes. Data analysis was performed using NVivo software (NVivo Qualitative Data Analysis Software; QSR International Pty Ltd., 12th edition, 2018).

3. Results

3.1. Demographic and clinical characteristics

Interviews were conducted with 27 patients undergoing chemotherapy, including 13 in the early stages and 14 in the late stages of treatment. The duration of interviews ranged from 7 to 35 minutes, with a median duration of 18 minutes. The average age of participants was 58.19 years, with 15 female patients and 23 individuals in stages III–IV of the disease. Details of the demographic and clinical characteristics are presented in **Table 2**. The three themes and eight subthemes identified in this study are summarized in **Table 3**.

Table 2. Demographic and clinical characteristics of the patients ($n = 27$)

Patient	Age	Gender	Education	Occupation	Surgical history of pancreatic cancer	Pathological stage	Chemotherapy	
							Cycle	Stage
P2	34	Male	Junior high school	Unemployed	No	IV	3	Early
P7	65	Female	No formal education	Farmer	No	III	2	Early
P9	59	Female	Junior high school	Farmer	No	IV	1	Early
P10	53	Male	Primary school	Unemployed	No	IV	2	Early
P11	50	Male	Junior high school	Laborer	No	III	3	Early
P13	66	Female	College or undergraduate	Retired	Yes	IV	2	Early
P14	50	Female	Primary school	Unemployed	No	IV	2	Early
P17	78	Male	Primary school	Farmer	No	IV	1	Early
P18	70	Male	Junior high school	Farmer	Yes	II	3	Early
P20	72	Female	Junior high school	Unemployed	Yes	IV	1	Early
P21	58	Female	Primary school	Unemployed	Yes	IV	3	Early
P22	60	Male	Junior high school	Unemployed	No	IV	2	Early
P27	56	Female	Primary school	Unemployed	Yes	IV	1	Early
P1	69	Female	Primary school	Retired	Yes	I	4	Late
P3	57	Female	College or undergraduate	Retired	Yes	IV	4	Late

Table 2 (Continued)

Patient	Age	Gender	Education	Occupation	Surgical history of pancreatic cancer	Pathological stage	Chemotherapy	
							Cycle	Stage
P4	56	Male	College or undergraduate	Civil servant or corporate or institution staff	No	II	4	Late
P5	61	Female	High school or vocational school	Retired	Yes	IV	6	Late
P6	41	Male	College or undergraduate	Civil servant or corporate or institution staff	No	III	4	Late
P8	51	Female	Primary school	Unemployed	Yes	IV	4	Late
P12	57	Female	High school or vocational school	Retired	Yes	IV	4	Late
P15	68	Male	Primary school	Laborer	Yes	IV	4	Late
P16	54	Female	Primary school	Farmer	Yes	I	5	Late
P19	54	Male	High school or vocational school	Farmer	No	IV	5	Late
P23	54	Female	College or undergraduate	Civil servant or corporate or institution staff	No	III	6	Late
P24	61	Male	Junior high school	Laborer	No	IV	4	Late
P25	55	Female	High school or vocational school	Retired	Yes	IV	6	Late
P26	62	Male	Junior high school	Retired	No	IV	4	Late

Table 3. Themes and subthemes

Themes	Subthemes	Content
Symptom experience	Varied symptom presentation	Pain
		Fatigue
		Lack of appetite
		Nausea
		Numbness
		Fever
		Itchy skin
	Dynamic symptom perception	Fluctuations within a cycle
		Variability between cycles
		Perception of severity
	Multidimensional symptom impact	Emotion
		Social interaction
		Daily activity
		Walking
		Work

Table 3 (Continued)

Themes	Subthemes	Content
Self-coping patterns	External support as the main approach	Seeking medical attention proactively
		Seeking multifaceted support from healthcare providers, family members, and friends
	Self-care as the main approach	Transforming behavioral patterns and lifestyle
		Redirecting attention
		Emotional regulation
		Self-endurance
Existing obstacles	Accessing medical resources	Insufficient feedback from healthcare providers
		Resource constraints
		Cumbersome disposal procedures
		Inconvenient access to medical care
	Negative attitude towards seeking support	Imposing an additional burden on others
		Barriers to effective communication
	Insufficient awareness of symptom management	Improper medication usage
		Lack of common knowledge
	Facing challenges in emotional regulation	Perceiving others as incapable of providing support or assistance
		Social impairments
		Disorder of negative emotion management

3.2. Symptom experience

The symptoms experienced by the patients were notably diverse, affecting multiple bodily systems. Variations were observed in the symptom presentation reported by patients at different stages of chemotherapy, as well as in their perceptions of symptoms and their impact (**Figure 1**).

3.2.1. Varied symptom presentation

Patients reported a total of 27 distinct physical symptoms, with a median of six symptoms per individual. The symptoms were categorized based on the International Classification of Functioning, Disability, and Health (ICF) anatomical structures, encompassing eight neurological symptoms, 11 gastrointestinal symptoms, one cardiovascular and respiratory symptom, three endocrine and metabolic symptoms, and four skin and related structural symptoms. A detailed list of symptoms and their reporting percentages is provided in **Figure 2**.

Symptoms related to the nervous system, endocrine and metabolic systems, and skin structures were reported more frequently during the early stages of chemotherapy.

P1 (69-year-old, female, cycle 4): “During the first two or three cycles, eating wasn’t really affected, but later it got worse. I started feeling nauseous, and food felt greasy and heavy.”

P5 (61-year-old, female, cycle 6): “I felt very weak, like my whole body was exhausted. My legs felt shaky when I walked.”

P13 (66-year-old, female, cycle 2): “I’m constipated now. We’ve tried everything, and I haven’t had a bowel movement in three days.”

P22 (60-year-old, male, cycle 2): “The worst part is the pain. It hurts right here (touching the abdomen).”

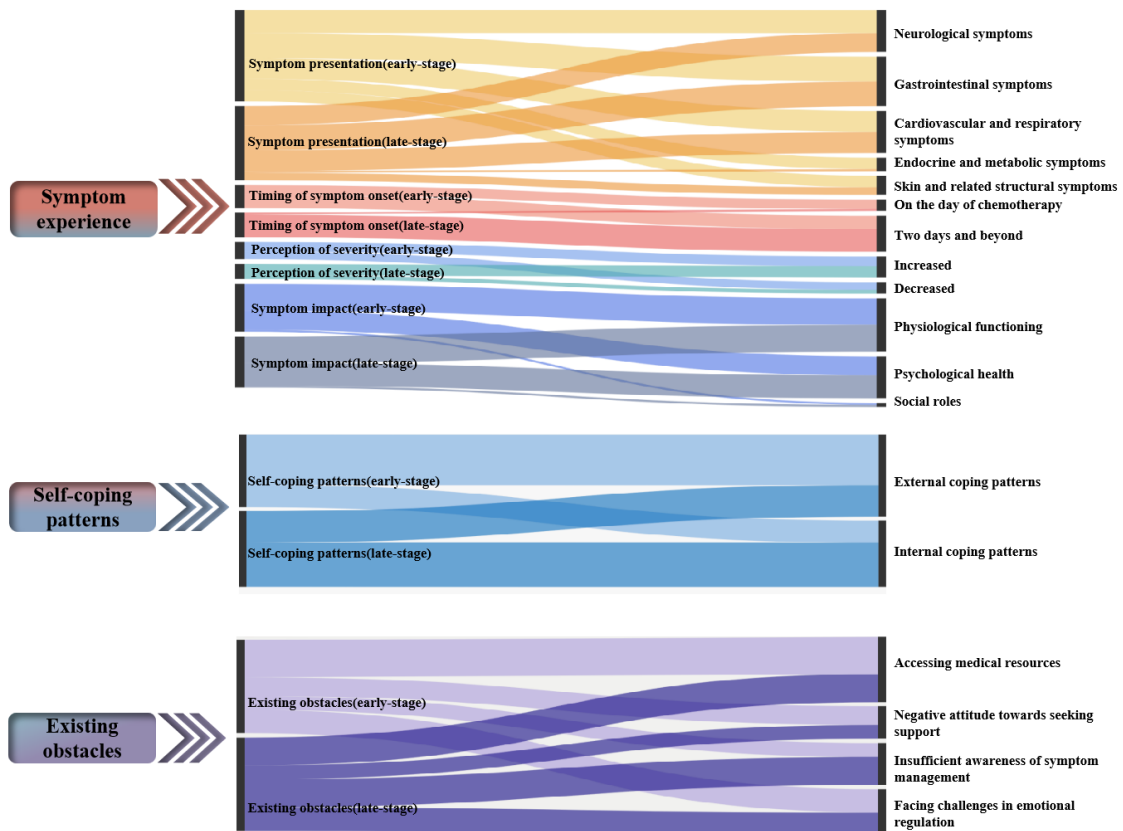


Figure 1. Description of symptom experience, self-coping patterns, and existing obstacles in the early and late stages of chemotherapy

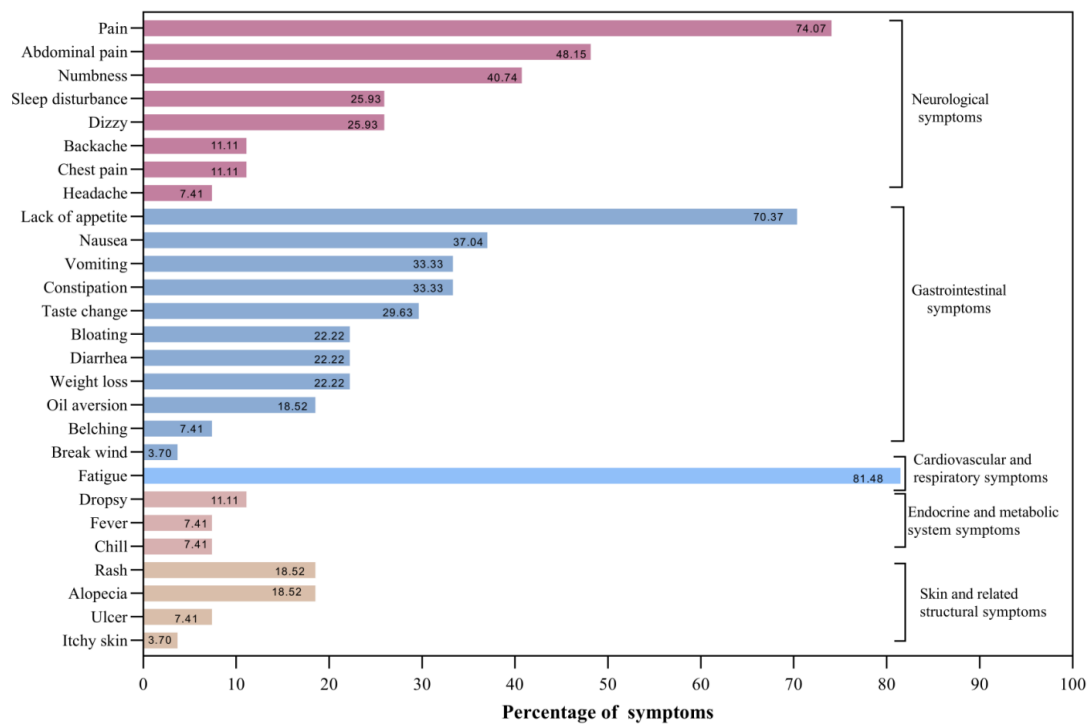


Figure 2. Detailed list of symptoms reported by patients, accompanied by the prevalence percentage for each individual symptom

3.2.2. Dynamic symptom perception

The demanding nature of the chemotherapy regimen imposes significant physical and psychological burdens on some patients. Variations in the onset and recovery of symptoms were observed both within the intervals between treatment cycles and across different stages of chemotherapy.

Nineteen patients reported experiencing adverse reactions within two to three days of returning home, of whom 12 were in the late stage of chemotherapy. Conversely, six patients noted the emergence of symptoms on the day of treatment itself, with five of these patients being in the early stages of chemotherapy.

P6 (41-year-old, male, cycle 4): “Usually, symptoms showed up two to three days after chemo. After those two or three days, they disappeared.”

P13 (66-year-old, female, cycle 2): “I throw up about a day after the chemo, that’s usually the day it started.”

Symptoms generally subsided over a span of approximately one week; however, fatigue persisted as a chronic issue for many.

P3 (57-year-old, female, cycle 4): “Fatigue is just part of the routine. It’s always been like this.”

P22 (60-year-old, male, cycle 2): “For example, I got the chemo today, and the worst is usually tomorrow and the day after. It’ll be around six or seven days before I start feeling better.”

Eleven patients reported increasingly severe or unpredictable symptoms as their treatment progressed. Conversely, six patients described developing a gradual tolerance to the symptoms, with four of these patients being in the early stages of chemotherapy.

P7 (65-year-old, female, cycle 2): “I had two cycles of chemotherapy before, and my stomach doesn’t hurt as much now. It feels like it’s getting a bit better.”

P12 (57-year-old, female, cycle 4): “... By the third cycle, I couldn’t recover for a week. By the fourth cycle, when I was supposed to rest for two weeks, I still couldn’t recover in that time.”

3.2.3. Multidimensional symptom impact

The symptoms associated with chemotherapy had a multifaceted negative impact, affecting patients’ physiological functioning, psychological well-being, and social roles.

Although differences in emotional distress between the early and late stages of chemotherapy were not clearly captured, many patients reported psychological challenges, including negative emotions and social impairments related to self-image and physical appearance. A total of 22 patients reported experiencing anxiety, irritability, restlessness, and pessimism due to chemotherapy-related symptoms.

P7 (65-year-old, female, cycle 2): “I’m quick to lose my temper and snap when I’m feeling down.”

P15 (68-year-old, male, cycle 4): “I’ve generally had a pretty good attitude, but this illness has really been affecting me.”

P21 (58-year-old, female, cycle 3): “Even after just two or three days back home, I still didn’t feel like eating. It left me feeling anxious and worried.”

Physiological challenges included difficulties with walking and performing daily activities, which were reported more frequently by patients in the late stages of chemotherapy.

P11 (50-year-old, male, cycle 3): “I do walk around a bit, but mostly I stay in bed. When I get up to go to the bathroom, I stumble around.”

P20 (72-year-old, female, cycle 1): “Anyway, I haven’t really gone downstairs. We live on the fourth floor, so I just walk around the house a bit, eat, stand around, and I feel like I have no energy at all.”

The impact on social roles was evident, with younger patients reporting work-related disruptions due to discomfort.

P2 (34-year-old, male, cycle 3): “Because I have already stopped working.”

P19 (54-year-old, male, cycle 5): “I can’t get a job again. No one wants to hire me for anything, not even for picking up garbage.”

3.3. Self-coping patterns

Patients primarily employed two self-coping strategies when dealing with distressing symptoms: seeking external support and engaging in self-care. These self-coping patterns varied depending on the stage of treatment (**Figure 1**).

3.3.1. External coping patterns

Some patients predominantly relied on external assistance to cope with their symptoms. The external coping strategies included proactive healthcare engagement (20/27), seeking help from healthcare providers as well as family and friends (9/27), and obtaining public information (4/27). For these patients, healthcare providers played a significant role in alleviating unpleasant symptoms associated with chemotherapy.

P2 (34-year-old, male, cycle 3): “After my second round of chemo, I told my attending physician about my insomnia, and he prescribed me some sleeping pills. I also mentioned that I had occasional abdominal pain, so he gave me some painkillers.”

P7 (65-year-old, female, cycle 2): “My son and daughter-in-law told me that keeping up with nutrition is important for my immune system, especially since chemo is so damaging. They’d tell me what to eat and what to buy each day.”

P11 (50-year-old, male, cycle 3): “What else can I do? I just take some medicine... get a prescription, take the pills, and go see the doctor.”

P18 (70-year-old, male, cycle 3): “I’ve been watching a lot of educational videos; they all say to eat light, eat whole grains, and cut back on main staples like rice.”

3.3.2. Internal coping patterns

Other patients adopted self-centered coping strategies, including behavioral and lifestyle modifications (12/27), redirecting attention (8/27), and emotional regulation (6/27). These efforts were aimed at improving their overall quality of life (QOL). Notably, 10 patients endured their suffering in silence, forming a group that warrants significant attention and support in the future.

P5 (50-year-old, male, cycle 6): “I’d listen to audiobooks or music... just to take my mind off things and try to relax a bit.”

P7 (65-year-old, female, cycle 2): “I’m worried that it’s getting worse. How will I manage? There are so many rounds left, a few more cycles to go.”

P12 (57-year-old, female, cycle 4): “At home, I’d move around a bit and use a hot water bottle. That was about it. What else could I do?”

P19 (54-year-old, male, cycle 5): “When I had symptoms, they would gradually go away. By then, I already knew how it worked.”

P23 (54-year-old, female, cycle 3): “Actually, I think you can consult patients more from a psychological perspective or guide them. I believe this is important.”

3.3.3. Differences in self-coping patterns based on the stage of chemotherapy

Patients undergoing the initial three cycles of chemotherapy exhibited a cheerful outlook and were more inclined to seek external support. There were six more patients in the early stages of chemotherapy who primarily employed external coping strategies compared to those in the late stages. Conversely, patients who had undergone more than three cycles of chemotherapy tended to manage their suffering independently, relying on self-care. In the late stages of chemotherapy, patients were more oriented toward internal self-coping strategies compared to those in the early stages.

3.4. Existing obstacles

Although patients often take proactive measures to manage unpleasant symptoms, they encounter various obstacles in addressing their condition. A larger proportion of patients in the early stages of chemotherapy reported challenges in accessing medical resources (14/27). Conversely, more patients in the late stages of chemotherapy displayed a negative attitude toward seeking support (7/27) and demonstrated insufficient awareness of symptom management (9/27). Emotional regulation disorders were observed across different stages of treatment (10/27).

3.4.1. Accessing medical resources

Patients frequently experienced physical discomfort during consultations and pharmacological interventions. Due to the unique nature of their illnesses and treatment modalities, 14 patients encountered such challenges, eight of whom were in the early stages of chemotherapy. These issues included insufficient or delayed feedback from healthcare providers (6/27), resource constraints (4/27), and cumbersome medical procedures (2/27).

P11 (50-year-old, male, cycle 3): “We’ve tried a lot of ways, but in the end, they just tell us to go to the hospital. But when we get there, there’s no available bed.”

P12 (57-year-old, female, cycle 4): “I asked the doctor, and they said these are just the side effects of the treatment. There’s nothing we can do.”

P20 (72-year-old, female, cycle 1): “The process is too complicated. They take so much blood at once, three or four vials.”

In addition, some patients expressed frustration due to difficulties in accessing medical care (2/27). Geographical distance from healthcare facilities often hindered their ability to obtain analgesics regularly and address their concerns promptly.

P9 (59-year-old, female, cycle 1): “We can ask other patients or doctors at the hospital, but when we go back to our hometown, there’s no one to ask.”

P22 (60-year-old, male, cycle 2): “I had to travel far just to get some painkillers. What can I do?”

3.4.2. Negative attitude towards seeking support

Seven patients faced challenges in seeking external support from hospitals and family, with four of these patients in the late stages of chemotherapy. Psychological burdens contributed to their reluctance to seek assistance, as they were mindful of the busy schedules of healthcare providers and the additional strain on their family members (4/27). Furthermore, stigma associated with their condition and communication barriers, particularly in older patients, discouraged them from seeking help (3/27).

P1 (69-year-old, female, cycle 4): “When I got sick, the whole family started to revolve around me, and it just added to the stress.”

P2 (34-year-old, male, cycle 3): *“I feel like if I can solve things on my own, I won’t have to bother my family or the doctors and nurses.”*

P5 (65-year-old, female, cycle 2): *“I just feel like I don’t want to interact with anyone, don’t want to communicate with others. It means I feel pretty lonely and isolated, you know? I guess I’m just feeling a bit down.”*

3.4.3. Insufficient awareness of symptom management

Nine patients demonstrated a lack of understanding regarding effective symptom management, with six of them primarily relying on internal self-coping strategies in the late stages of chemotherapy. Fear of potential addiction to medications or the belief that such drugs might obscure critical bodily signals led some patients to avoid using analgesics or sedatives (3/27). Many opted to endure discomfort until their physical condition became untenable.

P10 (53-year-old, male, cycle 2): *“I did buy those sleeping pills; the doctor prescribed me sleeping pills and painkillers, but I haven’t taken any. If I start taking them, I’ll have to rely on them all the time.”*

P20 (72-year-old, female, cycle 1): *“If I take the medicine, it’ll just mask the issues happening in my body. So, I can’t know what’s wrong with my body.”*

Additionally, some patients believed that others were incapable of offering meaningful support (7/27), prompting them to reject counseling.

P12 (57-year-old, female, cycle 4): *“The doctors don’t really have a solution now. No matter how they try to help, they can’t solve these problems for me.”*

3.4.4. Facing challenges in emotional regulation

Emotional regulation disorders were evenly distributed among patients at different stages of chemotherapy. Many patients struggled to regulate their emotional states in response to distressing symptoms (8/27). Anxiety over the potential ineffectiveness of treatments, fear of worsening conditions, and uncertainty about future therapies, particularly when faced with severe adverse reactions, were common concerns.

P7 (65-year-old, female, cycle 2): *“I’m worried that it’s getting worse. How will I manage? There are so many rounds left, a few more cycles to go.”*

P13 (66-year-old, female, cycle 2): *“I can’t help but think about it—this pain here and there. Is it spreading somewhere else?”*

Feelings of inferiority, driven by fear of judgment or stigma, further discouraged social interactions (3/27).

P18 (70-year-old, male, cycle 3): *“That’s why I don’t want to tell people about this. In rural areas, people tend to look down on it.”*

5. Discussion

This study revealed that patients with pancreatic cancer experience a complex and diverse range of symptoms during chemotherapy, with variations in their experiences and coping patterns at different stages of treatment. Patients in the early stages of chemotherapy were more likely to adopt external self-coping patterns to manage their symptoms, whereas those who had undergone more than three cycles of chemotherapy tended to rely on internal self-coping strategies. These findings provide valuable insights for healthcare providers, supporting the implementation of ongoing symptom monitoring and personalized self-coping strategies.

Patients reported a wide range of physical symptoms affecting various systems during chemotherapy, including the neurological, cardiovascular, gastrointestinal, and other systems^[19]. Symptoms related to the

nervous, endocrine, metabolic systems, and skin structures were more prevalent among patients in the early stages of chemotherapy compared to those in later stages. Additionally, patients in the early stages of chemotherapy tended to perceive the onset of symptoms earlier than those in the later stages. This may be attributed to an increased threshold for symptom perception as chemotherapy progresses, consistent with previous findings that cancer patients' perception of symptoms can change over time ^[20].

The diverse symptoms experienced by patients have multidimensional effects. Physiologically, walking difficulties were more prevalent among patients in the late stages of chemotherapy, potentially linked to the prolonged symptom burden and the coping strategies employed. Psychologically, the impact of symptoms was significant but often overlooked by patients. Over time, emotional avoidance may inadvertently lead to a decline in quality of life (QOL) ^[21]. These findings underscore the importance of conducting symptom assessments at regular intervals during chemotherapy. Frequent symptom assessments can provide critical insights into the patient's physiological condition and identify when interventions are needed outside the hospital. By employing high-frequency symptom monitoring, variations and patterns in symptom severity can be accurately identified, enabling timely interventions to mitigate adverse outcomes ^[22]. This study provides a qualitative foundation for the development of assessment tools for patients with pancreatic cancer. Continuous symptom monitoring during consultations, combined with real-time decision support, represents a promising strategy for addressing these challenges ^[23].

The findings also revealed that seeking external support was the primary self-coping strategy for patients in the early stages of chemotherapy. These patients tended to adopt problem-focused coping strategies ^[24], driven by the fear of "unknown" consequences of treatment, as they were unfamiliar with chemotherapy during its initial stages. In contrast, self-care emerged as the predominant coping approach among patients in the late stages of chemotherapy. This strategy was not primarily focused on addressing specific problems but was instead characterized by an emotion-focused approach. Previous studies have demonstrated that patients employing problem-focused coping strategies tend to be more proactive, while those relying on emotion-focused strategies are more likely to experience severe anxiety ^[25].

Patients face numerous obstacles in managing their symptoms due to both internal and external factors, which persist throughout chemotherapy. These barriers are closely tied to the self-coping patterns patients adopt. It was observed that a greater number of patients in the early stages of chemotherapy felt that support from healthcare providers was insufficient, likely due to communication challenges and limited medical resources ^[26,27]. This aligns with the finding that patients in advanced stages require more comprehensive care and support ^[28]. In contrast, some patients demonstrated a reluctance to seek help, choosing instead to endure discomfort silently due to psychological burdens and a tendency to conceal their symptoms ^[29]. Many of these patients preferred to manage their discomfort independently.

By addressing the existing obstacles and understanding the self-coping patterns of patients, symptom management can be significantly improved. Between chemotherapy sessions, timely access to support and effective self-care are critical for recovery. Remote monitoring and management systems offer a promising solution for alleviating the burden on healthcare providers while addressing patients' needs in the future ^[30].

5. Limitations

Due to the characteristics of qualitative research and the late-stage diagnosis of pancreatic cancer, a larger proportion of the participants interviewed were in the advanced stages of the disease. While the limited sample size

may affect the representativeness of the findings, the study nonetheless captures specific disease characteristics. The principle of data saturation was followed, with data collection ceasing when no new themes emerged. Additionally, the retrospective nature of the interviews may have introduced recall bias. Future research should consider adopting a longitudinal qualitative design or a quantitative approach to gain a more comprehensive understanding of the symptom burden and barriers faced by patients with pancreatic cancer.

6. Conclusion

Patients with pancreatic cancer experience a multifaceted and dynamic spectrum of symptoms throughout chemotherapy. Significant differences were observed between the early and late stages of chemotherapy in terms of symptom experiences and self-coping patterns. Patients in the early stages exhibited heightened sensitivity to symptoms and predominantly sought external support, whereas those in the late stages increasingly relied on self-care strategies. These differing self-coping patterns were frequently associated with distinct obstacles to symptom management. Enhancing collaboration among healthcare providers, families, and patients is essential. Regular symptom monitoring during chemotherapy, identification of primary burdens at different stages, and implementation of tailored management strategies aligned with patients' preferred coping styles are crucial for optimizing care and improving outcomes.

Acknowledgments

We sincerely thank all the patients who voluntarily participated in this interview and dedicated their time to our research. Allowing us to see issues from their perspective has greatly enriched our understanding.

Ethics approval and informed consent

This study was approved by the ethics committees of Mianyang Central Hospital (No: S202203501) and Chengdu Seventh People's Hospital (No: QT202300101). All participants provided written or electronic informed consent.

Consent for participation

Informed consent was obtained from all individual participants included in the study.

Funding

This work was supported by the State Key Laboratory of Ultrasonic Medical Engineering/the Chongqing Science and Technology Bureau (Project No. 2022KFKT7011), the Postdoctoral Fellowship Program of CPSF (GZC20233357), the Health Commission of Sichuan Province Medical Science and Technology Program (24QNMP007) and the Medical Research Program of Health Commission of Chengdu (2023535).

Disclosure statement

The authors declare no conflict of interest.

References

- [1] Bray F, Laversanne M, Sung H, et al., 2024, Global Cancer Statistics 2022: GLOBOCAN Estimates of Incidence and Mortality Worldwide for 36 Cancers in 185 Countries. *CA Cancer J Clin*, 74(3): 229–263. <https://doi.org/10.3322/caac.21834>
- [2] Park W, Chawla A, O'Reilly EM, 2021, Pancreatic Cancer: A Review. *JAMA*, 326(9): 851–862. <https://doi.org/10.1001/jama.2021.13027>. Erratum in *JAMA*, 326(20): 2081. <https://doi.org/10.1001/jama.2021.19984>
- [3] Yu KH, 2024, Advances in Systemic Therapy in Pancreatic Cancer. *Hematol Oncol Clin North Am*, 38(3): 617–627. <https://doi.org/10.1016/j.hoc.2024.03.002>
- [4] Weiss L, Fischer LE, Heinemann V, et al., 2024, Changes Over Time in the Course of Advanced Pancreatic Cancer Treatment with Systemic Chemotherapy: A Pooled Analysis of Five Clinical Trials from Two Decades of the German AIO Study Group. *ESMO Open*, 9(4): 102944. <https://doi.org/10.1016/j.esmoop.2024.102944>
- [5] Evans D, Ghassemi N, Hajibandeh S, et al., 2024, Meta-Analysis of Adjuvant Chemotherapy Versus No Adjuvant Chemotherapy for Resected Stage I Pancreatic Cancer. *Surgery*, 175(6): 1470–1479. <https://doi.org/10.1016/j.surg.2023.11.027>
- [6] Altman AM, Wirth K, Marmor S, et al., 2019, Completion of Adjuvant Chemotherapy After Upfront Surgical Resection for Pancreatic Cancer is Uncommon Yet Associated with Improved Survival. *Ann Surg Oncol*, 26(12): 4108–4116. <https://doi.org/10.1245/s10434-019-07602-6>
- [7] Chen J, Chen L, Yu J, et al., 2019, Meta-Analysis of Current Chemotherapy Regimens in Advanced Pancreatic Cancer to Prolong Survival and Reduce Treatment-Associated Toxicities. *Mol Med Rep*, 19(1): 477–489. <https://doi.org/10.3892/mmr.2018.9638>
- [8] Takeda T, Sasaki T, Mie T, et al., 2021, The Prognostic Impact of Tumour Location and First-Line Chemotherapy Regimen in Locally Advanced Pancreatic Cancer. *Jpn J Clin Oncol*, 51(5): 728–736. <https://doi.org/10.1093/jjco/hyab014>
- [9] Lelond S, Ward J, Lambert PJ, et al., 2021, Symptom Burden of Patients with Advanced Pancreas Cancer (APC): A Provincial Cancer Institute Observational Study. *Curr Oncol*, 28(4): 2789–2800. <https://doi.org/10.3390/curroncol28040244>
- [10] Liu C, Liu L, Chen M, 2023, Experience of Living with Symptom Clusters in Postoperative Pancreatic Cancer Patients. *Eur J Oncol Nurs*, 62: 102266. <https://doi.org/10.1016/j.ejon.2022.102266>
- [11] Tang CC, Draucker C, Tejani M, et al., 2018, Symptom Experiences in Patients with Advanced Pancreatic Cancer as Reported During Healthcare Encounters. *Eur J Cancer Care (Engl)*, 27(3): e12838. <https://doi.org/10.1111/ecc.12838>
- [12] Tang CC, Von Ah D, Fulton JS, 2018, The Symptom Experience of Patients With Advanced Pancreatic Cancer: An Integrative Review. *Cancer Nurs*, 41(1): 33–44. <https://doi.org/10.1097/NCC.0000000000000463>
- [13] Giesinger JM, Wintner LM, Zabernigg A, et al., 2014, Assessing Quality of Life on the Day of Chemotherapy Administration Underestimates Patients' True Symptom Burden. *BMC Cancer*, 14: 758. <https://doi.org/10.1186/1471-2407-14-758>
- [14] Komatsu H, Yagasaki K, Hirata K, et al., 2019, Unmet Needs of Cancer Patients with Chemotherapy-Related Hand-Foot Syndrome and Targeted Therapy-Related Hand-Foot Skin Reaction: A Qualitative Study. *Eur J Oncol Nurs*, 38: 65–69. <https://doi.org/10.1016/j.ejon.2018.12.001>
- [15] Henly SJ, Kallas KD, Klatt CM, et al., 2003, The Notion of Time in Symptom Experiences. *Nurs Res*, 52(6): 410–417. <https://doi.org/10.1097/00006199-200311000-00009>
- [16] Rha SY, Park M, Lee J, 2019, Stability of Symptom Clusters and Sentinel Symptoms During the First Two Cycles of

Adjuvant Chemotherapy. *Support Care Cancer*, 27(5): 1687–1695. <https://doi.org/10.1007/s00520-018-4413-9>

- [17] Braun V, Clarke V, 2019, Novel Insights into Patients' Life-Worlds: The Value of Qualitative Research. *Lancet Psychiatry*, 6(9): 720–721. [https://doi.org/10.1016/S2215-0366\(19\)30296-2](https://doi.org/10.1016/S2215-0366(19)30296-2)
- [18] Zhang J, Wang S, Zhou Z, et al., 2023, Unpleasant Symptoms of Immunotherapy for People with Lung Cancer: A Mixed-Method Study. *Int J Nurs Stud*, 139: 104430. <https://doi.org/10.1016/j.ijnurstu.2022.104430>
- [19] Livshits Z, Rao RB, Smith SW, 2014, An Approach to Chemotherapy-Associated Toxicity. *Emerg Med Clin North Am*, 32(1): 167–203. <https://doi.org/10.1016/j.emc.2013.09.002>
- [20] Nunes KZ, Grippa WR, Lopes AB, et al., 2024, Cancer Symptom Clusters, Cardiovascular Risk, and Quality of Life of Patients with Cancer Undergoing Chemotherapy: A Longitudinal Pilot Study. *Medicine (Baltimore)*, 103(16): e37819. <https://doi.org/10.1097/MD.00000000000037819>
- [21] Davis S, Serfaty M, Low J, et al., 2023, Experiential Avoidance in Advanced Cancer: A Mixed-Methods Systematic Review. *Int J Behav Med*, 30(5): 585–604. <https://doi.org/10.1007/s12529-022-10131-4>
- [22] Yu H, Lei C, Wei X, et al., 2024, Electronic Symptom Monitoring After Lung Cancer Surgery: Establishing a Core Set of Patient-Reported Outcomes for Surgical Oncology Care in a Longitudinal Cohort Study. *Int J Surg*, 110(10): 6591–6600. <https://doi.org/10.1097/JS9.0000000000001855>
- [23] Mooney K, Whisenant MS, Beck SL, 2019, Symptom Care at Home: A Comprehensive and Pragmatic PRO System Approach to Improve Cancer Symptom Care. *Med Care*, 57 Suppl 5 Suppl 1(Suppl 5 1): S66–S72. <https://doi.org/10.1097/MLR.0000000000001037>
- [24] Folkman S, Lazarus RS, Gruen RJ, et al., 1986, Appraisal, Coping, Health Status, and Psychological Symptoms. *J Pers Soc Psychol*, 50(3): 571–579. <https://doi.org/10.1037//0022-3514.50.3.571>
- [25] Silva AVD, Zandonade E, Amorim MHC, 2017, Anxiety and Coping in Women with Breast Cancer in Chemotherapy. *Rev Lat Am Enfermagem*, 25: e2891. <https://doi.org/10.1590/1518-8345.1722.2891>
- [26] Khan NN, Maharaj A, Evans S, et al., 2022, A Qualitative Investigation of the Supportive Care Experiences of People Living with Pancreatic and Oesophagogastric Cancer. *BMC Health Serv Res*, 22(1): 213. <https://doi.org/10.1186/s12913-022-07625-y>
- [27] Challinor JM, Alqudimat MR, Teixeira TOA, et al., 2020, Oncology Nursing Workforce: Challenges, Solutions, and Future Strategies. *Lancet Oncol*, 21(12): e564–e574. [https://doi.org/10.1016/S1470-2045\(20\)30605-7](https://doi.org/10.1016/S1470-2045(20)30605-7)
- [28] Temiz G, Durna Z, 2020, Evaluation of Quality of Life and Health Care Needs in Cancer Patients Receiving Chemotherapy. *J Cancer Educ*, 35(4): 796–807. <https://doi.org/10.1007/s13187-019-01533-2>
- [29] Riegel B, Page SD, Aryal S, et al., 2024, Symptom Characteristics, Perceived Causal Attributions, and Contextual Factors Influencing Self-Care Behaviors: An Ecological Daily Assessment Study of Adults with Chronic Illness. *Patient Educ Couns*, 123: 108227. <https://doi.org/10.1016/j.pec.2024.108227>
- [30] Maguire R, McCann L, Kotronoulas G, et al., 2021, Real Time Remote Symptom Monitoring During Chemotherapy for Cancer: European Multicentre Randomised Controlled Trial (eSMART). *BMJ*, 374: n1647. <https://doi.org/10.1136/bmj.n1647>. Erratum in *BMJ*, 374: n2116. <https://doi.org/10.1136/bmj.n2116>

Publisher's note

Bio-Byword Scientific Publishing remains neutral with regard to jurisdictional claims in published maps and institutional affiliations.

The Predictive Value of *SPP1* Gene Expression for the Survival of Advanced Liver Cancer Treated with Transarterial Chemoembolization

Yu Cai¹, Pu Yan^{1*}, Chang Tian², Yuqing Li³, Yuanyuan Jia², Siqi Wang²

¹Department of General Surgery, The First Affiliated Hospital of Xi'an Medical University, Xi'an 710000, Shaanxi Province, China

²Faculty Development and Teaching Evaluation Office, The First Affiliated Hospital of Xi'an Medical University, Xi'an 710000, Shaanxi Province, China

³Xi'an Medical University, Xi'an 710000, Shaanxi Province, China

*Corresponding author: Pu Yan, sxyanpu@163.com

Copyright: © 2025 Author(s). This is an open-access article distributed under the terms of the Creative Commons Attribution License (CC BY 4.0), permitting distribution and reproduction in any medium, provided the original work is cited.

Abstract: *Objective:* To evaluate the predictive value of *secreted phosphoprotein 1 (SPP1)* gene expression for postoperative survival in patients with advanced liver cancer undergoing hepatic artery interventional chemoembolization treatment. *Method:* Bioinformatics methods, including gene ontology (GO) and Kyoto Encyclopedia of Genes and Genomes (KEGG) pathway analysis, were used to identify genes related to survival prognosis in hepatocellular carcinoma (HCC) patients. A retrospective analysis of 115 advanced liver cancer patients treated between January 2016 and October 2017 was conducted. Patients were categorized into *SPP1* high-expression ($n = 89$) and low-expression groups ($n = 26$). Additionally, 115 healthy individuals served as the control group. The relationship between *SPP1* expression and clinical pathological features was analyzed. A 60-month follow-up and logistic regression analysis identified risk factors affecting survival. *Results:* *SPP1* mRNA expression was significantly higher in liver cancer patients compared to healthy controls ($P < 0.05$). *SPP1* expression levels were significantly associated with tumor size, Child-Pugh grading, lymph node metastasis, and BCLC staging ($P < 0.05$). High *SPP1* expression, along with tumor size, Child-Pugh grading, lymph node metastasis, and BCLC staging, were independent risk factors for survival ($P < 0.05$). The 60-month survival rate was 17.39%, with a median survival of 40 months in the low-expression group versus 18 months in the high-expression group ($P < 0.05$). *Conclusion:* *SPP1* expression is significantly upregulated in advanced liver cancer patients and has predictive value for postoperative survival following hepatic artery chemoembolization treatment. *SPP1*, combined with clinical indicators such as tumor size, Child-Pugh grading, lymph node metastasis, and BCLC staging, may serve as a prognostic biomarker for interventional treatment outcomes.

Keywords: *SPP1*; Transarterial chemoembolization; Advanced liver cancer; Survival period; Predictive value

Online publication: February 13, 2025

1. Introduction

Liver cancer is one of the most prevalent malignant tumors worldwide, characterized by high incidence and mortality rates. However, most patients with liver cancer seek medical attention only after the disease has progressed to an advanced stage. Consequently, early diagnosis is of critical importance for effective treatment ^[1]. Currently, alpha-fetoprotein (AFP) serves as a diagnostic biomarker for liver cancer, but it has limitations in diagnostic accuracy. Studies indicate that 32% to 59% of liver cancer patients exhibit normal AFP levels. Moreover, understanding the prognosis of cancer patients is crucial for improving their quality of life and optimizing treatment strategies. This underscores the necessity of identifying novel, more accurate biomarkers to enhance patient survival and prognosis.

Secretory phosphoprotein 1 (SPP1) is a chemokine-like glycoprotein secreted by cells and is recognized as a significant mediator of tumor-associated inflammation. In prostate cancer research, SPP1 expression has been shown to be significantly upregulated, contributing to the development of multidrug resistance and complicating clinical management. Additionally, bioinformatics analyses have revealed that SPP1 expression is markedly elevated in hepatocellular carcinoma tissues. However, the relationship between SPP1 expression and postoperative survival in patients with advanced liver cancer remains unclear. This study aims to assess the predictive value of *SPP1* gene expression for postoperative survival in patients with advanced liver cancer undergoing hepatic artery interventional chemoembolization treatment.

2. Methods

2.1. Expression difference analysis

R software version 4.13 was used to process and convert the downloaded data for analysis. The “ggpuber” R package was employed to analyze the differential expression of SPP1 mRNA between HCC tissue and normal tissue. Statistical significance was considered at $P < 0.05$.

2.2. Survival analysis and clinical feature correlation analysis

SPP1 was divided into high-expression and low-expression groups based on the median SPP1 mRNA expression in HCC tissue (median = 5.32768). The “survival” and “survminer” R packages, along with Kaplan-Meier curves, were used to analyze the relationship between *SPP1* expression levels and the survival of HCC patients. Univariate Cox regression analysis was conducted to evaluate the relationship between *SPP1* expression levels and patient prognosis, and receiver operating characteristic (ROC) curves were plotted. Statistical significance was defined as $P < 0.05$.

2.3. Differential gene analysis and functional enrichment analysis

Differential genes between the *SPP1* high-expression and low-expression groups were identified using the “limma” R package. Upregulated and downregulated genes underwent Gene Ontology (GO) biological function annotation and Kyoto Encyclopedia of Genes and Genomes (KEGG) signaling pathway enrichment analysis using the “circularize” and “clusterProfiler” R packages. Statistical significance was defined as $P < 0.05$, with the adjusted P -value (P_{adj}) and false discovery rate (FDR) q -value less than 0.05.

2.4. Research subjects

A retrospective analysis was conducted on 115 patients with advanced liver cancer treated at the First Affiliated Hospital of Xi'an Medical College from January 2016 to October 2017.

Inclusion criteria: (1) Patients meeting diagnostic and treatment criteria for liver cancer ^[4], aligned with the American College of Hepatology or the European College of Hepatology guidelines; (2) Barcelona Clinic Liver Cancer (BCLC) staging Phase B or C; (3) Underwent hepatic artery interventional chemoembolization; (4) Possessed basic language and hearing abilities, with informed consent obtained from patients and families; (5) No prior treatment before the study; (6) Karnofsky performance status exceeding 60 points.

Exclusion criteria: (1) Combined malignancies (e.g., gastric or lung cancer); (2) Severe abnormalities in liver, kidney, or heart function; (3) Intolerance to hepatic artery chemoembolization; (4) Abnormal coagulation function or infectious diseases.

Based on the optimal ROC-determined threshold value ($SPP1 = 2.03$), patients were divided into two groups: the *SPP1* low-expression group (26 cases, $SPP1 \leq 2.03$) and the *SPP1* high-expression group (89 cases, $SPP1 > 2.03$). A control group of 115 healthy individuals was also included. The study was approved by the hospital ethics committee and adhered to relevant medical ethics principles.

2.5. Hepatic artery interventional chemoembolization

Patients received traditional hepatic artery interventional chemoembolization ^[5]. An emulsion of 2–20 mL iodized oil, doxorubicin (10–40 mg), and mitomycin (2–10 mg) was injected selectively into the tumor's feeding artery via a hepatic artery catheter. Gelatin sponge or PVA particles were used for arterial embolization until blood flow to the main feeding artery ceased. Enhanced CT scans were performed 4–8 weeks post-procedure. Patients with residual active lesions and adequate liver function underwent repeated treatment as necessary.

2.6. Real-time fluorescence quantitative PCR (RT-PCR) for *SPP1* detection

Peripheral blood mononuclear cells were collected from 8 mL of fasting venous blood from liver cancer patients three days post-surgery and from healthy controls during physical exams. Density gradient centrifugation was used for separation. RNA was extracted using the TRIZOL method, and RNA purity was assessed via UV spectrophotometry (acceptable range: 1.8–2.1). Primer design was completed using Primer5 software, and *SPP1* mRNA expression was quantified using the $2^{-\Delta\Delta CT}$ method, with GAPDH serving as the internal reference.

2.7. Observational indicators

The relationship between *SPP1* expression and clinical-pathological characteristics was analyzed, including age, gender, smoking history, tumor size, Child-Pugh grading ^[6], lymph node metastasis, BCLC staging, and cirrhosis presence.

2.8. Follow-up

Patients were followed up through telephone or outpatient visits. The follow-up period began after surgical treatment and lasted 60 months. Factors influencing patient survival were analyzed.

2.9. Statistical analysis

SPSS 24.0 software was used for data analysis. Metric data were expressed as mean \pm standard deviation (SD) and analyzed using *t*-tests. Count data were expressed as [*n* (%)] and analyzed using χ^2 tests. Logistic regression

models identified risk factors influencing survival, while Kaplan-Meier survival curves assessed the relationship between *SPP1* expression and prognosis. Statistical significance was defined as $P < 0.05$.

3. Results

3.1. Expression of *SPP1* mRNA in HCC and normal tissues

The results demonstrated that the expression level of *SPP1* mRNA was significantly increased in HCC tissues compared to normal tissues ($P < 0.05$), as illustrated in **Figure 1**.

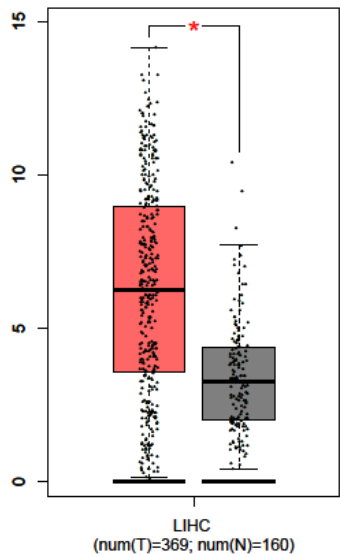


Figure 1. *SPP1* expression level significantly increased in HCC tissue ($P < 0.05$)

3.2. Relationship between *SPP1* expression levels and survival prognosis in HCC patients

Kaplan-Meier curve analysis revealed that the OS of HCC patients with low *SPP1* expression was significantly higher than that of patients with high *SPP1* expression ($P < 0.005$, **Figure 2A**). Univariate Cox regression analysis demonstrated that the *SPP1* expression level (OS:HR = 1.127, 95% CI: 1.072–1.184, $P < 0.005$) was an independent risk factor for poor prognosis in HCC patients, as shown in **Figure 2B**.

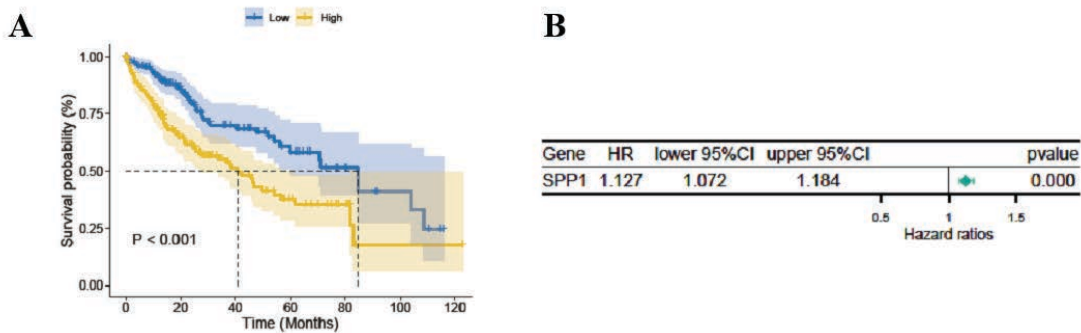


Figure 2. Relationship between *SPP1* expression level and survival prognosis of HCC patients. **(A)** Kaplan-Meier analysis of *SPP1* survival curve. **(B)** Univariate Cox regression analysis of the relationship between *SPP1* expression level and prognosis in HCC patients.

3.3. Differentially expressed genes and functional enrichment analysis

A total of 455 differentially expressed genes (DEGs) were identified between the high and low *SPP1* expression groups, including 380 upregulated and 75 downregulated genes (**Figure 3A**). GO enrichment analysis indicated that these DEGs were enriched in biological processes (BP) such as hormone metabolism, cellular components (CC) including extracellular matrix containing collagen, and molecular functions (MF) such as receptor-ligand activity (**Figures 3B–3D**). KEGG pathway analysis demonstrated significant enrichment in pathways related to neuroactive ligand-receptor interactions, bile secretion, and retinol metabolism (**Figure 3E**).

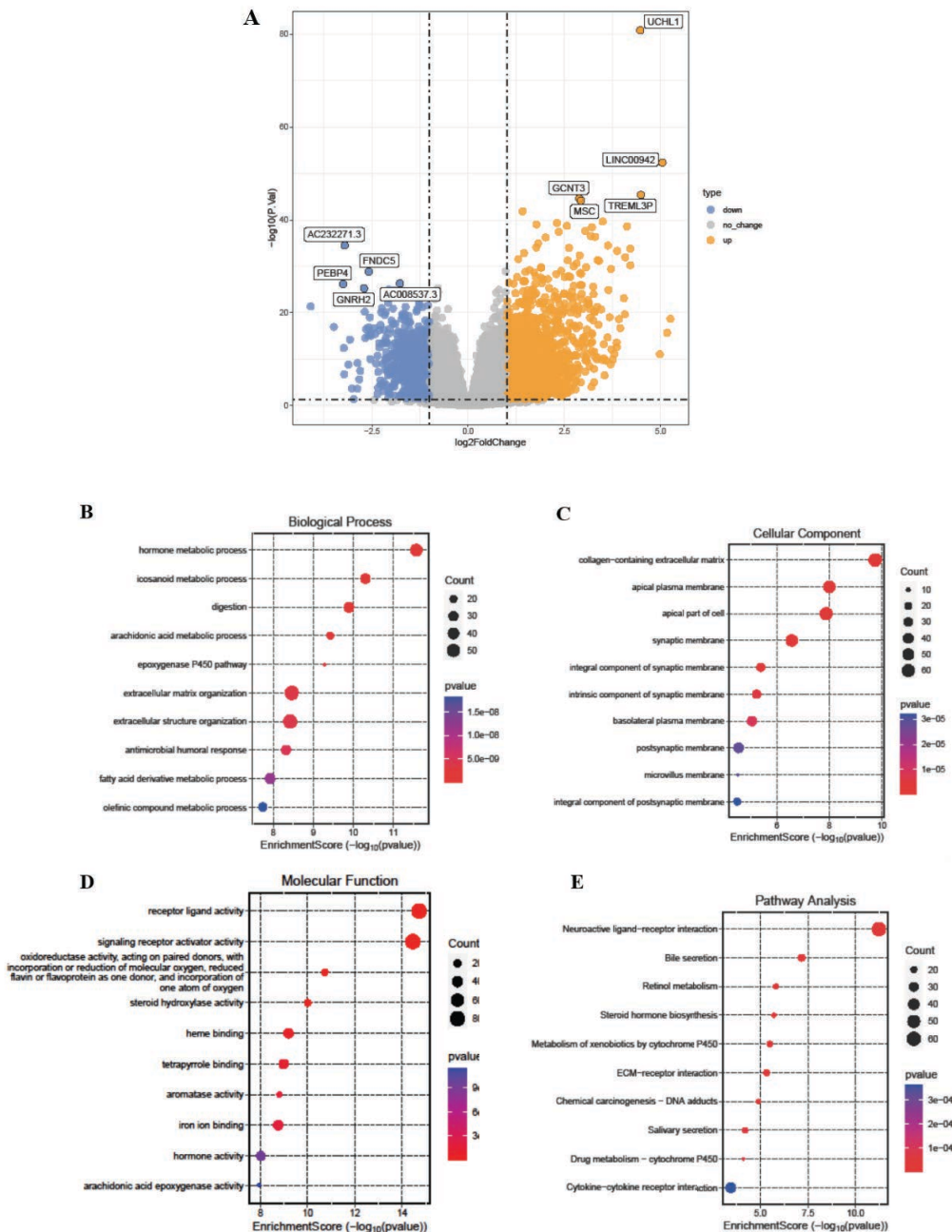


Figure 3. Functional enrichment analysis of *SPP1*-related DEGs in HCC based on the GO and KEGG methods. **(A)** Differential gene expression. **(B–D)** GO enrichment analysis. **(E)** KEGG pathway enrichment analysis.

3.4. Comparison of SPP1 mRNA expression between patients with liver cancer and the control group

The expression level of SPP1 mRNA in peripheral blood mononuclear cells of patients with liver cancer was significantly higher than that of the healthy control group ($P < 0.05$), as presented in **Table 1**.

Table 1. Comparison of SPP1 mRNA expression between liver cancer patients and the healthy control group

Group	<i>n</i>	SPP1 mRNA
Liver cancer group	115	5.15 ± 1.23
Healthy control group	115	1.38 ± 0.20
<i>t</i>		32.443
<i>P</i>		< 0.001

3.5. Correlation between SPP1 expression and clinicopathological characteristics

Patients in the high-expression group of *SPP1* demonstrated statistically significant differences in tumor size, Child-Pugh grading, lymph node metastasis, and BCLC staging ($P < 0.05$). No statistically significant differences were observed for age, gender, smoking history, or cirrhosis ($P > 0.05$), as shown in **Table 2**.

Table 2. Relationship between SPP1 expression and clinicopathological characteristics of advanced HCC patients.

Indicator	<i>n</i>	SPP1		χ^2	<i>P</i>
		Low expression group (<i>n</i> = 26)	High expression group (<i>n</i> = 89)		
Age (years)				1.663	0.197
< 55	67	18 (69.23)	49 (55.06)		
≥ 55	48	8 (30.77)	40 (44.94)		
Gender				0.087	0.768
Female	56	12 (46.15)	44 (49.44)		
Male	59	14 (53.85)	45 (50.56)		
Smoking history				1.311	0.252
Yes	55	15 (57.69)	40 (44.94)		
No	60	11 (42.31)	49 (55.06)		
Tumor size (cm)				11.440	0.001
≤ 5	39	16 (61.54)	23 (25.84)		
> 5	76	10 (38.46)	66 (74.14)		
Child-Pugh Classification				7.443	0.006
A	71	22 (84.62)	49 (55.06)		
B+C	44	4 (15.38)	40 (44.94)		
Lymphatic metastasis				5.151	0.023
Yes	44	5 (19.23)	39 (43.82)		
No	71	21 (80.77)	50 (56.18)		

Table 2 (Continued)

Indicator	<i>n</i>	SPP1		χ^2	<i>P</i>
		Low expression group (<i>n</i> = 26)	High expression group (<i>n</i> = 89)		
BCLC Staging				6.169	0.013
Stage B	55	18 (69.23)	37 (41.57)		
Stage C	60	8 (30.77)	52 (58.43)		
Liver cirrhosis				0.530	0.467
Yes	46	12 (46.15)	34 (38.20)		
No	49	14 (53.85)	55 (61.80)		

3.6. Univariate analysis of survival in patients with advanced liver cancer

Univariate analysis revealed statistically significant differences ($P < 0.05$) between the survival and death groups in terms of tumor size, Child-Pugh grading, lymph node metastasis, BCLC staging, and *SPP1* expression, as detailed in **Table 3**.

Table 3. Univariate analysis of survival in patients with advanced liver cancer

Indicator	<i>n</i>	Survival group (<i>n</i> = 20)	Death group (<i>n</i> = 95)	<i>t</i>	<i>P</i>
Age (years)				0.452	0.501
< 55	67	13 (65.00)	54 (56.84)		
≥ 55	48	7 (35.00)	41 (43.16)		
Gender				0.017	0.898
Female	56	10 (50.00)	46 (48.42)		
Male	59	10 (50.00)	49 (51.58)		
Smoking history				0.594	0.441
Yes	55	8 (40.00)	47 (49.47)		
No	60	12 (60.00)	48 (50.53)		
Tumor size (cm)				7.351	0.007
≤ 5	39	12 (40.00)	27 (28.42)		
> 5	76	8 (60.00)	68 (71.58)		
Child-Pugh Classification				5.546	0.019
A	71	17 (85.00)	54 (56.84)		
B+C	44	3 (15.00)	41 (43.16)		
Lymphatic metastasis				8.186	0.004
Yes	44	2 (10.00)	42 (44.21)		
No	71	18 (90.00)	53 (55.79)		
BCLC staging				4.771	0.029
Stage B	55	14 (70.00)	41 (43.16)		
Stage C	60	6 (30.00)	54 (56.84)		

Table 3 (Continued)

Indicator	<i>n</i>	Survival group (<i>n</i> = 20)	Death group (<i>n</i> = 95)	<i>t</i>	<i>P</i>
Liver cirrhosis				1.009	0.315
Yes	46	6 (30.00)	40 (42.11)		
No	69	14 (70.00)	55 (57.89)		
SPP1				19.345	< 0.001
Low expression	26	12 (60.00)	14 (14.74)		
High expression	89	8 (40.00)	81 (85.26)		

3.7. Multivariate analysis of survival in patients with advanced liver cancer

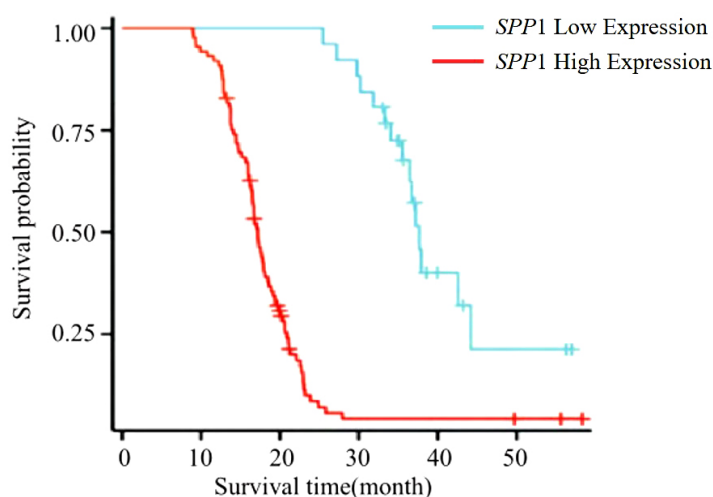
Logistic regression analysis identified tumor size, Child-Pugh grading, lymph node metastasis, BCLC staging, and high *SPP1* expression as independent risk factors affecting survival ($P < 0.05$), as summarized in **Table 4**.

Table 4. Multivariate analysis of survival in patients with advanced liver cancer

Indicator	<i>B</i>	<i>SE</i>	Wald	<i>P</i>	OR (95% CI)
Tumor size (cm)	1.213	0.415	6.605	0.023	3.751 (1.375–10.215)
Child-Pugh Classification	2.112	0.649	11.107	0.004	8.189 (2.267–18.233)
Lymphatic metastasis	1.112	0.469	4.718	0.012	2.771 (1.115–7.027)
BCLC Staging	0.998	0.511	3.781	0.026	2.752 (1.995–7.382)
<i>SPP1</i> high expression	1.326	0.570	7.852	0.033	5.412 (1.236–10.749)

3.8. SPP1 expression and survival prognosis

Follow-up was conducted over a 60-month period for the 115 patients included in the study, resulting in a survival rate of 17.39% (20/115). Kaplan-Meier survival curve analysis revealed that the median survival time for the low *SPP1* expression group was 40 months, significantly longer than the 18 months observed for the high-expression group ($P < 0.05$), as shown in **Figure 4**.

**Figure 4.** Kaplan-Meier analysis of the relationship between *SPP1* expression levels and survival prognosis

4. Discussion

Liver cancer ranks as the sixth most commonly diagnosed cancer and the fourth leading cause of cancer-related deaths globally. According to relevant statistics ^[7], the incidence rate of liver cancer is highest in East Asia, accounting for 35.5% of the global cases. The pathogenesis of liver cancer is complex and multifactorial. Chronic hepatitis B virus, hepatitis C virus, aflatoxin-contaminated food, excessive alcohol consumption, smoking, and type 2 diabetes are significant risk factors associated with liver cancer development ^[8]. Modern medical research has demonstrated that the liver possesses a low level of pain sensation, and even when liver disease occurs, the body often fails to detect it through pain feedback mechanisms ^[9]. As a result, the clinical manifestations of liver disease are relatively subtle. Consequently, many patients with liver cancer are diagnosed only in the advanced stages, leading to a poor prognosis. Therefore, early identification of diagnostic and prognostic markers for liver cancer is essential for improving diagnostic accuracy, enhancing treatment efficacy, improving patient outcomes, and reducing mortality rates.

SPP1, a crucial extracellular matrix component, is secreted by various cell types, including tumor cells, immune cells, fibroblasts, osteoclasts, smooth muscle cells, lymphocytes, and epithelial cells ^[10]. Studies have revealed that the upregulation of *SPP1* in tumor tissues and plasma correlates with poor prognosis in patients with various cancers ^[11]. The findings of this study indicated that the expression level of *SPP1* is significantly elevated in advanced liver cancer tissues. Furthermore, *SPP1* expression is closely associated with tumor size, Child-Pugh grading, lymph node metastasis, BCLC staging, and patient survival prognosis. Analyzing the expression level of *SPP1* may, therefore, hold significant value in evaluating disease progression and predicting patient survival outcomes.

Additionally, the study identified tumor size, Child-Pugh grading, lymph node metastasis, BCLC staging, and high *SPP1* expression as independent risk factors affecting survival in patients with advanced liver cancer. Advanced liver cancer often entails large tumor size or metastasis, which increases treatment complexity and mortality risk. Specifically, larger liver tumors exhibit higher growth rates, greater invasiveness, and stronger metastatic potential. These larger tumors are more prone to invading adjacent blood vessels and tissues, leading to complications such as liver dysfunction, portal hypertension, and ascites, ultimately increasing the risk of mortality ^[12]. The Child-Pugh scoring system remains a critical tool for evaluating liver function. Higher Child-Pugh grades indicate progressively severe liver dysfunction and diminishing therapeutic effectiveness ^[13]. Furthermore, lymphangiogenesis and lymph node metastasis serve as crucial prognostic indicators for malignant hepatobiliary tumors and are closely linked to poorer outcomes. The liver produces approximately 25% to 50% of the body's lymphatic fluid and contains an extensive lymphatic network. The lymphatic system plays an integral role in immune and inflammatory responses ^[14].

Luan *et al.* ^[15] reported a negative correlation between *SPP1* expression and overall survival in patients with lung adenocarcinoma, noting its association with clinical stage, lymph node metastasis, and survival status. Their findings suggest that *SPP1* could serve as a valuable molecular marker for the diagnosis, treatment, and prognosis evaluation of lung adenocarcinoma. Similarly, the Kaplan-Meier survival curve analysis in this study demonstrated that patients with low *SPP1* expression exhibited longer survival periods. This finding underscores the significant correlation between elevated blood *SPP1* expression and poorer prognosis in patients with advanced liver cancer following hepatic artery interventional chemotherapy embolization. Thus, *SPP1* may be a valuable biomarker for predicting prognosis.

This study, however, has certain limitations. The research duration was relatively short, and the sample size

was comparatively small. Additionally, the mechanism through which *SPP1* influences survival prognosis in patients with liver cancer remains unclear. Future research should focus on elucidating the underlying mechanisms and exploring the development of *SPP1*-targeted therapies for liver cancer treatment.

5. Conclusion

SPP1 is significantly upregulated in advanced liver cancer tissues and holds potential value in predicting the survival outcomes of patients with advanced liver cancer undergoing hepatic artery chemoembolization treatment. *SPP1* is anticipated to serve as a potential prognostic indicator for evaluating the outcomes of interventional treatments. Furthermore, it can be utilized in conjunction with clinical indicators, including tumor size, Child-Pugh grading, lymph node metastasis, and BCLC staging, to predict or assess the postoperative survival of patients with liver cancer.

Funding

- (1) Medical Research Project of Xi'an Science and Technology Bureau "Molecular Mechanism of miR-1305 Competitive Endogenous circRNA in the Development of Liver Cancer" (Project No. 22YXYJ0134)
- (2) General Project of Key Research and Development Program of Shaanxi Provincial Department of Science and Technology "Mechanism Study on the Inhibition of Liver Cancer Invasion and Metastasis by Downregulating METTL3 and Reducing the m6A Modification Level of MMP3 with Honokiol" (Project No. 2023-YBSF-631)

Disclosure statement

The authors declare no conflict of interest.

References

- [1] Huang G, Li Z, Ding X, 2022, The Transcription Factor AP-2 α Regulates the Expression of SOX9 Gene. Chinese Journal of Laser Biology, 31(6): 512–517.
- [2] Pu G, Xu Y, Gong R, et al., 2022, The Diagnostic Value of AFP Combined with ALT and T-Bil Detection in Hepatocellular Carcinoma. Western Medical Journal, 34(2): 304–308 + 312.
- [3] Han X, 2022, The Impact of CRISPR/Cas9 Mediated SPP1 Gene Knockout on the Biological Functions of Prostate Cancer Cells, dissertation, Zhengzhou University.
- [4] Kim TH, Kim H, Joo I, et al., 2020, Combined Hepatocellular-Cholangiocarcinoma: Changes in the 2019 World Health Organization Histological Classification System and Potential Impact on Imaging-Based Diagnosis. Korean J Radiol, 21(10): 1115–1125. <https://doi.org/10.3348/kjr.2020.0091>
- [5] Chen YG, Yang CW, Chung CH, et al., 2022, The Association Between Metabolic Risk Factors, Nonalcoholic Fatty Liver Disease, and the Incidence of Liver Cancer: A Nationwide Population-Based Cohort Study. Hepatol Int, 16(4): 807–816. <https://doi.org/10.1007/s12072-021-10281-9>. Erratum in Hepatol Int, 16(2): 488. <https://doi.org/10.1007/s12072-022-10308-9>
- [6] Thüring J, Rippel O, Haarbuerger C, et al., 2020, Multiphase CT-based Prediction of Child-Pugh Classification: A Machine Learning Approach. Eur Radiol Exp, 4(1): 20. <https://doi.org/10.1186/s41747-020-00148-3>

- [7] Bray F, Ferlay J, Soerjomataram I, et al., 2018, Global Cancer Statistics 2018: GLOBOCAN Estimates of Incidence and Mortality Worldwide for 36 Cancers in 185 Countries. *CA Cancer J Clin*, 68(6): 394–424. <https://doi.org/10.3322/caac.21492>. Erratum in *CA Cancer J Clin*, 70(4): 313. <https://doi.org/10.3322/caac.21609>
- [8] Liu C, Yu J, Wu P, 2022, Research Progress on the Treatment of Advanced Primary Liver Cancer. *Shandong Medical Journal*, 62(28): 91–95.
- [9] Anwanwan D, Singh SK, Singh S, et al., 2020, Challenges in Liver Cancer and Possible Treatment Approaches. *Biochim Biophys Acta Rev Cancer*, 1873(1): 188314. <https://doi.org/10.1016/j.bbcan.2019.188314>
- [10] Liu M, Liu L, 2021, Analysis of the Expression and Clinical Significance of Type 10 Collagen Alpha 1 Chain and Secreted Phosphoprotein 1 in Lung Adenocarcinoma Based on Multiple Datasets. *Cancer Progression*, 19(24): 2540–2543 + 2577.
- [11] Zhang D, Xu J, 2021, Differential Expression and Mechanism of SPP1 in Non-Small Cell Lung Cancer. *Journal of Clinical Pulmonary Medicine*, 26(11): 1724–1729.
- [12] Yan B, Bai DS, Qian JJ, et al., 2020, Differences in Tumour Characteristics of Hepatocellular Carcinoma between Patients With and Without Cirrhosis: A Population-based Study. *J Cancer*, 11(19): 5812–5821. <https://doi.org/10.7150/jca.46927>
- [13] Guo D, Liu B, Liu B, 2021, Value Analysis of Gadolinium Diamine Enhanced MRI and CT in the Diagnosis of Child Pugh A Hepatocellular Carcinoma with Liver Function. *Liver*, 26(11): 1264–1267.
- [14] Kong J, Li H, Zeng X, et al., 2022, Clinical and Pathological Characteristics and Prognostic Analysis of Regional Lymph Node Metastasis in Primary Liver Cancer. *Chinese Journal of Cancer Prevention and Treatment*, 29(4): 290–295 + 301.
- [15] Luan Y, Liang C, Han Q, et al., 2022, The Expression of SPP1 Gene in Lung Adenocarcinoma and Its Correlation with Prognosis. *Journal of Clinical Pulmonary Medicine*, 27(6): 884–891.

Publisher's note

Bio-Byword Scientific Publishing remains neutral with regard to jurisdictional claims in published maps and institutional affiliations.

Clinical Efficacy and Safety Analysis of Toripalimab Combined with GC Chemotherapy for Advanced Urothelial Carcinoma

Song Xue¹, Dongli Ruan^{2*}

¹Xi'an People's Hospital (Xi'an Fourth Hospital), Xi'an 710000, Shaanxi Province, China

²Shaanxi Provincial People's Hospital, Xi'an 710000, Shaanxi Province, China

*Corresponding author: Dongli Ruan, 745501416@qq.com

Copyright: © 2025 Author(s). This is an open-access article distributed under the terms of the Creative Commons Attribution License (CC BY 4.0), permitting distribution and reproduction in any medium, provided the original work is cited.

Abstract: *Objective:* To analyze the clinical efficacy and safety of toripalimab combined with the GC chemotherapy regimen in the treatment of advanced urothelial carcinoma. *Methods:* A retrospective study was conducted on 102 patients with advanced urothelial carcinoma treated at our hospital between March 2021 and August 2024. Based on treatment regimens, patients were divided into a chemotherapy group ($n = 52$) and a combination group ($n = 50$). The chemotherapy group received the GC chemotherapy regimen, while the combination group received GC chemotherapy combined with toripalimab. Both groups underwent 4–6 cycles of treatment based on patient tolerance. Clinical efficacy, immune-related factor levels, survival outcomes, and safety were observed and compared. *Results:* The disease control rate (DCR) and overall response rate (ORR) in the combination group were slightly higher than those in the chemotherapy group, but the differences were not statistically significant ($P > 0.05$). After treatment, levels of IFN- γ and IL-2 increased significantly, while VEGF levels decreased significantly in both groups ($P < 0.05$), with superior outcomes observed in the combination group ($P < 0.05$). Follow-up analysis showed progression-free survival (PFS) and median overall survival (OS) in the chemotherapy group were 5.19 and 10.15 months, respectively, compared to 8.24 and 18.23 months in the combination group, with statistically significant differences ($P < 0.05$). During treatment, the incidence of adverse reactions such as rash, immune-related pneumonia, and immune-related diarrhea was higher in the combination group than in the chemotherapy group ($P < 0.05$). However, the incidence of gastrointestinal reactions, fever, and leukopenia did not differ significantly between the two groups ($P > 0.05$). *Conclusion:* The use of toripalimab combined with the GC chemotherapy regimen for advanced urothelial carcinoma can effectively improve clinical outcomes and extend patient survival, with good overall safety. However, attention should be given to preventing adverse reactions such as rash and pneumonia during treatment.

Keywords: Urothelial carcinoma; Toripalimab; Chemotherapy; Survival; Efficacy; Safety

Online publication: February 13, 2025

1. Introduction

Urothelial carcinoma (UC) arises from the epithelial tissues of the renal calyces, renal pelvis, bladder, and ureters, and is one of the most common tumors, accounting for 5–10% of urinary tract malignancies. It is associated with poor prognosis and high recurrence and metastasis rates ^[1]. UC often presents without obvious early clinical symptoms, and most patients are diagnosed at an advanced stage, missing the optimal treatment window. For patients with advanced UC who cannot undergo surgical resection, systemic chemotherapy remains the primary treatment approach.

Clinical studies have shown that the gemcitabine-cisplatin (GC) chemotherapy regimen improves patient prognosis with a relatively low incidence of adverse reactions ^[2]. However, long-term survival outcomes following this regimen remain suboptimal, necessitating the exploration of more effective therapeutic strategies.

In recent years, immunotherapy has emerged as one of the most successful approaches for UC treatment and is now the standard of care for both in situ urothelial carcinoma and superficial bladder tumors ^[3]. This study retrospectively analyzed the clinical data of UC patients to evaluate the clinical efficacy and safety of immunotherapy combined with the GC chemotherapy regimen in treating advanced UC.

2. Materials and methods

2.1. General information

A retrospective study was conducted on 102 patients with advanced urothelial carcinoma treated at our hospital from March 2021 to August 2024. Based on treatment regimens, patients were divided into a chemotherapy group ($n = 52$) and a combination group ($n = 50$). In the chemotherapy group, there were 29 males and 23 females, aged 50–80 years, with an average age of (64.32 ± 6.22) years. Cancer types included ureteral cancer (6 cases), renal pelvic cancer (4 cases), bladder cancer (40 cases), and others (2 cases). The Karnofsky Performance Status (KPS) scores ranged from 65 to 90 points [4], with an average score of (74.91 ± 4.57) points. In the combination group, there were 30 males and 20 females, aged 52–80 years, with an average age of (65.01 ± 5.96) years. Cancer types included ureteral cancer (5 cases), renal pelvic cancer (5 cases), bladder cancer (39 cases), and others (1 case). KPS scores ranged from 63 to 90 points, with an average score of (76.14 ± 6.03) points. The baseline data of the two groups were comparable ($P > 0.05$). This study was approved by the hospital ethics committee.

2.2. Inclusion and exclusion criteria

Inclusion criteria:

- (1) Pathologically confirmed urothelial carcinoma ^[5].
- (2) Clinical stage III B to IV.
- (3) Ineligible for surgery or showing recurrence/metastasis after surgery.
- (4) Eastern Cooperative Oncology Group (ECOG) performance score of 0–2.
- (5) KPS score ≥ 60 points.
- (6) Estimated survival time ≥ 3 months.

Exclusion criteria:

- (1) Severe damage to other vital organs.
- (2) Autoimmune or hematological diseases.
- (3) Brain metastasis.

- (4) History of immunotherapy.
- (5) Poor compliance or cooperation during treatment and follow-up.

Elimination criteria:

- (1) Patients with an estimated survival quality of < 3 months.

2.3. Methods

The chemotherapy group received the GC chemotherapy regimen: gemcitabine (2,500 mg/m²) on days 1 and 8, and cisplatin (70 mg/m²) on day 2. Each chemotherapy cycle was 21 days.

The combination group received GC chemotherapy as described above, combined with immunotherapy using toripalimab (240 mg) every 2 weeks via intravenous infusion.

Both groups underwent 4–6 cycles of treatment based on patient tolerance. During cisplatin administration, adequate hydration was ensured to maintain urine output $\geq 2,000$ mL/day. Blood counts and liver and kidney function were monitored regularly during chemotherapy. In cases of thrombocytopenia or leukopenia, treatment with hematopoietic growth factors was initiated. Symptomatic treatments, including fluid replacement and antiemetics, were provided for adverse reactions.

2.4. Observational indicators and evaluation criteria

The study assessed clinical efficacy, immune-related factor levels, survival outcomes, and safety in both groups:

- (1) Clinical efficacy: Assessed according to the WHO criteria for solid tumors, including progressive disease (PD), stable disease (SD), partial response (PR), and complete response (CR). Disease control rate (DCR) = (SD + PR + CR cases) / total cases $\times 100\%$. Objective response rate (ORR) = (PR + CR cases) / total cases $\times 100\%$ [6].
- (2) Immune-related factor levels: Peripheral blood samples were collected before treatment and after 4 treatment cycles. Serum levels of interferon-gamma (IFN- γ), interleukin-2 (IL-2), and vascular endothelial growth factor (VEGF) were measured using enzyme-linked immunosorbent assay (ELISA) kits.
- (3) Survival outcomes: Patients were followed monthly after treatment to assess survival. Progression-free survival (PFS) was defined as the time from treatment initiation to disease progression. Overall survival (OS) was defined as the time from treatment initiation to death due to cancer. The follow-up lasted for 1 year.
- (4) Safety: Adverse events during treatment were analyzed, including gastrointestinal reactions, fever, leukopenia, and immune-related adverse events (e.g., rash, immune-related pneumonia, immune-related diarrhea).

2.5. Statistical analysis

SPSS 26.0 was used for statistical analysis. Measurement data (mean \pm standard deviation) were analyzed using *t*-tests, while categorical data [*n* (%)] were analyzed using χ^2 tests. A *P*-value < 0.05 was considered statistically significant.

3. Results

3.1. Comparison of clinical efficacy between the two groups

The DCR and ORR in the combination group were slightly higher than those in the chemotherapy group, but the differences were not statistically significant (*P* > 0.05). See **Table 1**.

Table 1. Comparison of clinical efficacy between the two groups [*n* (%)]

Group	PD	SD	PR	CR	DCR	ORR
Chemotherapy (<i>n</i> = 52)	18 (34.62)	10 (19.23)	22 (42.31)	2 (3.85)	34 (65.38)	17 (32.69)
Combination (<i>n</i> = 50)	17 (34.00)	14 (28.00)	19 (38.00)	0 (0.00)	36 (72.00)	19 (38.00)
χ^2					0.518	0.314
<i>P</i>					0.472	0.575

3.2. Comparison of immune-related factor levels between the two groups

Before treatment, there were no significant differences in IFN- γ , IL-2, and VEGF levels between the two groups ($P > 0.05$). After treatment, both groups showed significant increases in IFN- γ and IL-2 levels and significant decreases in VEGF levels ($P < 0.05$). The combination group exhibited superior changes compared to the chemotherapy group ($P < 0.05$). See **Table 2**.

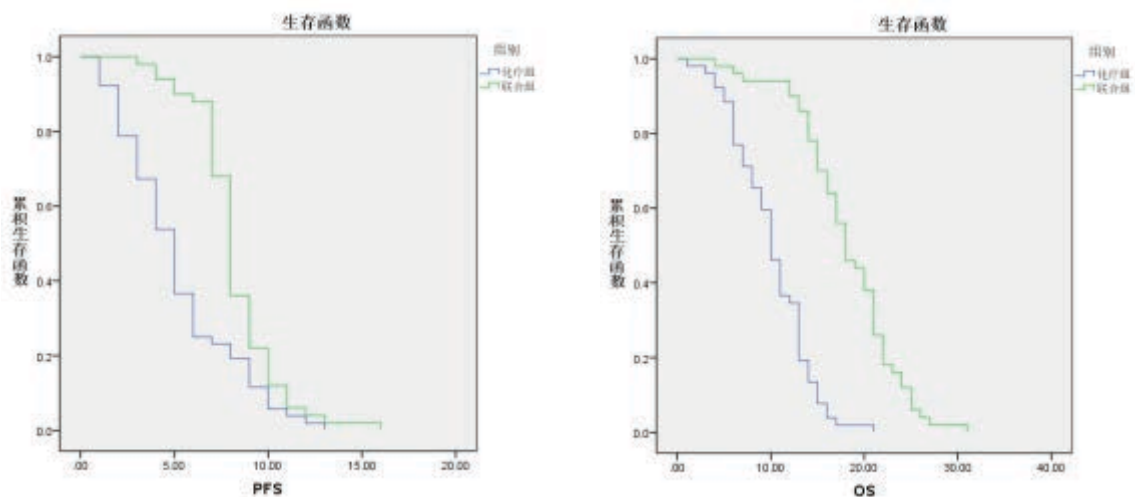
Table 2. Comparison of immune-related factor levels between the two groups (mean \pm SD)

Group	IFN- γ ($\mu\text{g/L}$)		IL-2 (ng/mL)		VEGF (ng/L)	
	Before treatment	After treatment	Before treatment	After treatment	Before treatment	After treatment
Chemotherapy (<i>n</i> = 52)	1.17 \pm 0.19	3.51 \pm 0.77*	1.98 \pm 0.52	12.33 \pm 2.01*	34.97 \pm 4.46	18.32 \pm 1.89*
Combination (<i>n</i> = 50)	1.14 \pm 0.33	34.82 \pm 4.47*	2.04 \pm 0.47	176.44 \pm 19.22*	36.02 \pm 5.01	9.66 \pm 1.71*
<i>t</i>	0.565	49.758	0.611	61.237	1.119	24.236
<i>P</i>	0.573	< 0.001	0.543	< 0.001	0.266	< 0.001

*Note: Comparison within the same group before and after treatment, $P < 0.05$.

3.3. Survival analysis

Follow-up results showed that the PFS and median OS in the chemotherapy group were 5.19 and 10.15 months, respectively, compared to 8.24 and 18.23 months in the combination group. The differences were statistically significant ($P < 0.05$). See **Figure 1**.

**Figure 1.** PFS (left) and OS (right) of patients in the two groups

3.4. Comparison of adverse reaction incidence between the two groups

During treatment, the incidence of rash, immune-related pneumonia, and immune-related diarrhea was higher in the combination group compared to the chemotherapy group ($P < 0.05$). There were no significant differences in the incidence of gastrointestinal reactions, fever, or leukopenia between the two groups ($P > 0.05$). See **Table 3**.

Table 3. Comparison of adverse reaction incidence between the two groups [n (%)]

Group	Gastrointestinal reactions	Fever	Leukopenia	Rash	Immune-related pneumonia	Immune-related diarrhea
Chemotherapy (<i>n</i> = 52)	14 (26.92)	22 (42.31)	7 (13.46)	3 (3.85)	1 (1.92)	4 (7.69)
Combination (<i>n</i> = 50)	13 (26.00)	19 (38.00)	10 (20.00)	11 (22.00)	8 (16.00)	13 (26.00)
χ^2	0.011	0.197	0.785	5.671	6.279	6.151
<i>P</i>	0.916	0.657	0.376	0.017	0.012	0.013

4. Discussion

Patients with advanced urothelial carcinoma often present with clinical symptoms such as weight loss, fatigue, hematuria, and difficulty urinating, which severely impact their safety and quality of daily life ^[7]. Various chemotherapy regimens have demonstrated certain clinical efficacy in treating urothelial carcinoma. Among these, the GC chemotherapy regimen has become the first-line treatment due to its high efficacy and relatively low incidence of adverse reactions ^[8]. Studies using the GC regimen for advanced bladder cancer have shown an objective survival rate of approximately 35% and a median survival time of 14 months ^[9]. However, despite its efficacy, the long-term survival benefits of the GC regimen remain limited, necessitating further improvements in treatment strategies.

In recent years, immunotherapy has garnered attention for its efficacy in cancer treatment. This approach activates antitumor immunity and reduces tumor immune evasion, offering hope for extending patient survival. Toripalimab, a recombinant humanized anti-PD-1 monoclonal antibody injection, binds with high affinity to PD-1 and selectively blocks the interaction between PD-1 and PD-L1, reactivating T cells and enhancing tumor cytotoxicity. It has been successfully applied in cancers such as liver and gastric cancers, with notable therapeutic effects ^[10,11].

In this study, the combination group achieved a DCR of 72.00% and an ORR of 38.00%, higher than the chemotherapy group (65.38% and 32.69%, respectively), though the differences were not statistically significant ($P > 0.05$). Additionally, follow-up results revealed that the PFS and median OS in the combination group were 8.24 and 18.23 months, respectively, significantly longer than those in the chemotherapy group ($P < 0.05$). These findings suggest that GC combined with toripalimab effectively improves ORR and extends survival in patients with advanced urothelial carcinoma.

The study also showed that VEGF levels significantly decreased in both groups after treatment, with a more pronounced reduction in the combination group. VEGF is closely associated with tumor angiogenesis and is significantly related to tumor metastasis and progression. These results indicate that toripalimab combined with GC chemotherapy can inhibit tumor neovascularization. Moreover, levels of IFN- γ and IL-2 increased after treatment. This can be attributed to the GC regimen: gemcitabine enhances cisplatin's chemosensitivity

and promotes immunogenic cell death in tumors. The action of the PD-1 inhibitor enhances the recognition and presentation of tumor antigens by dendritic and macrophage cells, leading to increased levels of IFN- γ and IL-2. These changes recruit and activate large numbers of T cells and cytotoxic cells, improving immune function and thus enhancing treatment efficacy and prolonging survival ^[12].

Regarding safety, patients treated with the combination of toripalimab and chemotherapy experienced higher incidences of rash, immune-related pneumonia, and immune-related diarrhea. However, the incidences of gastrointestinal reactions, fever, and leukopenia were comparable between the two groups. This highlights the need for effective measures to prevent rash, pneumonia, and other adverse events to ensure medication safety during treatment with the combination regimen.

5. Conclusion

In conclusion, the combination of the GC chemotherapy regimen with toripalimab effectively improves clinical outcomes and extends survival in patients with advanced urothelial carcinoma while maintaining acceptable safety. However, attention should be given to preventing adverse reactions such as rash and pneumonia to ensure treatment safety.

Disclosure statement

The authors declare no conflict of interest.

References

- [1] Gandhi J, Chen JF, Al-Ahmadie H, 2022, Urothelial Carcinoma: Divergent Differentiation and Morphologic Subtypes. *Surg Pathol Clin*, 15(4): 641–659. <https://doi.org/10.1016/j.path.2022.07.003>
- [2] Coleman JA, Yip W, Wong NC, et al., 2023, Multicenter Phase II Clinical Trial of Gemcitabine and Cisplatin as Neoadjuvant Chemotherapy for Patients With High-Grade Upper Tract Urothelial Carcinoma. *J Clin Oncol*, 41(8): 1618–1625. <https://doi.org/10.1200/JCO.22.00763>
- [3] Uccello M, Adeleke S, Moschetta M, et al., 2023, Immunotherapy for Advanced Urothelial Carcinoma (UC): Rational and Current Evidence. *Ann Palliat Med*, 12(6): 1345–1354. <https://doi.org/10.21037/apm-22-1350>
- [4] Liu W, Shen H, 2023, Efficacy of PD-1 Monoclonal Antibody Combined with GC Chemotherapy in the Treatment of Advanced Urothelial Carcinoma and Its Impact on Tumor Malignancy. *Chongqing Medicine*, 52(21): 3274–3278 + 3282.
- [5] Xu L, Zhang C, Wang D, et al., 2023, Neoadjuvant Immunotherapy Combined with Chemotherapy Followed by Surgical Treatment of Locally Advanced Upper Urinary Tract Urothelial Carcinoma: A Case Report. *Practical Oncology Journal*, 38(5): 476–480.
- [6] Yang X, Wu Y, 2004, RECIST Criteria for Evaluating the Efficacy of Solid Tumor Treatments. *Evidence-based Medicine*, 4(2): 25–30.
- [7] Xiang Y, 2024, Prognostic Significance of Urea and Immune-Inflammatory Markers in Advanced Urothelial Carcinoma Treated with Immunotherapy, dissertation, Jilin University.
- [8] Li H, Chen H, Wang L, et al., 2024, Nutritional Risk and Influencing Factors During Chemotherapy in Patients with

Urothelial Carcinoma. *Tumor Metabolism and Nutrition Electronic Journal*, 11(1): 60–64.

- [9] Liu T, 2018, The Impact of Kushen Injection Combined with GC Chemotherapy on Chemotherapy Tolerance and Median Survival in Patients with Advanced Bladder Cancer. *Drug Evaluation*, 15(9): 35–38.
- [10] Wu X, Deng J, Luo T, 2024, Efficacy of Toripalimab Combined with Lenvatinib TACE in the Treatment of Advanced Liver Cancer and Its Impact on Tumor Markers for Prognosis. *Hebei Medicine*, 30(10): 1745–1751.
- [11] Li M, Han M, Li Z, 2023, Clinical Observation of Hepatic Arterial Chemoembolization Combined with Toripalimab in the Treatment of Liver Cancer. *Tianjin Pharmacy*, 35(3): 53–56.
- [12] Xie Q, 2024, Efficacy of Different Chemotherapy Regimens in the Treatment of Advanced Urothelial Carcinoma and Their Impact on Immune Function. *Jilin Medical Journal*, 45(2): 276–279.

Publisher's note

Bio-Byword Scientific Publishing remains neutral with regard to jurisdictional claims in published maps and institutional affiliations.

Application of Artificial Neural Networks in Predicting Malignant Lung Nodules on Chest CT Scans

Wenhui Li, Yuping Yang*, Yixian Liang, Pengliang Xu, Qiuqiang Chen

Department of Thoracic Surgery, Huzhou First People's Hospital, Huzhou 313000, Zhejiang Province, China

*Corresponding author: Yuping Yang, 13819281694@163.com

Copyright: © 2025 Author(s). This is an open-access article distributed under the terms of the Creative Commons Attribution License (CC BY 4.0), permitting distribution and reproduction in any medium, provided the original work is cited.

Abstract: *Objective:* To explore a simple method for improving the diagnostic accuracy of malignant lung nodules based on imaging features of lung nodules. *Methods:* A retrospective analysis was conducted on the imaging data of 114 patients who underwent lung nodule surgery in the Thoracic Surgery Department of the First People's Hospital of Huzhou from June to September 2024. Imaging features of lung nodules were summarized and trained using a BP neural network. *Results:* Training with the BP neural network increased the diagnostic accuracy for distinguishing between benign and malignant lung nodules based on imaging features from 84.2% (manual assessment) to 94.1%. *Conclusion:* Training with the BP neural network significantly improves the diagnostic accuracy of lung nodule malignancy based solely on imaging features.

Keywords: Lung nodule; Malignant lung tumor; Neural network; Chest CT

Online publication: February 13, 2025

1. Introduction

Lung cancer, as a cancer type with an increasing incidence rate ^[1], poses severe consequences and high mortality if not treated promptly ^[2]. Early screening and treatment are therefore of great significance ^[3]. Chest CT, as the most important examination for detecting lung nodules ^[4], has been widely implemented as part of routine physical check-ups in recent years. However, lung nodules identified on chest CT can be either benign or malignant. Benign solitary lung nodules are often granulomatous lesions or hamartomas. Unless the nodules are large and cause compression symptoms, surgical treatment of such benign nodules does not benefit patients. Therefore, in addition to detecting lung nodules, distinguishing between benign and malignant nodules is a critical aspect of chest CT interpretation ^[5].

This study aims to assess the lung cancer positivity rate among surgical lung nodule cases handled in our department and to summarize a straightforward machine-learning-assisted diagnostic method suitable for clinical application.

2. Materials and methods

This study was approved by the Ethics Committee of the First People's Hospital of Huzhou. It included 114 patients who underwent lung nodule surgery at the hospital from June to September 2024.

Inclusion criteria: (1) Completion of preoperative chest CT examination at this hospital; (2) Clear pathological diagnosis after surgery.

Exclusion criteria: (1) Resection of small, non-primary lesions; (2) Unclear pathological diagnosis after surgery.

Chest CT interpretation and data collection were independently completed by three thoracic surgeons from the research team. The final data was confirmed after verifying the consistency of the results. The imaging features of lung nodules, including lobulation, spiculation, burr sign, pleural indentation, vacuole sign, and ground-glass opacity (**Figure 1**), were recorded. Positive features were recorded as 1, and negative features as 0. Pathological results were recorded as 1 for malignant and 0 for benign.

General information such as the gender and age of the surgical patients was compiled, and the proportion of malignant nodules among the surgical cases was recorded. The proportions of ground-glass opacity, burr sign, spiculation, vacuole sign, lobulation, and pleural indentation were calculated and compared between benign and malignant groups.

Statistical methods: χ^2 tests were used for statistical analysis, performed using SPSS 21.0 software.

Neural network algorithm: A Back Propagation (BP) neural network was selected for analysis. Its architecture includes an input layer, a hidden layer, and an output layer.

- (1) The input layer consisted of six neurons, corresponding to six imaging features of lung nodules from chest CT scans.
- (2) The hidden layer contained seven neurons, chosen based on MATLAB's official recommendations.
- (3) The output layer consisted of two neurons, corresponding to benign or malignant nodules (**Figure 2**).

The dataset was divided into training, validation, and testing sets, with proportions of 70%, 15%, and 15%, respectively. The training was performed using the conjugate gradient algorithm. The entire training process was conducted using MATLAB 2022b software.

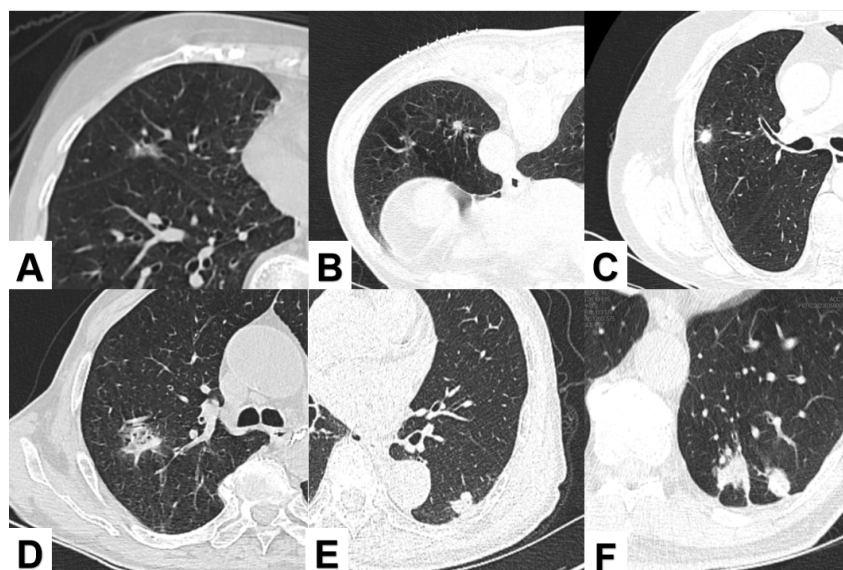


Figure 1. (A) Ground-glass opacity; (B) Burr sign; (C) Spiculation; (D) Vacuole sign; (E) Lobulation; (F) Pleural indentation

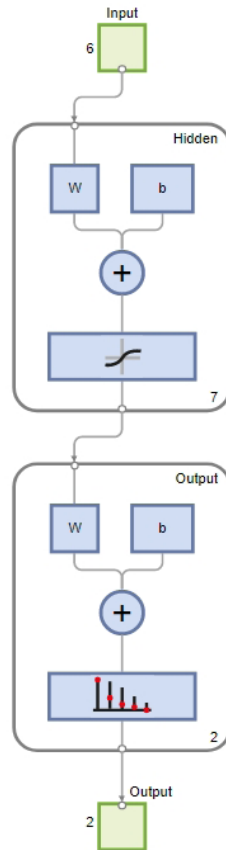


Figure 2. The BP neural network consists of three layers: input, hidden, and output. The data flows from the input layer to the hidden layer, where it is multiplied by weights (w) and added to biases (b), then passed through a sigmoid function to the output layer. Similarly, in the output layer, the data undergoes multiplication by weights and the addition of biases before being passed through a sigmoid function. The squared error between the output value and the expected value is back-propagated to calculate the partial derivatives of weights for each neuron, which are adjusted accordingly. The network learning ends when the error reaches the expected value.

3. Results

3.1. Basic information

Among the 114 patients included, 47 were male (42.23%), and 67 were female (57.77%), with an average age of 64.25 ± 12.21 years. Postoperative pathological results showed 96 cases of malignancy (84.21% of the total) and 18 cases of benign lesions (**Table 1**).

Among the cases, ground-glass opacity, burr sign, spiculation, vacuole sign, lobulation, and pleural indentation were observed in 79.17%, 62.50%, 70.83%, 28.13%, 65.63%, and 28.13% of patients, respectively. For patients with benign nodules, these features appeared at rates of 16.67%, 33.33%, 55.56%, 55.56%, 27.78%, and 22.22%, respectively. A comparison between the two groups showed that ground-glass opacity, burr sign, spiculation, vacuole sign, and lobulation were more frequently observed in patients with lung cancer, with statistical significance ($P < 0.05$). Although pleural indentation was more common in malignant cases, the difference was not statistically significant ($P = 0.609$, **Table 2**). This may be because many lung nodules, whether malignant or benign, were not located near the pleural surface, which limited the manifestation of pleural

indentation. Subgroup analysis focusing on nodules on the pleural surface revealed that malignant nodules were significantly more likely to exhibit pleural indentation than benign ones ($P < 0.05$, **Table 3**).

Table 1. Gender, age, and proportion of malignant nodules in 114 patients

Gender		Age (years)	Postoperative pathology	
Male	Female		Malignant	Benign
47 (42.23%)	67 (57.77%)	64.25 ± 12.21	96 (84.21%)	18 (15.79%)

Table 2. Proportions of imaging features in 114 patients and comparison between malignant and benign groups

Feature	Malignant		Benign		P value
	n	%	n	%	
Ground-glass	76	79.17%	3	16.67%	2.32E-08
Burr sign	60	62.50%	6	33.33%	0.021
Spiculation	68	70.83%	1	55.56%	3.93E-08
Vacuole	27	28.13%	1	55.56%	0.0416
Lobulation	63	65.63%	5	27.78%	0.002
Pleural indentation	27	28.13%	4	22.22%	0.609

Table 3. Comparison of pleural surface nodules with pleural indentation in malignant and benign groups

Item	Malignant		Benign		P value
	n	%	n	%	
Pleural indentation	27/35	87.10%	4/9	44.44%	0.038

3.2. Neural network training results

Cross-entropy, a measure of the difference between two probability distributions, was used to evaluate the predictive model's deviation from actual results. In the training, validation, and testing sets, the cross-entropy values were 0.0375, 0.0588, and 0.0375, respectively, indicating high agreement between the predictive model and actual data (**Table 4**).

The BP neural network achieved a diagnostic accuracy of 96.2% for malignant lung nodules in the training set, 100% in the validation set, and 94.1% in the testing set (**Table 5**).

Table 4. Cross-entropy and error values for neural network training

	Observation	Cross-entropy	Error value
Training	80	0.0765	0.0375
Validation	17	0.0239	0.0588
Testing	17	0.1193	0.0375

Table 5. Confusion matrices of BP neural network training results

Training confusion matrix				Validation confusion matrix					
Output class	1	66	2	97.1%	Output class	1	15	0	100%
		82.5%	2.5%	2.9%			88.2%	0.0%	0.0%
	2	1	11	91.7%		2	0	2	100%
		1.2%	13.8%	8.3%			0.0%	11.8%	0.0%
		98.5%	84.6%	96.2%			100%	100%	100%
		1.5%	15.4%	3.7%			0.0%	0.0%	0.0%
		1	2			1	2		
Target class				Target class					
Testing confusion matrix				Cumulative confusion matrix					
Output class	1	14	1	93.3%	Output class	1	95	3	96.9%
		82.4%	5.9%	6.7%			83.3%	2.6%	3.1%
	2	0	2	100%		2	1	15	93.8%
		0.0%	11.8%	0.0%			0.9%	13.2%	6.2%
		100%	66.7%	94.1%			99.0%	83.3%	96.5%
		0.0%	33.3%	5.9%			1.0%	16.7%	3.5%
		1	2			1	2		
Target class				Target class					

4. Discussion

Interpreting lung nodule imaging is undoubtedly a fundamental skill for thoracic surgeons, who are directly responsible for determining the surgical indications for lung nodules. Most lung nodule surgeries aim to address malignancy concerns and proceed with radical lung cancer surgery. Thoracic surgeons assess the benign or malignant nature of lung nodules primarily through chest CT imaging, focusing on reading the radiographic characteristics of the nodules ^[6]. These include lobulation, spiculation, burr sign, pleural indentation, air bronchogram, calcification, ground-glass opacity, solid components, and mixed features, among others ^[7]. While individual imaging features may have statistical significance in predicting malignancy, they are insufficient for definitive characterization. Determining malignancy requires a combination of multiple features, which introduces ambiguity and inevitably leads to misdiagnosis or missed diagnoses ^[8]. In this study, the positive rate of lung cancer among surgical patients with lung nodules was only 84.2%. This indicates room for improvement, and the identification of malignant lung nodules requires additional diagnostic tools.

Artificial intelligence (AI) aims to mimic human thought processes ^[8], performing specific tasks via computer systems to enhance its performance. AI has been widely applied in areas such as image recognition and natural language processing. Its general principle involves setting a loss function, where the loss minimizes when a specific target is reached and increases otherwise. Among these algorithms, gradient descent (GD), particularly the back-propagation algorithm (BP), is widely used. The basic principle involves inputting information through the input layer, processing it in the hidden layer, and outputting it via the output layer. The output is then compared

with the expected value. If the error is large, it propagates back to the hidden layer, where weights in the data transmission process are purposefully adjusted based on the magnitude and direction of the error. Ultimately, this process brings the output closer to the expected value. In medical subspecialties supported by large datasets, machine learning has naturally found a significant role. For instance, in pathology, machine learning has been used to analyze large volumes of pathological slides to diagnose gastric cancer^[9,10], lung cancer^[11], renal cancer^[12], prostate cancer^[13], and hypopharyngeal squamous cell carcinoma^[14]. Similarly, imaging has improved diagnostic accuracy for breast cancer^[15], liver cancer^[16], gallbladder cancer^[17], and pituitary tumors^[18] using CT imaging.

Currently, AI-based chest CT interpretation for screening lung nodules and distinguishing between benign and malignant lesions has been applied clinically^[19]. However, its use comes at a significant cost and is mostly limited to large hospitals. Even in cases where AI is used for imaging in radiology departments, it is rarely extended to thoracic surgeons. Moreover, many radiologists do not make definitive judgments about the benign or malignant nature of lung nodules in chest CT reports, leaving the decision to thoracic surgeons. As mentioned earlier, most lung nodule surgeries are managed by attending surgeons or above, yet the positive rate for lung cancer remains only 84.2%. Therefore, simple AI-assisted diagnostic tools hold significant potential value for thoracic surgeons.

To balance simplicity and accuracy, we focused exclusively on chest CT nodule features without considering patient characteristics such as gender and age, as their association with malignant lung nodules is relatively weak. Among lung nodule-related features, we studied only those closely related to distinguishing between benign and malignant nodules, such as burr signs, spiculation, and pleural traction. In this study, the discrimination accuracy for malignant lung nodules exceeded 94% across the training, validation, and test groups while requiring only six imaging features. This achieved a favorable balance between simplicity and accuracy.

Funding

Zhejiang Medical and Health Technology Project (Project No. 2020PY072)

Disclosure statement

The authors declare no conflict of interest.

References

- [1] Zhang J, 2023, Research on Semantic Segmentation Algorithm for Pulmonary Nodules Based on 3D U-Net, dissertation, Northwest A&F University.
- [2] Pei Q, Luo Y, Chen Y, et al., 2022, Artificial Intelligence in Clinical Applications for Lung Cancer: Diagnosis, Treatment and Prognosis. *Clin Chem Lab Med*, 60(12): 1974–1983. <https://doi.org/10.1515/cclm-2022-0291>
- [3] Yang X, Zhou Y, Chen F, et al., 2024, Construction and Practice of a Comprehensive Management Model for Pulmonary Nodules/Lung Cancer Based on “Internet+”. *West China Medical Journal*, 39(4): 613–618.
- [4] Chen Q, Zhu Q, Gu J, et al., 2023, Comparative Value of HRCT Targeted Scanning with Physiological Ventilation Assistance and Thin-Section CT Reconstruction in Diagnosing Pulmonary Ground-Glass Nodules. *Chinese Journal of Medical Computer Imaging*, 29(1): 26–31.
- [5] Zhao S, Meng L, Guo J, 2022, Construction of a Multimodal Combined Model Nomogram Based on CT Targeted Scanning for Evaluating Solitary Pulmonary Nodules. *Radiologic Practice*, 37(10): 6.

- [6] Feng X, Zhang M, Wu B, et al., 2020, Application Value of High-Resolution CT Combined with Serum CEA and NSE in Differential Diagnosis of Benign and Malignant Solitary Pulmonary Nodules. *Chinese Journal of CT and MRI*, 18(6): 3.
- [7] Liu J, Qian W, Li L, et al., 2024, Diagnostic Value of Imaging Features and Quantitative Parameters in Differentiating Benign and Malignant Pulmonary Nodules. *Chinese Medical Engineering*, 32(3): 25–30.
- [8] Fu Y, Xue P, Xiao T, et al., 2023, Semi-Supervised Adversarial Learning for Improving the Diagnosis of Pulmonary Nodules. *IEEE J Biomed Health Inform*, 27(1): 109–120. <https://doi.org/10.1109/JBHI.2022.3216446>
- [9] Li J, Song Z, Chen W, et al., 2024, Discussion on the Impact of Different Staining Modes on AI Diagnosis of Gastroscopy Tissue Pathology. *Journal of Diagnostic Pathology*, 31(9): 910–912.
- [10] Zhang J, Song Z, Wang S, et al., 2024, Research on a Classification Model Based on Pathological Data Features of Gastric Tumors. *Journal of Instrumentation and Measurement*, Online ahead of print.
- [11] Wang H, Guo M, Sun Y, et al., 2024, Research and Diagnostic Value of AI-Based Cytopathology Diagnostic System for Lung Cancer. *Journal of PLA Medical College*, 45(5): 463–468.
- [12] Hou N, Zhai W, Zheng J, 2024, Micro Knowledge through Macro Vision: Application Status and Challenges of AI in Digital Pathology of Renal Cancer. *Chinese Journal of Cancer Prevention and Treatment*, 16(2): 143–151.
- [13] Fan L, Song Z, Deng L, et al., 2024, Research Progress of AI in Pathological Diagnosis and Molecular Typing of Prostate Cancer. *Journal of Naval Medical University*, 45(9): 1141–1146.
- [14] Xie Y, 2023, Application of AI in Pathological Diagnosis and Prognosis of Metastatic Lymph Nodes in Hypopharyngeal Squamous Cell Carcinoma, dissertation, Shandong University.
- [15] Zhai T, Zhang M, Li D, 2024, Research Progress of AI in Imaging Diagnosis and Treatment of Breast Cancer. *Journal of Molecular Imaging*, 47(9): 1003–1006.
- [16] Chu X, Fu Y, Zheng S, et al., 2024, Opportunities and Challenges of AI in Imaging of Primary Liver Cancer. *Radiologic Practice*, 39(9): 1244–1249.
- [17] Wu Y, Hao J, 2024, Research Progress of Radiomics in Diagnosis and Treatment of Gallbladder Cancer. *International Journal of Medical Radiology*, 47(5): 594–598.
- [18] Jia W, Wang L, 2024, Research Progress of AI in MRI of Pituitary Tumors. *Magnetic Resonance Imaging*, 15(9): 162–166.
- [19] Deng B, Huang W, Jiang Y, 2024, Advances in AI-Based Precision Diagnosis and Treatment of Lung Cancer Using CT Imaging. *Chongqing Medicine*, Online ahead of print.

Publisher's note

Bio-Byword Scientific Publishing remains neutral with regard to jurisdictional claims in published maps and institutional affiliations.

Study on the Clinical Efficacy of Levofloxacin Combined with Ambroxol in the Treatment of Elderly Patients with Chronic Obstructive Pulmonary Disease and Pulmonary Infection

Yuanyuan Chen*

The 960th Hospital of the Joint Logistic Support Force of the Chinese People's Liberation Army, Jinan 250031, Shandong Province, China

*Corresponding author: Yuanyuan Chen, 15665733858@163.com

Copyright: © 2025 Author(s). This is an open-access article distributed under the terms of the Creative Commons Attribution License (CC BY 4.0), permitting distribution and reproduction in any medium, provided the original work is cited.

Abstract: *Objective:* To investigate the clinical efficacy of levofloxacin combined with ambroxol in the treatment of elderly patients with chronic obstructive pulmonary disease (COPD) and pulmonary infection. *Methods:* A total of 80 elderly COPD patients with pulmonary infection, treated between December 2022 and November 2023, were randomly divided into a control group and an observation group, with 40 cases in each group. The control group was treated with levofloxacin hydrochloride, while the observation group received ambroxol hydrochloride injection in addition to the treatment in the control group. Laboratory indices (white blood cell count, procalcitonin, C-reactive protein, and apolipoprotein E levels), imaging-based pulmonary lesion absorption time, hospital stay, and incidence of adverse reactions were compared between the two groups. *Results:* After treatment, the biochemical indices of the observation group were significantly lower than those of the control group, with highly significant differences ($P < 0.001$). Compared to the control group, the imaging-based pulmonary lesion absorption time and hospital stay of the observation group were significantly shorter ($P < 0.001$). Additionally, the incidence of adverse reactions in the observation group was significantly lower than in the control group ($P < 0.05$). *Conclusion:* Levofloxacin combined with ambroxol demonstrates advantages in improving biochemical indices, shortening imaging-based pulmonary lesion absorption time and hospital stay, and reducing adverse reaction rates in elderly COPD patients with pulmonary infection. It holds significant clinical application value.

Keywords: Levofloxacin; Ambroxol; Elderly chronic obstructive pulmonary disease; Pulmonary infection

Online publication: February 14, 2025

1. Introduction

Chronic obstructive pulmonary disease (COPD), a common chronic respiratory disease, has a high prevalence, and heavy disease burden, and poses a severe threat to the health of the elderly. It is one of the leading causes

of death in older adults ^[1,2]. The primary characteristics of COPD include chronic respiratory symptoms such as dyspnea, cough, and sputum production, typically presenting as persistent and progressively worsening airflow obstruction. This leads to a gradual decline in respiratory function and significantly affects the patient's quality of life. Clinically, COPD not only has a high incidence but is also frequently accompanied by pulmonary infections, which exacerbate the condition. Pulmonary infections aggravate symptoms like dyspnea, increased cough, and sputum production, severely impairing quality of life, increasing hospitalizations, and raising mortality rates ^[3].

Timely and effective treatment is critical to improving the prognosis of these patients. Antibiotic therapy is one of the most important measures for controlling pulmonary infections associated with COPD ^[4]. Levofloxacin hydrochloride, a commonly used quinolone antibiotic, exhibits broad-spectrum antibacterial activity and effectively inhibits the growth and reproduction of various bacteria. It is widely used in treating COPD with pulmonary infections. However, the sole use of antibiotics sometimes fails to meet all treatment needs.

Ambroxol hydrochloride injection, a mucolytic agent, increases the secretion of serous glands in the respiratory tract, reduces mucus gland secretion, decreases sputum viscosity, and promotes sputum clearance. Additionally, ambroxol possesses antioxidant and anti-inflammatory properties, reducing pulmonary inflammation and improving lung function. Therefore, combining ambroxol with levofloxacin may achieve better therapeutic outcomes.

This study aims to explore the clinical efficacy of levofloxacin combined with ambroxol in the treatment of elderly COPD patients with pulmonary infection, providing a more effective clinical treatment plan.

2. Materials and methods

2.1. General information

Eighty elderly patients with COPD complicated by pulmonary infection who were hospitalized in the respiratory department of our hospital from December 2022 to November 2023 were selected as study subjects.

Inclusion criteria: (1) Patients meeting the diagnostic criteria in the “Chinese Expert Consensus on the Diagnosis and Treatment of Acute Exacerbations of Chronic Obstructive Pulmonary Disease (2023 Revision)” ^[5]; (2) Age ≥ 60 years; (3) Signed informed consent provided by the patients or their families.

Exclusion criteria: (1) Patients with severe cardiovascular or cerebrovascular diseases, or liver and kidney dysfunction; (2) Patients allergic to levofloxacin or ambroxol; (3) Patients who had used other antibiotics or immunomodulators within the past three months; (4) Patients with psychiatric disorders who could not cooperate with treatment.

The patients were randomly divided into a control group and an observation group using a random number table, with 40 cases in each group. The control group included 22 males and 18 females, aged 60–80 years, with a COPD duration of 5–15 years and a pulmonary infection duration of 3–10 days. The observation group included 20 males and 20 females, aged 62–82 years, with a COPD duration of 4–14 years and a pulmonary infection duration of 2–9 days. No statistically significant differences were observed between the two groups in terms of gender, age, COPD duration, or pulmonary infection duration ($P > 0.05$), indicating comparability (see **Table 1**).

Table 1. Comparison of general information between the two groups

Group	<i>n</i>	Gender (<i>n</i>)		Mean age (mean ± SD, years)	Mean COPD duration (mean ± SD, years)	Mean pulmonary infection duration (mean ± SD, days)
		Male	Female			
Control	40	22	18	68.51 ± 5.37	9.24 ± 3.15	5.67 ± 2.26
Observation	40	20	20	69.17 ± 5.84	8.94 ± 2.92	5.24 ± 2.08
χ^2 / t	-	0.201		0.526	0.442	0.885
<i>P</i>	-	0.654		0.600	0.660	0.379

2.2. Methods

2.2.1. Control group

Patients were treated with levofloxacin sodium chloride injection (manufacturer: Beijing Jiluohua Pharmaceutical Co., Ltd.; specification: 100 mL containing levofloxacin 0.5 g and sodium chloride 0.9 g; approval number: H20020636). The dosage was 0.5 g once daily via intravenous infusion, with a treatment course of 10–14 days. During treatment, routine symptomatic and supportive care, such as oxygen therapy, antitussive therapy, and bronchodilation, was provided based on the patient's condition.

2.2.2. Observation group

On the basis of the control group treatment, patients received ambroxol hydrochloride injection (manufacturer: Shandong Luoxin Pharmaceutical Group Co., Ltd.; specification: 4 mL containing 30 mg; approval number: H20133026). The dosage was 30 mg twice daily via intravenous infusion, with the same treatment course as the control group. Other routine symptomatic and supportive treatments were identical to those in the control group.

2.3. Observation indicators

- (1) Laboratory indices: After treatment, venous blood was collected from the patient's inner elbow. A blood routine analyzer was used to measure white blood cell count (WBC), immunostaining to measure procalcitonin (PCT), enzyme-linked immunosorbent assay (ELISA) to measure C-reactive protein (CRP), and immunoturbidimetric assay to measure apolipoprotein E (ApoE).
- (2) Imaging-based pulmonary lesion absorption time and hospital stay: Chest X-ray or CT was used to observe changes in pulmonary lesions and the time required for complete absorption of the lesions was recorded. The length of hospital stay was also recorded, from admission to discharge.
- (3) Incidence of adverse reactions: Adverse reactions such as nausea, vomiting, diarrhea, and rash were monitored and recorded during treatment, and the incidence rate was calculated.

2.4. Statistical methods

Data analysis was performed using SPSS 27.0 statistical software. Measurement data were expressed as mean ± standard deviation (SD) and analyzed with the *t*-test. Categorical data were expressed as [*n* (%)] and analyzed with the χ^2 test. A *P*-value < 0.05 was considered statistically significant.

3. Results

3.1. Comparison of laboratory indices

After treatment, the levels of WBC, PCT, CRP, and ApoE in the observation group were significantly lower than those in the control group, with highly significant differences ($P < 0.001$). See **Table 2**.

Table 2. Comparison of laboratory indices after treatment between the two groups (mean \pm SD)

Group	WBC ($\times 10^9/L$)	PCT (ng/mL)	CRP (mg/L)	ApoE (mg/L)
Control ($n = 40$)	10.22 \pm 3.10	1.18 \pm 0.37	44.31 \pm 6.39	61.27 \pm 7.45
Observation ($n = 40$)	7.44 \pm 3.02	0.61 \pm 0.21	25.14 \pm 5.63	40.03 \pm 6.20
<i>t</i>	4.023	8.474	14.236	13.860
<i>P</i>	< 0.001	< 0.001	< 0.001	< 0.001

3.2. Comparison of imaging-based pulmonary lesion absorption time and hospital stay

The pulmonary lesion absorption time and hospital stay were significantly shorter in the observation group compared to the control group, with highly significant differences ($P < 0.05$). See **Table 3**.

Table 3. Comparison of pulmonary lesion absorption time and hospital stay between the two groups (mean \pm SD, days)

Group	<i>n</i>	Pulmonary lesion absorption time	Hospital stay
Control ($n = 40$)	40	15.65 \pm 2.77	18.04 \pm 3.65
Observation ($n = 40$)	40	8.26 \pm 2.85	11.26 \pm 3.09
<i>t</i>		11.760	8.967
<i>P</i>		< 0.001	< 0.001

3.3. Comparison of adverse reaction incidence

The adverse reaction rate in the observation group was 5.00%, significantly lower than the 22.50% in the control group, with a statistically significant difference ($P = 0.023$). See **Table 4**.

Table 4. Comparison of adverse reaction incidence between the two groups [n (%)]

Group	<i>n</i>	Nausea and vomiting	Diarrhea	Rash	Total adverse reaction rate
Control ($n = 40$)	40	3 (7.50%)	3 (7.50%)	3 (7.50%)	9 (22.50%)
Observation ($n = 40$)	40	1 (2.50%)	0 (0.00%)	1 (2.50%)	2 (5.00%)
χ^2	-	-	-	-	5.165
<i>P</i>	-	-	-	-	0.023

4. Discussion

Levofloxacin, a fluoroquinolone antibiotic, exhibits a unique and powerful mechanism of action by inhibiting bacterial DNA gyrase and topoisomerase IV, both of which play critical roles in bacterial DNA replication, transcription, and repair [6]. By suppressing these enzymes, levofloxacin disrupts bacterial reproduction, preventing

normal synthesis of genetic material, accelerating DNA dissolution, and ultimately leading to bacterial death. Additionally, levofloxacin has a broad antibacterial spectrum, showing strong activity against Gram-positive bacteria, Gram-negative bacteria, and atypical pathogens. This broad-spectrum activity makes it effective in treating COPD with pulmonary infections, targeting a wide range of pathogens.

Ambroxol hydrochloride, also known as bromhexine hydrochloride, plays a significant role in regulating respiratory physiological functions. It enhances the production of lysosomes in bronchial wall cells, which contain hydrolases that can break down viscous components in sputum, thereby reducing its viscosity ^[7]. Furthermore, ambroxol inhibits the formation of fibrin, a key substance contributing to sputum viscosity, aiding in sputum dilution and expulsion. It also modulates mucus secretion from airway glandular cells, making the mucus thinner and easier to expectorate.

In elderly patients with COPD complicated by pulmonary infections, the combined use of levofloxacin and ambroxol exerts synergistic effects. Levofloxacin effectively controls pulmonary infections by inhibiting bacterial growth and reproduction, thereby addressing the root cause of the inflammatory response. Meanwhile, ambroxol improves pulmonary ventilation by promoting sputum clearance and alleviating airway inflammation, creating favorable conditions for levofloxacin to exert its antibacterial effects ^[8]. This combination not only better controls pulmonary infections but also improves respiratory function to some extent, enhancing the quality of life for patients ^[9].

This study demonstrates that the combination of levofloxacin and ambroxol excels in improving laboratory indices in elderly COPD patients with pulmonary infections. The combined therapy significantly reduces levels of WBC, PCT, CRP, and ApoE, strongly indicating its effectiveness in suppressing inflammatory responses and positively regulating physiological functions.

Regarding treatment progression, imaging-based pulmonary lesion absorption time and hospital stay are key evaluation metrics. The study data indicate that patients receiving the combined therapy showed significantly faster pulmonary lesion absorption and shorter hospital stays. This not only facilitates quicker recovery, reducing physical and psychological distress but also lowers medical costs and enhances the efficiency of healthcare resource utilization.

The safety profile of the combined therapy is also satisfactory, with a lower incidence of adverse reactions compared to traditional monotherapies. This can be attributed to the synergistic effects of the two drugs. Levofloxacin, with its potent antibacterial activity, precisely inhibits bacterial growth and reproduction, effectively controlling infections at their source. Ambroxol, by promoting sputum clearance, alleviates airway obstruction and exerts anti-inflammatory effects, improving the pulmonary microenvironment. Together, these drugs complement each other, providing better control of pulmonary infections while enhancing respiratory function, leading to smoother breathing and improved quality of life for patients. This offers an efficient and safe therapeutic option for elderly COPD patients with pulmonary infections ^[10,11].

5. Conclusion

In summary, the combination of levofloxacin and ambroxol for treating elderly COPD patients with pulmonary infections demonstrates excellent clinical efficacy and safety. This regimen improves multiple indices, shortens the disease course, and has a lower incidence of adverse reactions, making it worthy of clinical promotion. However, the study has limitations, including a relatively small sample size, which may not comprehensively represent all patient populations, and a short observation period, which limits the precise evaluation of long-term efficacy and

safety. Further in-depth research is required in the future.

Disclosure statement

The author declares no conflict of interest.

References

- [1] Zhong J, 2022, Clinical Efficacy of Levofloxacin in the Treatment of Lower Respiratory Tract Bacterial Infections in Patients with Acute Exacerbations of Chronic Obstructive Pulmonary Disease. *Journal of Clinical Rational Drug Use*, 15(28): 44–46.
- [2] Ren J, Ren D, 2020, Clinical Effects of High-Dose Ambroxol Combined with Levofloxacin in the Treatment of Elderly Patients with Chronic Obstructive Pulmonary Disease and Severe Pneumonia. *Journal of Clinical and Pathology*, 40(10): 2565–2568.
- [3] Zhou Y, Zhu G, 2020, Analysis of the Efficacy of Piperacillin Sodium and Sulbactam Sodium in the Treatment of Chronic Obstructive Pulmonary Disease with Acute Lower Respiratory Tract Infection. *Northern Pharmacy*, 17(1): 3–78.
- [4] Lu X, Cheng X, Li Y, 2022, Efficacy of Tanreqing Injection Combined with Levofloxacin in the Treatment of Acute Exacerbations of Chronic Obstructive Pulmonary Disease Complicated with Pneumonia and Its Effects on Pneumonia Severity, IL-6, PCT, and SAA Levels. *Journal of Traditional Chinese Medicine*, 40(5): 51–54.
- [5] Expert Group on Diagnosis and Treatment of Acute Exacerbations of Chronic Obstructive Pulmonary Disease, 2023, Chinese Expert Consensus on the Diagnosis and Treatment of Acute Exacerbations of Chronic Obstructive Pulmonary Disease (2023 Edition). *International Journal of Respiration*, 43(2): 132–149.
- [6] Chen L, Zhou Z, Zhang J, 2022, Efficacy Analysis of High-Dose Ambroxol Combined with Levofloxacin in the Treatment of Elderly Patients with Chronic Obstructive Pulmonary Disease and Severe Pneumonia. *Chinese Community Doctors*, 38(20): 45–47.
- [7] Wen J, Wu H, Huang X, 2023, Clinical Efficacy of Piperacillin Sodium and Sulbactam Sodium Combined with Levofloxacin Lactate in the Treatment of Senile Pneumonia Complicated with Chronic Obstructive Pulmonary Disease. *Clinical Rational Drug Use*, 16(14): 87–89.
- [8] Sheng X, 2021, Study on the Effect of Levofloxacin Combined with Cefoperazone-Tazobactam in the Treatment of Chronic Obstructive Pulmonary Disease Complicated with Infectious Pneumonia. *Jilin Medical Journal*, 42(6): 1419–1420.
- [9] Kong Y, 2021, Clinical Effects of High-Dose Ambroxol Combined with Levofloxacin in the Treatment of Elderly Patients with Chronic Obstructive Pulmonary Disease and Severe Pneumonia. *Medical Equipment*, 34(10): 77–78.
- [10] Liu L, 2021, Observation on the Effect of High-Dose Ambroxol Combined with Levofloxacin in the Treatment of Elderly Patients with Chronic Obstructive Pulmonary Disease and Severe Pneumonia. *Jilin Medical Journal*, 42(9): 2189–2190.
- [11] Wang C, Chen X, Song X, et al., 2023, Study on the Effects of Sequential Administration of Moxifloxacin and Levofloxacin on Respiratory Function and Microinflammation in Elderly Patients with Severe Chronic Obstructive Pulmonary Disease in the Acute Exacerbation Stage. *Hebei Medical Journal*, 29(4): 685–689.

Publisher's note

Bio-Byword Scientific Publishing remains neutral with regard to jurisdictional claims in published maps and institutional affiliations.

Plasma Technology: Unlocking a New Path for Precise Elimination of Cancer Cells

Jie Bai*

Peptide Holdings (Hainan) Group Co., Ltd., Haikou 571000, Hainan Province, China

*Corresponding author: Jie Bai, 13366667724@qq.com

Copyright: © 2025 Author(s). This is an open-access article distributed under the terms of the Creative Commons Attribution License (CC BY 4.0), permitting distribution and reproduction in any medium, provided the original work is cited.

Abstract: This paper systematically elucidates the application of plasma technology in cancer treatment, including its principles, case studies, comparative advantages over traditional methods, challenges, and countermeasures. Plasma technology targets and eliminates cancer cells with precision through physical, chemical, and immune-regulatory mechanisms, offering high accuracy and low side effects. International applications include plasma scalpels in the United States, combined chemotherapy and low-temperature plasma therapy in Russia, and plasma-targeted capture technology in China. However, plasma technology faces technical hurdles and clinical application barriers, requiring interdisciplinary collaboration and industry-academia-research cooperation to advance its development.

Keywords: Plasma technology; Cancer treatment; Precision; Side effects; Challenges

Online publication: February 13, 2025

1. Introduction

Cancer, a global health challenge, continues to escalate annually. In 2020, approximately 19.29 million new cases were reported globally, with about 9.96 million deaths. The cancer situation in China is particularly severe, with 4.57 million new cases, accounting for one-fourth of the global total. Confronted with the limitations of traditional treatment methods, plasma technology emerges as an innovative therapeutic approach. With its high activity and energy properties, plasma technology precisely disrupts cancer cell structures, induces oxidative stress responses, and inhibits cancer cell proliferation. Compared to traditional methods, plasma technology offers greater specificity, reduced side effects, personalized treatment, ease of operation, and faster recovery. This study aims to explore the application of plasma technology in cancer treatment, analyze its mechanisms and current status, and project future developments to address therapeutic gaps and contribute to precision cancer treatment.

2. Analysis of plasma technology principles

2.1. Material properties of plasma

Plasma can be categorized by temperature into high-temperature plasma and low-temperature plasma, with the latter further divided into cold plasma and thermal plasma. High-temperature plasma, where both electron and heavy particle temperatures exceed 10^6 K, is primarily used for generating nuclear fusion energy. However, the energy of high-temperature plasma is challenging to harness directly for industrial heating. In contrast, low-temperature cold plasma has heavy particle temperatures in the ambient range, while electron temperatures may exceed 10^4 K. Despite this, its energy density is very low, comparable to room-temperature atmospheric gases, rendering it unsuitable as a large-scale industrial energy source. Instead, it is mainly utilized to enhance chemical reactions for surface processing (e.g., etching, coating, doping, cleaning, biomedical applications, and nanomaterial growth and processing), gas treatment (e.g., ozone generation and harmful gas processing), and cold light sources. It is also employed for macroscopic material preparation, such as diamond growth ^[1].

Plasma, often referred to as the fourth state of matter, differs fundamentally from the traditional three states. It is an ionized gas composed of numerous free electrons, ions, free radicals, and neutral particles. On a microscopic level, its charged particles move at high speeds, interact with each other, and are coupled with external electromagnetic fields, resulting in high activity. These charged particles endow plasma with excellent conductivity, enabling it to rapidly conduct current under an electric field. Despite containing large numbers of charged particles, the positive and negative charge densities are nearly equal, resulting in macroscopic electrical neutrality. This ensures precise and controllable actions.

2.2. Mechanism of plasma generation

Plasma is artificially generated by supplying energy to ionize gases. The heating method increases the kinetic energy of gas molecules through sustained heating, causing electrons to detach from atoms, as seen in tokamak devices that heat plasma to billions of degrees. Electromagnetic excitation methods are more widely applied:

- (1) DC glow discharge: Direct current voltage applied between electrodes creates a glow region to generate plasma.
- (2) Radiofrequency discharge: Alternating electromagnetic fields ionize gases, allowing precise control over plasma properties, commonly used in cellular experiments.
- (3) Microwave discharge: Microwaves interact with gases to produce highly active plasma, enhancing the ability to kill cancer cells.

Plasma parameters influence its performance ^[2]. Electron temperature affects chemical reaction activity, ion temperature impacts diffusion and transport, plasma density determines action intensity, and the type of gas dictates plasma composition and activity. These parameters must be finely tuned to meet therapeutic requirements.

2.3. Mechanisms of plasma interaction with cancer cells

Plasma eliminates cancer cells through physical, chemical, and immunomodulatory mechanisms, achieving precise destruction.

- (1) Physical mechanism: High-energy charged particles in plasma, such as electrons and ions, collide with cancer cells, damaging their membranes and causing intracellular material leakage, osmotic imbalance, and apoptosis or necrosis. Plasma can also penetrate cancer cells, damaging organelles like mitochondria and the endoplasmic reticulum, disrupting energy metabolism and biosynthesis, thereby deactivating cancer cells.

- (2) Chemical mechanism: Plasma contains reactive oxygen species (ROS) and reactive nitrogen species (RNS), which are highly redox-active particles. These particles enter cancer cells and react with biomolecules such as nucleic acids, proteins, and lipids. They oxidize DNA bases, causing strand breaks, destabilizing the genome, and hindering DNA replication and transcription. They also interact with protein active groups, altering their conformation and function, disrupting cellular signaling pathways, and activating apoptotic proteins to promote cancer cell apoptosis.
- (3) Immunomodulatory mechanism: Plasma treatment alters cancer cell antigen epitopes, making them more recognizable to the immune system and activating innate and adaptive immunity ^[3]. Macrophages and natural killer (NK) cells engulf cancer cells, releasing cytokines to recruit immune cells, creating a localized immune-activated microenvironment. Additionally, the immune response triggered by plasma has a memory effect, monitoring and suppressing tumor recurrence, thus ensuring long-term cancer treatment and recovery.

3. Application cases of plasma technology in precise cancer cell elimination

3.1. Clinical exploration of plasma surgical tools in the United States

The United States has made significant progress in exploring plasma technology for cancer treatment, achieving innovative results. The Canady Helios Cold Plasma System and surgical tool, developed by US Medical Innovations LLC and the Jerome Canady Research Institute for Advanced Biological and Technological Sciences (JCRI/ABTS), represent a breakthrough after years of research. The system features a low-temperature plasma generator and a pen-like electrosurgical tool that emits blue cold plasma from its tip when activated, opening new possibilities for cancer treatment. Preliminary animal and cellular studies have demonstrated that cold plasma is a highly efficient and selective “cancer killer” ^[4]. ROS and other toxic molecules produced by the plasma can precisely target tumor cells. Due to the highly oxidative internal environment of cancer cells, ROS induces oxidative stress beyond their threshold, triggering apoptosis, while causing minimal damage to healthy cells.

Previously, three terminally ill patients were treated with the plasma surgical tool under the “compassionate use” principle, successfully clearing residual cancer cells. The research has since received FDA approval to commence Phase I clinical trials involving 20 patients with advanced solid tumors, including pancreatic, ovarian, and breast cancer patients.

3.2. Russia’s combination therapy of chemotherapy and cold plasma

Russia has pioneered a novel cancer treatment combining chemotherapy with cold plasma. Researchers tailor the therapy by selecting suitable chemotherapy drugs based on the type of cancer, patient-specific conditions, and disease progression. Concurrently, specialized equipment generates cold plasma, with parameters precisely controlled to ensure activity and efficacy. The two methods then work synergistically to combat cancer ^[5].

In cellular experiments, this combination therapy has demonstrated impressive anticancer efficacy, successfully targeting over 20 types of cancer cells. The mechanism involves two key aspects:

- (1) On the one hand, the ROS and RNS produced by the plasma exert strong oxidative and reductive effects, directly attacking critical components of cancer cells, disrupting metabolic processes, causing genetic information loss, and inducing apoptosis.
- (2) On the other hand, the plasma modifies the tumor microenvironment, enhancing the permeability of

chemotherapy drugs, thereby improving efficacy and reducing toxicity.

According to Namik Gusein-Zade, a director at Russia's National Pirogov Medical University, plasma can penetrate several centimeters deep into tissues. For deep tumors, plasma-treated fluids can be injected directly. In some cases, portable plasma generators are sufficient for treatment.

3.3. Plasma-targeted capture technology by Henan Guoshanglian in China

The Henan Guoshanglian Health Management Co., Ltd. has achieved groundbreaking advancements in plasma-targeted capture technology, bringing hope to cancer patients. This technology leverages the natural affinity between boron and cancer cells. By using a specially formulated boron compound beverage as a medium, boron is selectively enriched within cancer cells. Precisely controlled plasma is then applied to target these boron-enriched cells.

The high-energy particles from the plasma interact with boron, releasing immense energy to accurately destroy critical cancer cell structures such as cell membranes, mitochondria, and nucleic acids. This process disrupts the foundations of cancer cell proliferation and survival, efficiently eliminating cancer cells. Since normal cells lack boron, they remain unaffected, preserving the immune system and causing no side effects ^[6].

Certified by a top-tier inquiry agency under China's Ministry of Science and Technology, Guoshanglian's equipment has achieved a significant breakthrough in the depth of cancer cell eradication, reaching 13 cm—far surpassing similar products in the United States and placing it two generations ahead technologically. This positions the company at the forefront of the field.

Currently, Guoshanglian has developed a comprehensive cancer prevention and treatment system featuring five advanced devices, including cancer cell-clearing capsules and intelligent high-speed radiation cabins. These devices work in coordination to provide precise cancer clearance, functional regulation, and protective functions, offering personalized, one-stop solutions.

4. Advantages of plasma technology compared to traditional cancer treatments

4.1. Precision comparison

Surgical treatment often relies on the surgeon's experience and visual observation, making it challenging to completely remove cancer cells with unclear boundaries or microscopic size, particularly in high-risk procedures such as brain surgeries, which also involve slow recovery. Radiation therapy can destroy cancer cells but may cause damage to normal tissues due to scattered radiation, leading to side effects such as pneumonia and esophagitis. Chemotherapy drugs, lacking specificity, harm healthy cells, resulting in severe side effects and drug resistance ^[7].

In contrast, plasma technology employs imaging techniques such as CT and MRI for precise tumor localization. Specially designed catheters deliver plasma directly to the tumor site, where the reactive particles preferentially target and destroy cancer cells with minimal impact on normal cells. This greatly enhances the precision and safety of cancer treatment.

4.2. Side effects comparison

Traditional cancer treatments often come with severe side effects. Surgical recovery can be arduous, radiation therapy causes extensive tissue damage, and chemotherapy leads to systemic side effects that significantly impact the patient's quality of life.

Plasma technology, on the other hand, precisely targets cancer cells with minimal damage to normal tissues, resulting in only mild local reactions. Patients do not endure the intense pain and lengthy recovery associated with traditional surgeries. For skin cancers, plasma therapy results in smaller wounds, faster healing, and no inflammatory responses^[8]. Additionally, systemic side effects are nearly nonexistent, with no reports of nausea, vomiting, hair loss, or significant immune system disruptions. This significantly improves patients' quality of life, facilitating both treatment and recovery.

4.3. Treatment effectiveness comparison

Plasma ablation technology has demonstrated precision in treating early-stage liver cancer, effectively destroying tumor tissues and inducing rapid tumor necrosis. Post-treatment, patients often exhibit a significant reduction in tumor biomarkers and substantial tumor shrinkage. Patients recover quickly, experiencing less pain in the liver region, improved appetite, and an overall better quality of life.

In terms of long-term outcomes, plasma technology not only eradicates cancer cells but also stimulates the immune system, effectively preventing recurrence. For instance, Russia's combination therapy of chemotherapy and cold plasma has proven to increase the five-year survival rate of lung cancer patients while improving their quality of life ratings^[9].

5. Challenges and strategies for plasma technology

5.1. Technical challenges

Despite the availability of various plasma generation methods, such as gas discharge and laser irradiation, achieving stable and efficient generation of plasma with specific parameters inside complex biological environments remains challenging. The requirements for plasma parameters, such as electron and ion temperatures, vary depending on the type of cancer, tumor location, and patient-specific factors. For example, treating deep-seated tumors requires plasma with strong penetration capabilities, necessitating precise control over energy and particle concentration to balance energy attenuation and protect normal tissues. Current technology struggles to meet these demands.

Dose control and safety considerations are also critical. Plasma dosage directly impacts both efficacy and safety. Insufficient doses fail to eradicate cancer cells, while excessive doses induce oxidative stress that damages normal tissues, causing inflammation, fibrosis, and immune imbalance. Establishing precise, standardized dosage protocols is difficult due to variations in tumor characteristics and patient health, which significantly limits clinical adoption^[10].

Equipment development and clinical integration also face numerous obstacles. Existing plasma treatment devices are often bulky, and complex, and require specialized personnel for operation and maintenance, making them inaccessible for use in primary healthcare settings. Additionally, technical integration with cancer diagnosis, surgery, and rehabilitation remains problematic. For instance, using plasma technology during surgery requires clear visualization and seamless operation, which remains an urgent issue to resolve and hampers clinical translation.

5.2. Barriers to clinical application

In the clinical trial phase, large-scale, multi-center trials are scarce despite the technology's immense potential. Conducting such trials is costly and demands significant human, financial, and time resources, with challenges at every stage. For example, the Canady Helios low-temperature plasma scalpel trial in the United States required

years of preparation before its Phase I clinical trial began, following a decade of foundational research involving tasks like identifying chemical substances and determining tissue penetration properties. These requirements test the limits of research capacity, funding, and patience.

Interdisciplinary collaboration challenges further complicate trials. Communication gaps and inconsistent standards among researchers from different fields hinder the scientific rigor of experiments, delaying the clinical translation of the technology.

The lack of standardization in operation protocols and efficacy evaluation also limits development. Plasma-based cancer treatment currently lacks unified standards for procedures and outcome assessments. Equipment, parameters, and treatment protocols vary across teams and institutions. Critical parameters like optimal dosage, treatment frequency, and duration remain undefined, making it difficult to compare results across studies and objectively evaluate effectiveness. This leaves clinicians without clear guidance and patients with lingering doubts, impeding widespread adoption.

Additionally, physician training and patient awareness are critical issues. Many doctors have only a superficial understanding of emerging plasma technology and lack systematic training, increasing the risk of errors during implementation.

5.3. Strategies for addressing challenges

5.3.1. Interdisciplinary collaboration

Interdisciplinary collaboration is key to overcoming these challenges, as plasma technology spans multiple advanced fields.

- (1) Physicists: Develop highly efficient and precise plasma generation devices, optimize electromagnetic fields, and explore new discharge modes to achieve stable parameter control.
- (2) Chemists: Analyze chemical reactions to optimize plasma composition, enhance cancer cell targeting, and reduce damage to normal tissues.
- (3) Biologists: Investigate molecular biological pathways to provide precise therapeutic targets.
- (4) Medical Experts: Integrate this knowledge into diagnostic and therapeutic systems, creating personalized treatment plans to maximize efficacy.

5.3.2. Synergistic innovation between academia, industry, and clinical practice

Collaboration between universities, research institutions, and the private sector is essential for driving innovation and clinical translation.

- (1) Academia and research institutions: Increase investment in fundamental research, gather interdisciplinary talent, and solve core challenges.
- (2) Industry: Focus on commercializing research outcomes, and improving device portability, usability, and stability while reducing costs.
- (3) Healthcare institutions: Collaborate with companies to refine device performance for clinical use.
- (4) Government support: Provide incentives, establish funds, and create platforms to foster an ecosystem conducive to plasma technology development and clinical application.

By uniting efforts across disciplines and sectors, plasma technology can overcome its challenges and achieve its potential as a transformative tool in cancer treatment.

6. Conclusion

This study comprehensively explored the application of plasma technology in the precise eradication of cancer cells, analyzing its underlying principles and showcasing its remarkable efficacy in treating various types of cancer through international case studies. Compared with traditional methods, plasma technology demonstrates higher precision and fewer side effects, offering a novel approach to cancer treatment.

Although technical and application challenges remain, advancements in technology and interdisciplinary collaboration present promising prospects for the future development of plasma technology. It is anticipated that the technology will achieve more precise control, integrate with other treatment methods, and become accessible to more medical institutions. Ultimately, plasma technology is poised to become a mainstream cancer treatment method, offering new hope in the fight against cancer.

Disclosure statement

The author declares no conflict of interest.

References

- [1] Xia W, Shi K, Wang C, et al., 2023, Plasma Energy Supports China's Industrial Carbon Neutrality. *Chinese Journal of Theoretical and Applied Mechanics*, 55(12): 2779–2795.
- [2] Zhang H, Zhang J, Xu D, et al., 2023, Research Review on Plasma-Activated Water Solutions for Cancer Treatment. *Journal of Electrotechnics Technology*, 38(S1): 231–246.
- [3] Lin S, 2023, Photothermal-photodynamic Synergistic Treatment of Breast Cancer Cells Deep Within Tissue Using Gold Nanorods, dissertation, Fujian Normal University.
- [4] Han X, 2023, Construction of a Detection and Drug Delivery Platform for Cancer Biomarkers Based on Hybridization Chain Reaction, dissertation, Beijing University of Chemical Technology.
- [5] Wang H, 2023, Molecular Dynamics Simulation Study of Apoptosis in Cancer Cells Under the Synergistic Effects of Plasma Active Particles and Electric Fields, dissertation, Shandong University.
- [6] Shi H, Dang L, Lu M, et al., 2023, Risk Analysis and Control of Clinical Use of Plasma Surgical Knife Heads. *Medical Equipment and Facilities*, 44(6): 80–83.
- [7] Chen Y, Ni G, 2022, Development of a High-Voltage Pulse Power Supply for Low-Temperature Plasma Surgical Knives. *Power Electronics Technology*, 56(1): 99–102.
- [8] Xiao Q, Liu D, Gu Y, et al., 2023, Efficacy Analysis of Transoral Low-Temperature Plasma in the Removal of Tonsil Cancer. *Medical Research and Trauma Surgery*, 36(9): 940–943.
- [9] Li C, Jin H, 2023, Low-temperature Plasma-targeted Ablation Combined with Progressive Relaxation Training in Treating Lumbar Disc Herniation and Its Impact on Patients' Sleep Quality. *World Journal of Sleep Medicine*, 10(5): 960–962 + 967.
- [10] Chen C, 2023, Mechanism of Outer Membrane Lysis of *Salmonella typhimurium* Induced by Cold Plasma, dissertation, South China University of Technology.

Publisher's note

Bio-Byword Scientific Publishing remains neutral with regard to jurisdictional claims in published maps and institutional affiliations.



Integrated Services Platform of International Scientific Cooperation

Innoscience Research (Malaysia), which is global market oriented, was founded in 2016. Innoscience Research focuses on services based on scientific research. By cooperating with universities and scientific institutes all over the world, it performs medical researches to benefit human beings and promotes the interdisciplinary and international exchanges among researchers.

Innoscience Research covers biology, chemistry, physics and many other disciplines. It mainly focuses on the improvement of human health. It aims to promote the cooperation, exploration and exchange among researchers from different countries. By establishing platforms, Innoscience integrates the demands from different fields to realize the combination of clinical research and basic research and to accelerate and deepen the international scientific cooperation.

Cooperation Mode



Clinical Workers



In-service Doctors



Foreign Researchers



Hospital



University



Scientific institutions

OUR JOURNALS



The *Journal of Architectural Research and Development* is an international peer-reviewed and open access journal which is devoted to establish a bridge between theory and practice in the fields of architectural and design research, urban planning and built environment research.

Topics covered but not limited to:

- Architectural design
- Architectural technology, including new technologies and energy saving technologies
- Architectural practice
- Urban planning
- Impacts of architecture on environment

Journal of Clinical and Nursing Research (JCNR) is an international, peer reviewed and open access journal that seeks to promote the development and exchange of knowledge which is directly relevant to all clinical and nursing research and practice. Articles which explore the meaning, prevention, treatment, outcome and impact of a high standard clinical and nursing practice and discipline are encouraged to be submitted as original article, review, case report, short communication and letters.

Topics covered by not limited to:

- Development of clinical and nursing research, evaluation, evidence-based practice and scientific enquiry
- Patients and family experiences of health care
- Clinical and nursing research to enhance patient safety and reduce harm to patients
- Ethics
- Clinical and Nursing history
- Medicine



Journal of Electronic Research and Application is an international, peer-reviewed and open access journal which publishes original articles, reviews, short communications, case studies and letters in the field of electronic research and application.

Topics covered but not limited to:

- Automation
- Circuit Analysis and Application
- Electric and Electronic Measurement Systems
- Electrical Engineering
- Electronic Materials
- Electronics and Communications Engineering
- Power Systems and Power Electronics
- Signal Processing
- Telecommunications Engineering
- Wireless and Mobile Communication

